PHOTOSENSITIZING PROPERTIES OF NON-TRANSITION METAL PORPHYRAZINES TOWARDS THE GENERATION OF SINGLET OXYGEN

THESIS

Submitted to Rhodes University

in fulfilment of the requirements for

THE DEGREE OF MASTER OF SCIENCE IN CHEMISTRY

by

ITUMELENG SEOTSANYANA-MOKHOSI

January 2001

Department of Chemistry

Rhodes University

Grahamstown

Acknowledgments

I would like to express my deepest gratitude to my supervisor, Prof. T. Nyokong, for her guidance, commitment and unending encouragement throughout the project.

My heartfelt thanks to my mom and dad, `M'aisang and Thabo Seotsanyana who sacrificed a lot to enable me to further my studies. I would not have survived without their constant support and encouragement. I extend my thanks to the rest of my family especially, my kids, who had to survive without a mother for so long.

I would also like to thank Dr N. Kuznetsova, who was visiting from Organic Intermediates and Dyes Institute, Moscow, Russia who supplied knowledge and guidance in the course of this project.

I would also like to thank the following:

- Lesotho government for financial support.
- my friends and colleagues, especially, Joshua for proofreading my drafts and Dr Janice Limson for helping to proofread the thesis.
- members of the Chemistry Department Rhodes University, for their assistance in many different ways.

Abstract

Metallophthalocyanine complexes containing non-transition metals are very useful as sensitizers for photodynamic therapy, a cure for cancer that is based on visible light activation of tumour localized photosensitizers. Excited sensitizers generate singlet oxygen as the main hyperactive species that destroy the tumour. Water soluble sensitizers are sort after for the convenience of delivery into the body. Thus, phthalocyanine (pc), tetrapyridinoporphyrazines (tppa) and tetramethyltetrapyridinoporphyrazines (tmtppa) with non-transition central metal atoms of Ge, Si, Sn and Zn were studied. First was the synthesis of these complexes, followed by their characterisation. The characterisation involved the use of ultraviolet and visible absorption spectroscopy, infrared spectroscopy, nuclear magnetic resonance spectroscopy, electrochemical properties and elemental analysis.

Photochemical properties of the complexes were then investigated. Photolysis of these macrocycles showed two processes; -reduction of the dye and photobleaching, which leads to the disintegration of the conjugated chromophore structure of the dye. Photobleaching is the reductive quenching of the excited state of the sensitizers. The intensity of the quenching decreased progressively from tmtppa, tppa to pc metal complexes with photobleaching quantum yields, 6.6×10^{-5}, 1.8×10^{-5} and 5.4×10^{-6} for Zntmtppa, Zntppa and Znpc, respectively.

Efficiency of singlet oxygen sensitization is solvent dependent with very different values obtained for the same compound in different solvents, for example, 0.25 and 0.38 were observed as singlet oxygen quantum yields for Gepc complex in DMSO and DMF respectively. In DMSO the efficiency of $^1O_2$ generation decrease considerably from pc to tppa and finally tmtppa. In water Getmtppa exhibits much higher singlet oxygen quantum yield, hence promising to be effective as a sensitizer for

photodynamic therapy.

Table of contents Page

List of abbreviations

^{1}Sens*	=	singlet excited sensitizer
^{3}Sens*	=	triplet excited sensitizer
ADMA	=	α,α`-(anthracene-9,10-diyl)bimethylmalonate
ALA	=	5-Aminolaevulinic acid
BAS	=	Bio-Analytical Systems
CV	=	cyclic voltammetry
DABCO	=	Diazabicyclo-(2.2.2)-octane
DMF	=	N,N-Dimethylformamide
DMSO	=	Dimethylsulphoxide
DPBF	=	Diphenylisobenzofuran
H_2Pc	=	unmetallated phthalocyanine
HNMR	=	proton nuclear magnetic resonance
HOMO	=	highest occupied molecular orbital
HpD	=	haematoporphyrin derivative
I	=	Intensity of light from the lamp
I_{abs}	=	absorbed light
IR	=	infrared
L	=	ligand
LUMO	=	lowest unoccupied molecular orbital
m-MTHPC	=	m-tetrahydroxyphenyl chlorin

Mpc	=	metallophthalocyanine
Mtmtppa	=	NN`N``N```tetramethyltetrapyridinoporphyrazine
Mtspc	=	metallotetrasulphonated phthalocyanine
n.h.e	=	normal hydrogen electrode
NA	=	n-Nitrosodimethylanaline
p	=	porphyrin
pa	=	porphyrazine
pc	=	phthalocyanine
PDT	=	photodynamic therapy
PPIX	=	protoporphyrin
Pz*	=	excited porphyrazine molecule
SAR	=	structure activity relationship
Sens	=	sensitizer
T_1	=	triplet state energy level
TEAP	=	Tetraethyl ammonium perchlorate
tppa	=	tetrapyridinoporphyrazine
Tspc	=	tetrasulphonated phthalocyanine
UV/Vis	=	Ultraviolet and visible

List of symbols

Φ_{DPBF}^{Mpc}	=	quantum yield of DPBF in the presence of Mpc
Φ_{DPBF}^{Znpc}	=	quantum yield of DPBF in the presence of Znpc
α	=	fraction of light absorbed
β	=	beta
ΔE	=	separation between the peak potentials
λ_{max}	=	wavelength
π	=	pi orbital
π^*	=	pi antibonding orbital
Φ	=	quantum yield
Φ_{Δ}	=	quantum yield of singlet oxygen
$\Phi\tau$	=	triplet state quantum yield
Φ_{DPBF}	=	quantum yield of DPBF
Φ_f	=	fluorescence
$\Phi_{photobleaching}$	=	quantum yield of photobleaching
A	=	area of electrode
a_u	=	ungerade
C	=	bulk concentration
D	=	diffusion coefficient

E_a	=	anodic potential
E_c	=	cathodic potential
E_f	=	final potential
e_g	=	gerade
E_i	=	initial potential
$E°$	=	standard potential
$E_{½}$	=	half wave potential
F	=	Faraday`s constant
I_c	=	cathodic peak potential
I_i	=	anodic peak potential
kJ/Mol	=	kilojoules per mole
n	=	number of electrons
N_a	=	Avagadro`s number
nm	=	nanometer
$O_2(^1\Delta_g)$	=	singlet state oxygen
$O_2(^3\Sigma_g)$	=	triplet state oxygen
R	=	gas constant
r_o	=	radius of electrode
S_0	=	ground state energy level
S_1	=	singlet state energy level
v	=	scan rate
V	=	volts

List of Figures

List of Schemes

List of Table

Page

1.1 History of Phthalocyanines

Phthalocyanines (pc), Figure 1.1(a), are porphyrin-like structures with the systematic name, tetraazatetrabenzoporphyrins. Pcs form part of the big family of macrocycles known as porphyrazines which are porphyrin (p) derivatives, only more complicated. When compared with the structure of porphyrins, Figure 1.1(b), the pc has a similar inner backbone with the nitrogen aza bonds replacing the methine linkages of the porphyrins.

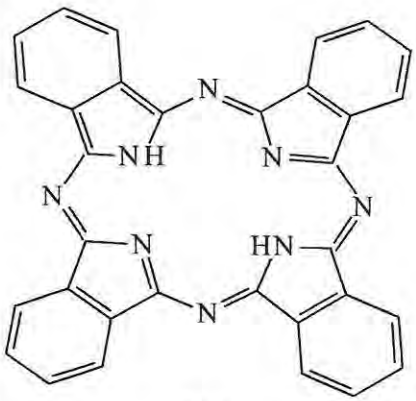

1(a)

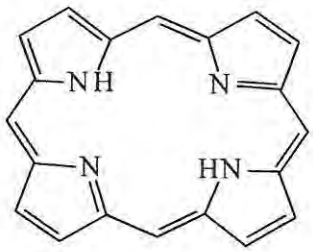

1(b)

Figure 1.1 Structural representation of metal free (a) phthalocyanine (H_2pc) and (b) porphyrin(p).

Phthalocyanines were first discovered in 1928 during the preparation of phthalamide in a fluke.[1,2] Messrs Scottish Dyes Ltd[1] were using iron vessels to prepare the phthalamide from phthalic

anhydride and ammonia but the product emerged contaminated with a stable dark blue insoluble complex which was later shown to be ferrous phthalocyanine. Only a year earlier a German chemist De Diesbach[1] had prepared a similar compound by reacting phthalodinitrile with a copper salt. The mystery of these two compounds was solved about four years later by Linstead who was able to characterise the complexes,[3] and that was followed by elucidation of their structure using x-ray diffraction analysis by Robertson.[4] The nomenclature to describe these molecules was suggested thereafter by the same Linstead. Needless to say, from their similar structures pcs and porphyrins exhibit similar properties, such as their remarkable ability to complex with central metals. Over the 70 years since their first discovery they have established themselves as metallophthalocyanine (Mpc) complexes through the replacement of the central hydrogen atoms with a variety of elements, of either metal or metalloid nature.

The pc dianion (pc^{-2}) is an 18 π-electron system with very strong characteristic absorptions in the ultraviolet and the visible (UV/Vis) region, between 200-1000nm. The absorbance in the visible region give the pcs their rich colour.[5] Mpcs such as Cupc exist in different polymorphic forms with slightly different properties of which the α and the β forms are the most important. Robertson[6] pioneered the study of the geometry of the Mpcs and from his findings together with subsequent results from the other research groups, the geometry of Mpc complexes was mapped. Commonly simplified co-ordination patterns rely on the binding power of the central metal. For a 6 co-ordinate centre a hexagonal sphere is observed, while a square pyramidal and a square planar result from 5 and

4 co-ordinate centres, respectively, Figure 1.2.

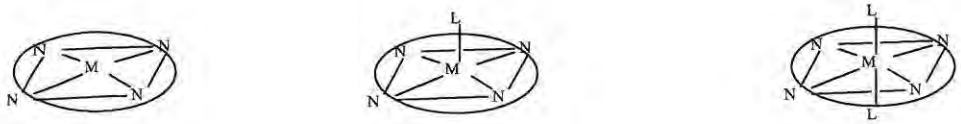

(a) (b) (c)

Figure 1.2 A depiction of the different Mpc co-ordination spheres: (a) 4 co-ordinate sphere (square planar), (b) 5 co-ordinate (pyramidal) sphere and (c) 6 co-ordinate (hexagonal) sphere. The rings with the nitrogen atoms represent the macrocycle of the pc, M is the metal and L is the ligand.

1.2 General synthetic methods for metallophthalocyanines.

Many research groups have worked on designing different new efficient methods of synthesizing Mpcs.[2] The usual methods are the cyclotetramerization reactions of metal-templates of the phthalonitrile derivatives.[7] The most commonly used methods include the condensation of phthalonitrile with a metal, a metal oxide or metal salt in the presence of a solvent, Scheme 1.

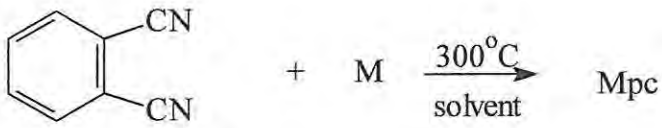

Scheme 1 Preparation of an Mpc from phthalonitrile.

The above method is not normally applied in industry because the starting material, phthalonitrile, is relatively expensive. However, when a product of high purity is needed then even industry uses this method. If the reactants are acid etched or when the metal is finely divided, offering a much larger surface area for the reaction, the reaction can become very vigorous and exothermic, rendering the method unsafe. A variation of the above method is the use of o-cyanobenzamide or phthalamide instead of the phthalonitrile as shown in Scheme 2.

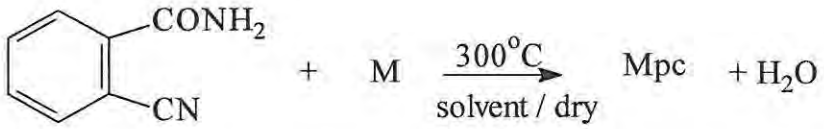

Scheme 2 Preparing an Mpc starting with o-cyanobenzamide.

Scheme 2 involves the condensation of the amide under anhydrous conditions. A solvent need not be used, a factor which produces a purer sample in the end. In another method, Scheme 3, 1,3-diiminoisoindole is the starting material. This then reacts with the metal or the metal salt to give a product of much higher purity and in relatively much higher yields.[8]

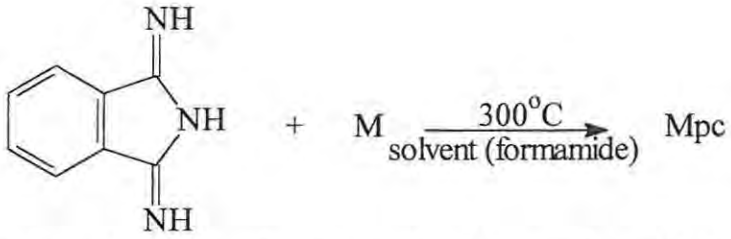

Scheme 3 Synthesis of Mpc from 1,3-diiminoisoindole

All the methods cited above can also be used to prepare a metal-free pc by omitting the addition of the metal. The metal can then be introduced at a later stage to give the Mpc. These methods are relatively cheap which is another factor that promotes the research on Mpcs. In industry the preferred method is to heat the phthalic anhydride with urea as a nitrogen source in the presence of a catalyst such as aluminium oxide or ammonium molybdate, Scheme 4.

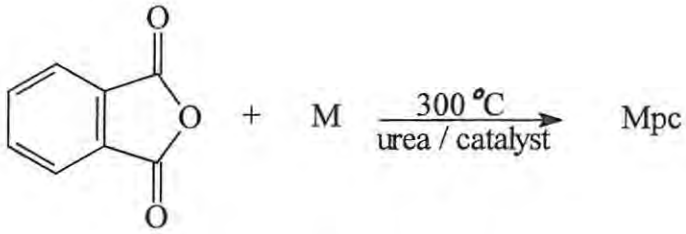

Scheme 4 Preparing an Mpc from phthalic anhydride.

To prepare Mpcs with axially substituted derivatives, Scheme1 can be modified by just using a metal salt whose anion is targeted as the ligand. The method applies mostly when the metal is of higher oxidation state than M(II). The metal salt that is normally used is the chloride which can later

be hydrolysed into ((OH)$_x$Mpc) by reacting with pyridine and ammonium hydroxide. The dihydroxy Mpc derivatives are chemically reactive and are normally used when synthesizing alkoxy derivatives.[9] Axial ligands can also be introduced by refluxing Mpc complexes in a co-ordinating solvent or in the presence of an excess of the axial ligand, Scheme 5.

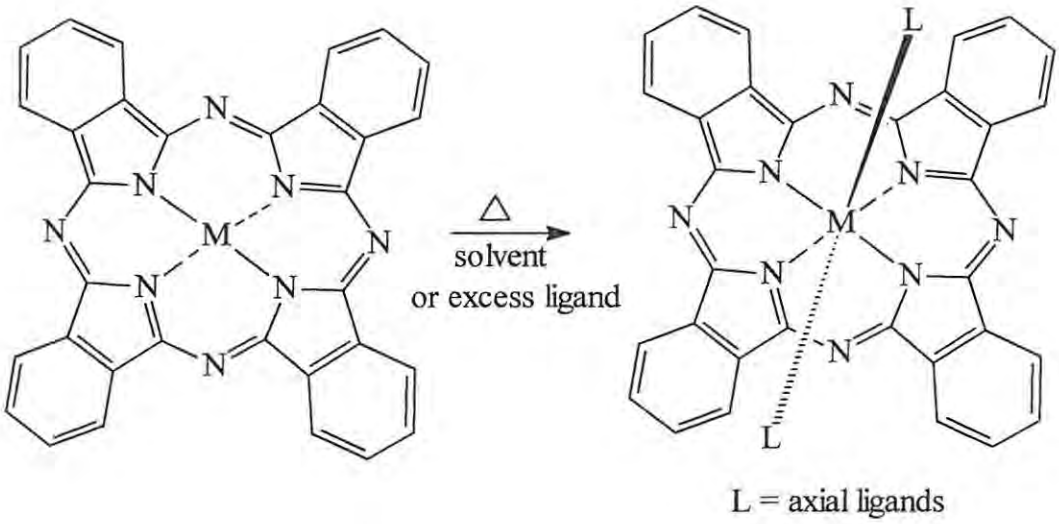

Scheme 5 Introduction of axial ligands in Mpc complexes.

Finally, it is important also to introduce substituents on the periphery of the ring. Derivatives of the Mpc complexes with substituents on the benzene ring have different properties from their unsubstituted counterparts. For example, halogenation of the Mpcs particularly with chloride or bromine atoms on the benzo moiety has the effect of stabilizing one polymorph form over the other, resulting in a bathochromic shift in spectra, and the change in colour from blue to green. Peripheral substitution by alkyl chains, amino groups, crown ethers and carboxyl groups greatly improve the

solubility of Mpcs.[10] The polarity of the Mpc can also be tempered with by introducing substituents on the periphery of the ring. For example, addition of sulphonate groups on Mpc gives tetrasulphonated phthalocyanine (Tspc) complexes which are soluble in aqueous media as opposed to the insoluble non-derivatised Mpcs. The importance of introducing the peripheral substituents is therefore greatly appreciated as it is a tool that can be used to generate Mpcs with desired properties. Scheme 6 shows one of the ways through which sulphonation can be acquired.

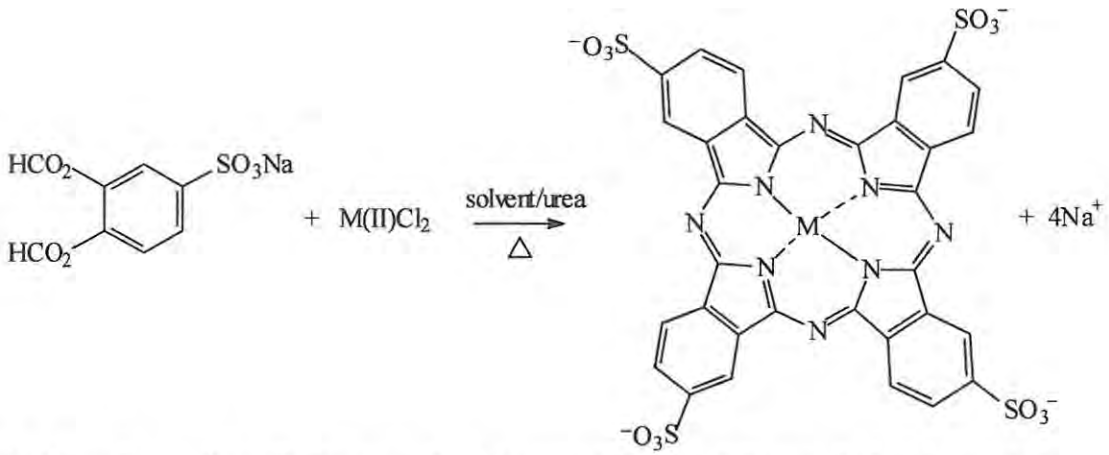

Scheme 6 A synthetic procedure for a metal tetrasulphonated phthalocyanine (MTspc)

A variety of peripherally substituted Mpc complexes can be prepared using substituted phthalonitrile as a starting material using Scheme1.

1.3 Synthesis of tetrapyridinoporphyrazines

Since some applications of the pcs strictly require solubility in aqueous solutions, thus related aza analogs with charged substituents have been of some interest. Alternative compounds of the same structure as the porphyrins and pcs are the tetrapyridinoporphyrazines (tppa), Figure 1.3 (a). Tppa complexes have the same structure as pcs except that the benzene groups have been replaced by the pyridine groups. The tppa molecules can be quartenized by attaching methyl groups to the pyridine nitrogens forming the N,N`,N``,N```-tetramethyltetrapyridinoporphyrazines complex (tmtppa), Figure 1.3(b), which are represented as Mtmtppa when metallated. Mtmtppa complexes are positively charged and are soluble in water.

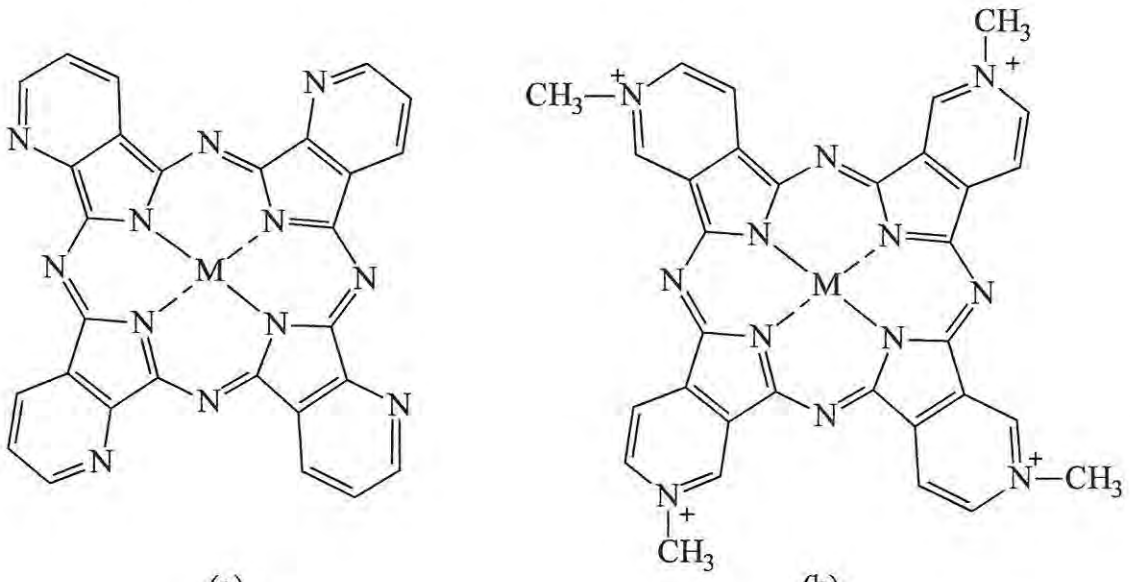

Figure 1.3 Structural representation of (a) metallo 2,3-tetrapyridinoporphyrazine (Mtppa) and (b) N, N`, N``, N```tetramethyl-3,4-pyridinoporphyrazine (Mtmtppa).

Methods of preparation for the Mtppa complexes have not been explored as much as they have been for Mpcs. However, a few methods are known which use template procedures analogous to that of phthalocyanines. The most common methods use α-dicyanopyridine or α-dicarboxypyridine. Mtppa has been using dicarboxypyridine as a starting material,[11, 12] Scheme 7. In this method, concentrated sulphuric acid is used during the purification stage and some Mtppa complexes get demetallated during this process.

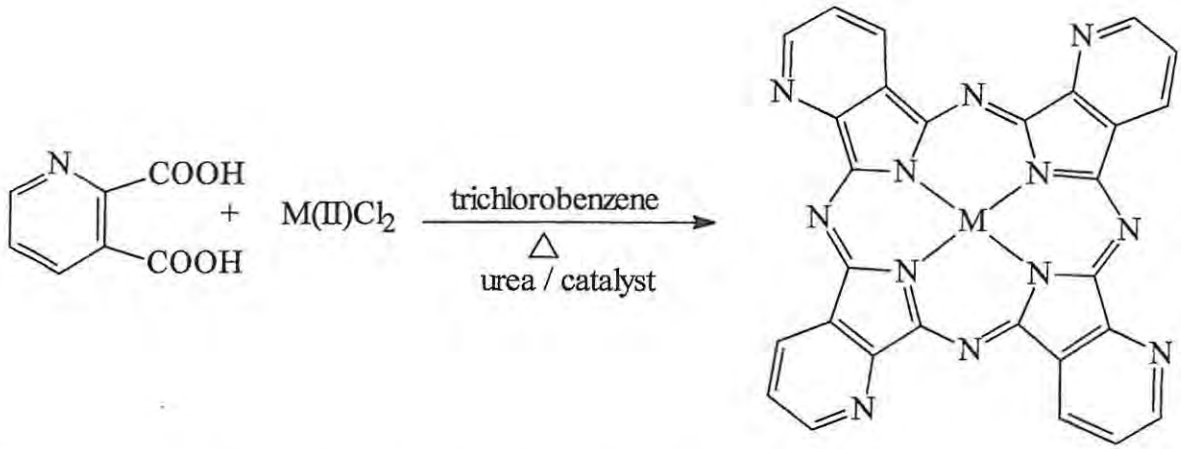

Scheme 7 Preparation of the metallopyridinoporphyrazine from dicarboxypyridine.

Obtaining the dicyanopyridine for use as starting material in a second method for synthesis is the challenging step in the method that uses this template. Danzig *et al.*[13] prepared dicyanopyridine through dehydration of the diamide using phosgene, while some research groups used phosphorus oxychloride instead of phosgene in synthesizing dicyanopyridine. The dinitrile can then be heated with a metal or a metal salt to get the Mtppa complexes.[13] Earlier method reported by Linstead and

co-workers involved the heating of a metal chloride, quinolinamide and ammonuim aminosulphonate but the Mtppa product was impure. Efforts to purify the Mtppa complex by precipitating from acid decomposed the sample.[3] Quartenization of the Mtppa complexes is done by refluxing the Mtppa complexes in dimethyl sulphate under deaerated conditions. The Scheme of this step is shown in section 2.1.4.

The tppa complexes with the extra nitrogens due to the pyridines have different electrochemical properties when compared to the parent pc molecule because of the electron withdrawing capacity of the nitrogen atoms.[14] Mtmtppas like the Mpcs have been shown to exhibit some electrocatalytic behaviour as reported by Sekota and Nyokong.[15] It has been suggested that unlike the water soluble MTspc which tend to aggregate in solution (depending on the level of sulphonation),[16] the Mtmtppas do not aggregate. Aggregation of complexes is not desired when the complexes are to be used as photocatalysts since aggregated species are photoinactive due to fragmentation of the aggregates which compromises the efficiency of the photoreaction.

1.4 Electronic absorption spectra of the Metallophthalocyanines.

The colour that makes the Mpcs so useful is a result of their absorption spectra in the visible region. Phthalocyanines have an absorption band in the red end of the visible spectrum between 600-800 nm, called the Q band, with a weaker absorption in the UV region called the B or the Soret band,

as shown in Figure 1.4.

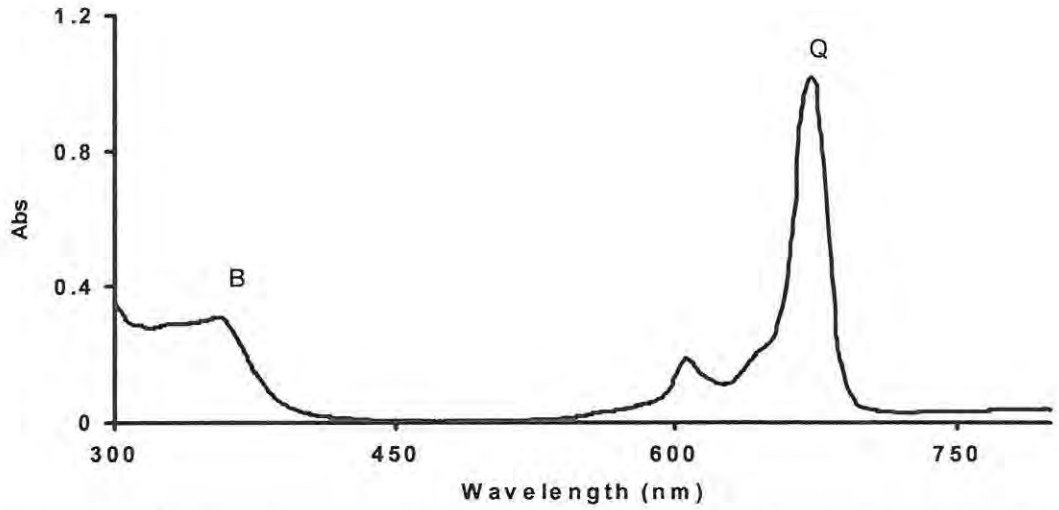

Figure 1.4 Absorption spectra of a metallophthalocyanine, showing the Q band and the B band.

In the case of unmetallated pcs the Q band is split. Metallation changes the symmetry from D_{2h} of H_2Pc to D_{4h} of Mpc in cases where the planarity is maintained. In Mpcs the highest occupied molecular orbital (HOMO) is the $1a_{1u}(\pi)$ followed by the second highest filled orbital, the $1a_{2u}(\pi)$. The lowest unoccupied molecular orbital (LUMO) is $1e_g(\pi^*)$. According to Gouterman's theory[17] that outlines the allowed transitions in the visible region, transitions are possible from the upper filled levels (the HOMO) to the lowest unfilled levels (the LUMO), Figure 1.5. The resultant spectrum shows an intense band, the Q band, which is due to the transition from the HOMO (a_{1u}) to the LUMO (e_g).[18,19] The transition from the a_{2u} to the e_g gives the B band in the absorption spectra.

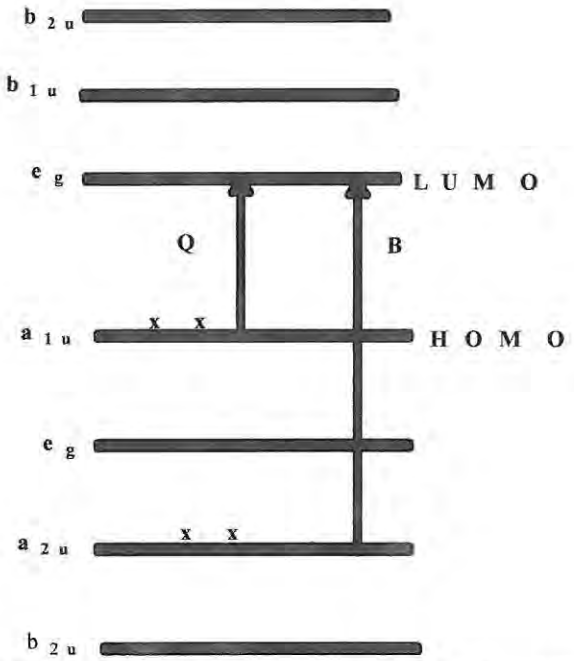

Figure 1.5 Energy level diagram showing, the origin of Q and the B band on the pc absorption spectra.

The absorption spectra maxima vary depending on the nature of the solvent, metal, ring substituents and the axial ligands.[19,20] Some solvents are more co-ordinating than others and may tend to donate electrons to the Mpc forming charge transfer transitions, resulting in new peaks in the spectra. Weakly co-ordinating solvents keep the environment around the Mpc consistent and offer an opportunity to compare the effect of either the insertion of different metals or different axial ligands.

The ring in Mpc complexes contains two negative charges hence the complexes are represented as Mpc^{2-} before reduction or oxidation. Reduction and oxidation of the metallophthalocyanines

results in colour changes of the complexes, this inherently means the details of the transitions also changes. The absorption spectra can be used to characterise the reduction and oxidation products. Singly ring reduced species of Mpcs show a change in colour from blue to purplish blue, with new absorption bands forming near 600 nm and 500 nm due to the formation of Mpc^{3-}, an anion radical that can further be reduced to Mpc^{4-} species. These new absorption bands are much weaker than the bands for the Mpc^{2-} dianion bands because of the perturbations in the ring. It is sometimes possible to tell whether the reduction is a single step process by doing spectroelectrochemistry which allows one to follow the spectral changes as the Mpc is electrochemically reduced.[21] Successive one-electron additions to the LUMO causes reduction at the ring up to Mpc^{-6}.[22] Reduction of the metal in Mpc^{2-} show a shift in the Q band but no considerable change in the intensity.[23]

Oxidation of the ring is also possible through the removal of electrons from the HOMO, leaving a 'sink' into which the lower lying $e_g(\pi)$ orbitals can transfer their electrons. The Q band loses its intensity on formation of the oxidized species and a new broad band is formed between 700 and 800 nm and a broader band near 500 nm. In general, reduced or oxidized Mpc species result in the broadening of the peaks and formation of weaker bands elsewhere in the spectrum. This can sometimes be attributed to the formation of dimers of the reduced or oxidised radicals. A broad band around 700 nm is associated with dimeric species following oxidation of Mpc.[24]

1.5 Application of phthalocyanines.

The properties of Mpc complexes have been studied and reviewed with growing interest because of their very diverse uses.[25] Major commercial uses of pcs are based on three of their characteristic factors namely; their clear intense colour with very strong tinting power, their chemical and heat stability and their fastness to light. Mpc complexes are very stable to heat hence the purification of their impure samples can be achieved by vacuum sublimation and they can be made into thin films for optical applications. Mpc complexes are also used in electrical materials such as optical computer read or write devices because they are electrochromic.[26,27] Due to their diverse redox behaviours, Mpcs have received attention as catalysts in technologically important applications in electrocatalysis,[28] medicine and materials science.[25,29]

1.5.1 Mpc as electrocatalysts.

Mpc are known to be effective homogeneous and heterogeneous catalysts of a wide range of chemical reactions. [30,31,32,33] Mpcs can be used as catalysts in the synthesis of organic chemicals and they have been widely tried as electrocatalysts in many reactions including the catalytic reduction of H_2O_2, O_2 and CO_2.[28, 30,33] The π bond conjugated system of Mpc complexes allow the molecules to act both as electron donors and acceptors. A new interest is growing towards the use of the Mpcs as sensors in biological systems due to their capability to electrocatalyse the oxidation or reduction of biologically important molecules such as NO, and other neurotransmitters, thus allowing the detection of biological compounds at very low concentrations.[34,35,36,37] This catalytic behaviour is

dependent on the nature of the central metal, with the electroactive Mpc complexes of Co and Fe being the best catalysts. Electroinactive metals can be used for making selective electrodes such as the use of lipophylic Sn(IV)pc on a poly vinyl chloride membrane to selectively analyse salicylate.[38]

1.5.2 Energy conversion.

With the growing concern over environmental issues the world as a whole is set on finding alternative energy sources that are environmental friendly and one such source is the solar energy which is very modestly utilized at present. For solar energy conversion photosensitsers that can collect light energy and convert it into excited electrons are needed. This is the same function that is performed by chlorophyll in photosynthesis. The electrons should then be conveyed from the sensitizer efficiently. In the meantime the sensitizer should also gain electrons from a sacrificial donor so as to keep the process continuous. Such a sensitizer would have a dual reducing and oxidising power. Non-transition metal porphyrins and pcs complexes such as zinc complexes have shown some promise in becoming the ideal compounds for this process.[1,39] Mpcs are already used in solar screen, flash fusion toner and in laser thermal transfer all of which involve some form of converting radiation into heat.[40]

1.5.3 Mpcs as dyes

Mpcs are most commonly used as commercial dyes due to their characteristic intense blue or green colour. They are widely used as dyes in ballpoint pen ink and for colouring of plastics and

metallic surfaces such as in paints for cars and in ink jet printers for paper. The use on synthetic fibre and open structure substrates such as cellulose has not been very successful because of the big size of the complexes which can not be incorporated into the fibres. However, conversion of the Mpc dyes into reactive dyes by attaching substituents on the Mpc has enabled the use as wash-fast colours on cotton, which is the most abundant textile fibre used.[40] Mpc dyes are used in electrophotography during imaging, for use in laser printers and photocopiers.[41]

1.5.4 Applications involving the absorption of light by Mpc complexes.

The chromophore property of Mpcs can be changed accordingly by attaching substituents on the ring. Some invisible infrared absorbing Mpc complexes can be obtained by attaching reactive bidentate nucleophiles such as the aryl thiolates or the amino substituents to the pc.[39,40] This modification enables selective absorption of radiation and high solubility in non-polar solvents. The thiol substituted pcs are used in optical storage and for security purposes because they are invisible to human eye but can be electronically detected. The thiol-amino bidentate Mpc complexes have much longer wavelengths and are used in camouflage applications.

Fastness to light is the behaviour that enables pcs to be used as sensitizers. Photosensitizers are molecules or atoms that absorb radiant energy becoming electronically excited in the process. The molecule then passes the energy, without itself reacting, onto another molecule or atom. From the description above we realize that a sensitizer can be catalytic, a necessity for use in optical data storage, energy conversion and as a sensitizer in photodynamic therapy (PDT) which will be discussed

in detail later. Znpcs can be used in washing powders as bleach because they are excellent sensitizers and singlet oxygen producers. The aim of this work is to study Mpcs, Mtmtppas and Mtppas as photosensitizers.

Mtmtppa complexes have not been as thoroughly investigated as their Mpc partners. There have been some reports on the use of Mtmtppa complexes as photosensitizers[14], and as electrocatalysts for the detection of some compounds.[42],[43] It can be assumed that their popularity did not reach the heights of the Mpcs because of their lack of outstanding stability to heat and chemicals. Some of the Mtmtppa are decomposed by simple extraction with high boiling solvents. Washing of the crystals with acid leads to decomposition or demetallation, so getting the right purity of the samples is difficult. They cannot be sublimed satisfactorily and they are very sensitive to pH changes.

1.6 Photosensitization

The use of Mtmtppa as photosensitizers is of interest because they have been claimed not to aggregate in aqueous solutions and therefore are expected to show good photosensitization behaviour. Processes such as PDT need sensitizers that are soluble in water, a character that unsubstituted Mpc lack but which Mtmtppas have.

The process of sensitization is the same for all complexes that do photosensitize. Sensitization in general occur via either a Type I (radical/ radical ion) or Type II (singlet oxygen) mechanism, but two other mechanisms that take place in anaerobic conditions have been reported.[44] Type I and II

mechanisms take place only after the sensitizer has been excited by absorbing a photon. Figure 1.6 represents a modified Jablonski diagram of an organic molecule such as the metallophthalocyanine as the sensitizer (Sens).

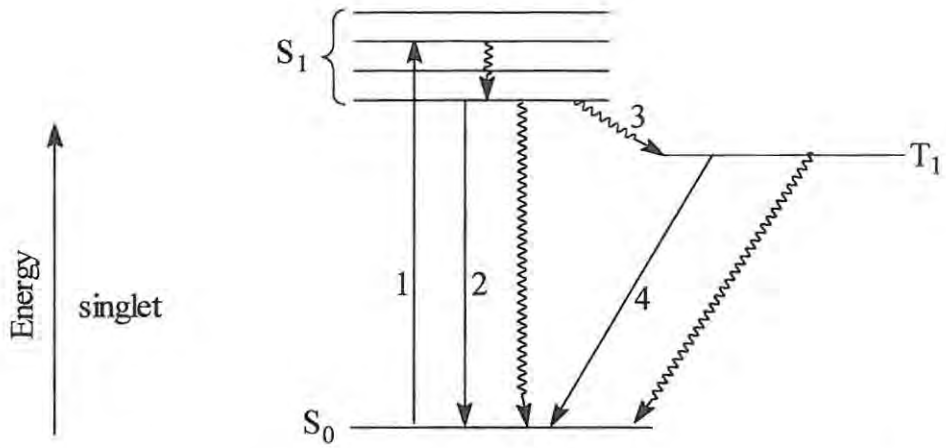

Figure 1.6 Simplified Jablonski diagram showing: 1 = absorption, 2 = fluorescence, 3 = intersystem crossing, 4 = phosphorescence. S_0, S_1, T_1 are the ground state , the singlet excited state and the triplet state respectively and the wavy lines represent non radiative processes.

The sensitizer in its ground state (Sens) through excitation from the S_0 to S_1levels absorbs the photon to produce an electronically singlet excited species, ^{1}Sens*. The fate of the excited species can be any of the following; flourescence (2), non-radiative deactivation (shown as a wavy lines from S_1 and T_1 to S_0) or intersystem crossing (3) giving ^{3}Sens*, Equation 1.[45] Intersystem crossing (ISC) involves a change of spin from singlet to triplet state. The ISC transitions (S_0 to T_1 and also T_1 to

S_0) are not allowed due to spin selection rule.[46] Therefore, the triplet state, with a lifetime in the order of microseconds to milliseconds, is a longer lived species than the singlet excited state due to the spin selection rule in which $T_1 \rightarrow S_0$, is spin forbidden.

$$\text{Sens} \xrightarrow{h\nu} {}^1\text{Sens}^* \xrightarrow{\text{ISC}} {}^3\text{Sens}^* \qquad \ldots 1$$

Triplet state favours bimolecular processes of Type I or Type II where it interacts with a quencher and gets deactivated by other molecules.[25] In Type I process, the mechanism of quenching occurs through the abstraction of H atom from the substrate or the transfer of electrons between the sensitizer and the substrate which results in radicals or radical ions, Equation 2. Radicals or radical ions are very reactive and can react with oxygen to form superoxides radical ions, $O_2^{\cdot -}$. Depending on the pH the superoxides can further protonate to the reactive $HO^{\cdot}{}_2$ radical. All these active forms of oxygen are capable of acting as reactive species which can oxidise molecules in their immediate surroundings.[45]

$$^3\text{Sens}^* \xrightarrow{\text{substrate}} \text{radicals/ radical ions} \xrightarrow{O_2(^1\Delta_g)} \text{oxidation products eg } O_2^{\cdot -} \qquad \ldots 2$$

In Type II mechanism the sensitizer transfers energy to the ground state oxygen to form singlet excited state of oxygen, $O_2\,(^1\Delta_g)$, which then oxidises the substrate, Equation 3 and 4.[45]

$$^3\text{Sens}^* + O_2\,(^3\Sigma_g) \rightarrow O_2\,(^1\Delta_g) \qquad \ldots 3$$

$O_2 (^1\Delta_g)$ + Substrate → Oxidation products ...4

The mechanisms above rely a lot on oxygen and understanding the photophysics of oxygen can help to appreciate them. Ground state electronic structure of oxygen could be described as a triplet state in which the highest occupied orbitals have unpaired electrons. The orbitals are degenerate π* in nature, Figure 1.7.[1]

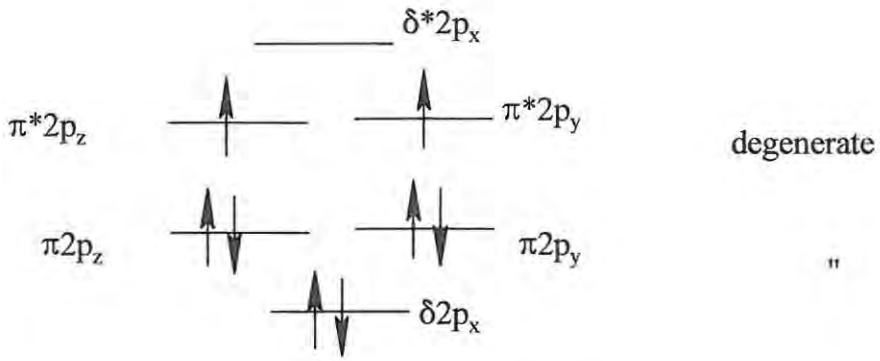

Figure 1.7 Electronic structure of ground state $O_2(^3\Sigma_g)$ excluding the fully filled 1s and 2s bonding and antibonding orbitals.

The above structure is created when two oxygen atoms come together so that their separate atomic orbitals overlap resulting in bonding and antibonding orbitals. Filling the orbitals with electrons starting from the lowest energy orbital fills the s-orbitals and leaves only the four p orbitals contributing in the bonding of the atoms. Eight electrons are then left to be distributed in the three p bonding and the three p antibonding orbitals. The resultant is the formation of one δ orbital

containing two electrons, two π orbitals with two electrons each and two unpaired electrons in the two π^*, antibonding molecular orbitals.

The two degenerate half filled molecular orbitals of the oxygen are the ones that make oxygen such a reactive species.[47] They create a "sink" for electrons which explains why oxygen will accept the electrons from the sensitizer during photosensitization. Accepting electrons into the half filled antibonding orbitals is one way of getting an excited state of oxygen, but the most common way is through pairing of the electrons in the highest level and fitting them into one π^* orbital forming O_2 ($^1\Delta_g$). The O_2 ($^1\Delta_g$) lies 94 kJmol^{-1} above the ground state of O_2 ($^3\Sigma_g$) requiring very small amounts of energy for the transition from one form to the other. Exposing O_2 ($^3\Sigma_g$) to energy radiation of 1270 nm which corresponds to the energy gap between the two oxygen species does not give O_2($^1\Delta_g$) because oxygen is transparent at this wavelength.[1] The transition from O_2 ($^3\Sigma_g$) to O_2 ($^1\Delta$g) can be achieved through photosensitization whereby O_2 ($^3\Sigma_g$) quenches the sensitizer by absorbing its triplet state, ^{3}Sens*, energy. For quenching to occur, the triplet excited state of the sensitizer must lie slightly above the O_2 ($^3\Sigma_g$) orbital in energy. Radiative or non-radiative deactivation of the excited oxygen will occur following the formation of O_2 ($^1\Delta_g$), while the molecule of the sensitizer generally returns unchanged to its ground state.[48]

Formation of the singlet oxygen is the most accepted mechanism of sensitization, however, it is possible to have both Type I and Type II mechanisms operating simultaneously. Reactions that utilize the process of sensitization include photodegradation of wastes and PDT.

The main aim of this thesis is to study the photosensitizing abilities of some Mpc, Mtppa and Mtmtppa complexes towards the generation of O_2 ($^1\Delta_g$) as the first step towards determining their effectiveness as photosensitizers for PDT.

1.7 Photodynamic therapy

1.7.1 Background on photodynamic therapy

The use of light in medicine is a known phenomenon which was first reported by Dane and Finsen[1] in the late 19th century when they showed that the facial lesions (*Lupus vulgaris*) from tuberculosis could be treated with ultra violet light.[49] Subsequent discovery on how microorganisms react to ultraviolet light and the treatment of rickets with light opened another door into the science of light and healing. The advent of lasers in the past two decades shone light on yet a more spectacular but very helpful device in surgery. Not only are lasers used as scalpels but now also in the treatment of cancer as energy sources.

Cancer can be described as uncontrolled growth and spread of abnormal cells, and it tops the charts in the United States as a killer disease.[50] Cancer is often detected through a growth of a malignant tumor which has the potential to grow and spread as long as it is not prevented from doing so. Causes of cancer vary very widely and thus it cannot be totally prevented by just avoiding the causes which range from exposure to chemicals, radiation, certain viruses, genetic inheritence, hormones and many others including just the lifestyle adopted.[51] Fighting cancer thus still entails the

prevention of the spread of the malignant tissue and the killing of the abnormal cells which can be primarily achieved by either radical surgery, radiotherapy or chemotherapy. Some degree of success can be achieved with these methods when used either individually or combined. However, these methods have a common shortfall that is of great concern to the scientists in that they destroy indiscriminately both the normal and the tumour tissue. Oncology has had to re-design its goals into, not only to find possible cancer cures, but also a selective tumour destruction. Photodynamic therapy has attracted much interest since it has a potential of selective tumour destruction.

Photodynamic therapy involves the use of red light usually from a laser in conjunction with light sensitive drugs, the photosensitizers, in an oxygen rich environment to combat a disease. The healing effect in PDT is produced via the light induced chemical reaction of the photosensitizer which produce a cytotoxic agent. Neither light alone nor the drug alone has independent biological effect.

The steps involved in treatment of cancer with PDT consists of the drug (the sensitizer) being administered intravenously to the patient, followed by an incubation period of 48-72 hours during which selective uptake or retention of the photosensitizer occurs in much higher concentration in malignant tissues than in normal tissue. Laser light tuned to the absorption maximum of the sensitizer is introduced via fibre optics and it is directed to the target tissue for varying lengths of times depending on the depth and location of the tumour. In the presence of this light, the sensitizer is activated, transferring the energy in a photochemical reaction, to produce a cytotoxic species through

either Type I or Type II mechanisms. One such species is singlet oxygen which participates in many photo-oxidative processes by interacting with proteins and lipids, hence destroying the cell membranes, the mitochondria, plasma membrane and other biological molecules.[52] Figure 1.8 shows the depiction of the PDT protocol.[53]

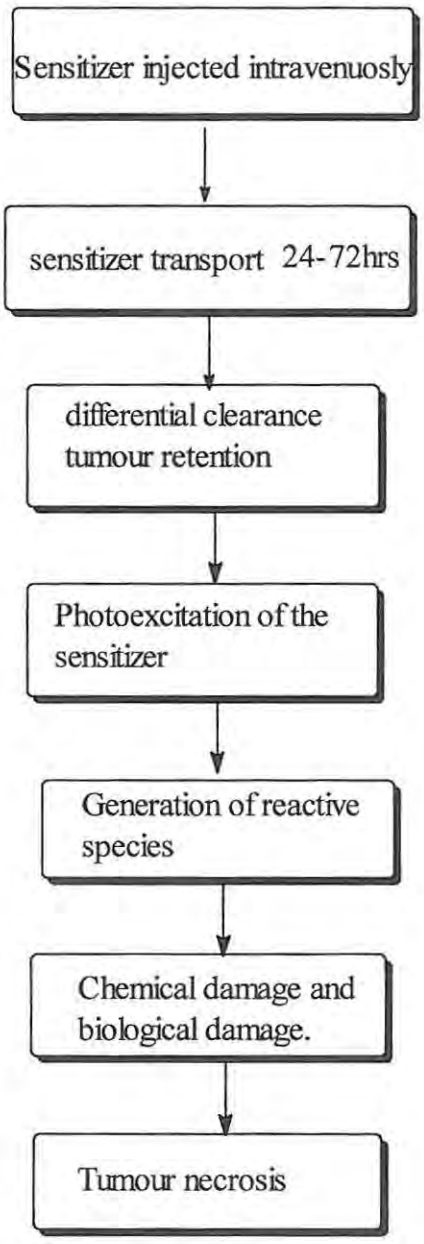

Figure 1.8 The protocol of events in PDT.

PDT has the following advantages over the already existing therapies; the recovery and regeneration of normal tissue after treatment is good, it can be coupled with other conventional cancer therapies and it allows *in-vivo* detection of the sensitizer which permits monitoring of the concentration of the drug during treatment. Detection of sensitizers is possible during surgery, on the body surface and also with endoscopic methods *via* their fluorescence when exposed to the blue light from a krypton laser source.[54]

Success of PDT relies on the quality of the sensitizer. A list of requirements for a good sensitizer may be summarised as follows ;[55]

(a) It must be red-light absorbing. The body tissue is generally transparent to red light therefore a substance embedded in the tissue that absorbs red light helps improve the amount of light that can penetrate the tissue. Increasing the wavelength of absorption from 630-700nm almost doubles the depth of light penetration.[56] Again, at the wavelength of the red light, enough energy is present to promote production of the singlet oxygen which is suspected to be the main destructive species.

(b) It must be a pure chemical compound and it must have a reproducible, preferably easy, synthetic route. This helps when conducting efficacy tests, for running the structure activity relationships (SAR) and for determining lethal doses.

(c) It must be non-toxic and it should not react in the absence of light. If the sensitizer only reacts when activated by light of a specific wavelength, then the threat of phototoxicity is also removed.

(d) It must be preferentially retained by the tumour. A sensitizer that is selectively retained in the tumour reduces the chances of destruction of the normal cells during treatment. In cases where the drug fluoresces, the tumour can be located and traced, this can even serve as a diagonistic device. (e) It must clear from the body rapidly after use. When a sensitizer is retained within the body for a long time, it makes the whole body light sensitive and prone to 'sun burns' even by ordinary light from a tungsten bulb, photocopiers and light used by dentists.

(f) It must be an efficient producer of its excited states and its triplet state must be long lived. The mode of action involves the excited states which, if efficiently generated could result in higher production of the cytotoxic species.

(g) It must be soluble in the body's tissue fluids. Solubility in the body's fluids helps to transport the sensitizer to the tumour and also to get it into the tumour, thus a balance between lipophilicity and hydrophilicity should be attained. The drug has to leave the body by leaching out during excretion so it must be soluble in water. It was realized that very high solubility in water results in a condition whereby the drug cannot stay in the body long enough for reasonable quantities to accumulate, so retention could be improved by making the drugs to also be fat soluble.

1.7.2 The history of porphyrin-based sensitizers

Finding a drug that fits the model of an ideal photosensitizer is the challenge to most chemists. Even sensitizers that have already been approved still fall short on some of these expectations. Of

the substances that have been used as photodynamic sensitizers, porphyrin-type molecules, were the first used. The emergence of the idea of phototherapy started when phototoxicicty caused by hematoporphyrin derivative (HpD) resulted when Meyer-Betz[57] had injected himself with it. He experienced no ill effects until he exposed himself to sunlight, whereupon he suffered extreme swelling which lasted for months.[57] This was followed by the discovery that porphyrins accumulated in malignant tissue. It took some 50 more years to realize that the two ideas combined could be used in the treatment of cancer.[1]

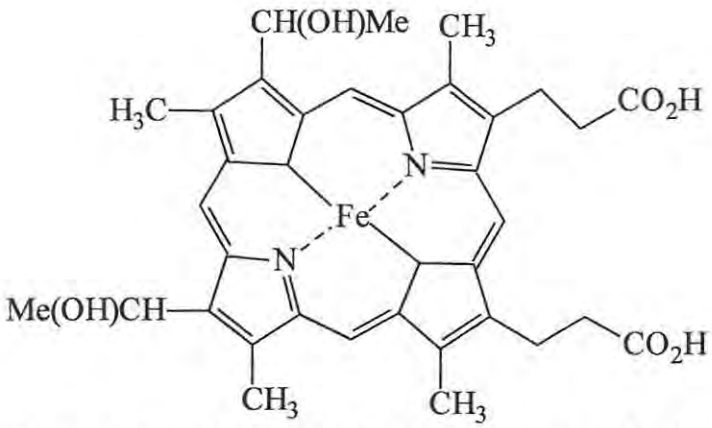

Figure 1.9 Structure of soluble haematoporphyrin.

HpD was found to be retained by malignant tissue. HpD is a complex mixture of oligomers, monomers and dimers derived from heamatoporphyrin (iron protoporphyrin), Figure 1.9. HpD can be obtained by extracting heam from blood, followed by acid hydrolysis using HBr and acetic acid. Purification is carried out by reacting the extract with acid, followed by alkali hydrolysis of the

acetoxy groups giving the HpD mixture. Although HpD is retained by the tumour, appreciable amounts of it are also retained in the skin. When used as PDT sensitizer HpD is slowly cleared and so it makes the body light sensitive for up a to month after application. HpD is a mixture of compounds which cannot be reproducibly obtained from batch to batch and thus it becomes impossible to get the same PDT properties from different samples. HpD`s absorption band in the red region is at 630nm which is not the wavelength that produces best absorption of light by the tissue The region for light absorption by the tissue that produces maximal penetration into the tumour occurs at 650-750nm.[58] For these reasons, HpD was not found to be a completely ideal sensitizer. A purified form of HpD known as Photofrin which is still a mixture has been made and has gone commercial. Like HpD, Photofrin still induces photosensitization, it is not a pure compound thus its production is difficult. Because Photofrin is obtained as a mixture of compounds, interpretation of its clinical and preclinical results is hard. Photofrin absorbs at 630 nm, in the red part of the optical spectrum.

1.7.3 Second generation sensitizers

To overcome the disadvantages of HpD a different breed of sensitizers known as second generation sensitizers were synthesized. The aim was to get better results through shifting the absorption to longer wavelengths to ensure that the chromophore had the desired absorption properties. This was chiefly achieved by either extending the macrocycle of the porphyrins to

produce the phthalocyanines, pentaphyrins, porphyrin vinylogues and many others or by reducing the porphyrin ring to make the chlorins.[1, 38] The second aim when designing the second generation sensitizers was to get a pure, stable compound. Phthalocyanines have an added advantage over the other second generation sensitizers in that they have a lower absorption in the ultra violet region of the spectra and are therefore less likely to cause phototoxicity.

Many complexes were designed and some were found to be promising enough to go into clinical trials. A few of the second generation drugs that are in clinical trials include, benzoporphyrin, tin etiopurpurin and *m*-tetrahydroxyphenylchlorin.[55,59] Benzoporphyrin derivative, Figure 1.10, a monoacid with two isomers which do not have the same PDT efficacy, is on trials in Canada.

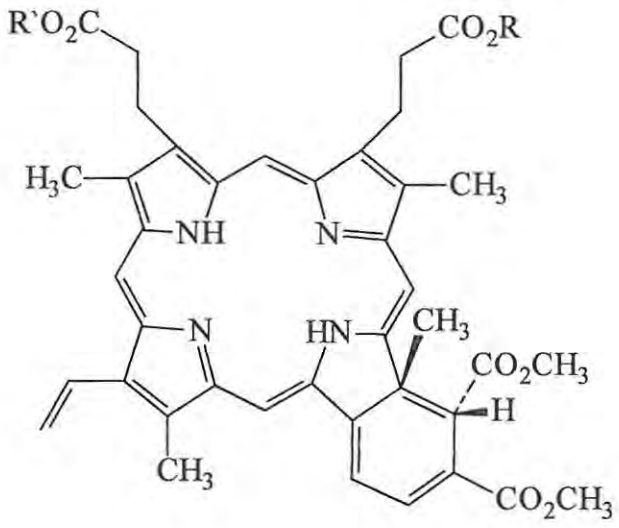

Figure 1.10 The structure of benzoporphyrin derivative monoacid. R and R` are H and CH_3, they are interchangeable but always a mixture.

Benzoporphyrin is in phase I/II trials for treatment of skin cancer and in clinical trials for basal cell carcinoma and metastatic skin lesions. The advantages of benzoporphyrin over HpD are that it has a longer wavelength absorption maxima at 690 nm and it shows no skin sensitization. The disadvantage is that it clears too quickly from the system thus accumulation in cancer might not be optimum by the time it is treated with light. Synthesis of benzoporphyrin results in two isomers of which only one is effective, unfortunately it is difficult to separate the two isomers because they have the same solubility.

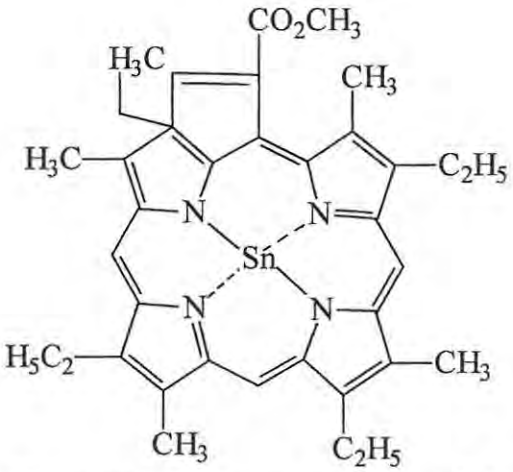

Figure 1.11 The structure of tin etiopurpurin.

Tin etiopurpurin (also called Purlytin), Figure1.11, is a metal based porphyrin sensitizer in phase II trials for prostrate cancer in United States of America.[58] Purlytin is also in preliminary trials for basal cell carcinoma and breast cancer, with 95% response observed in patients with basal

carcinoma.[58] It has also been tried for Kaposi`s sarcoma and the majority of the patients responded positively.[58] The problem with the use of Purlytin is its low solubility in aqueous media thus, it has been formulated into liposomes for administration, but this leads to the formation of toxic material in the dark. Purlytin has delayed phototoxicity which can be observed as late as two months after treatment. The advantages of Purlytin are; the availability of a diode laser that releases light within the limits of the drug and that it absorbs at longer wavelengths, 650 nm, hence deeper penetration into the tissue than Photofrin.

m-Tetrahydroxyphenylchlorin (*m*-THPC, Foscan), Figure1.12, is a very effective drug with very low doses needed for activity.

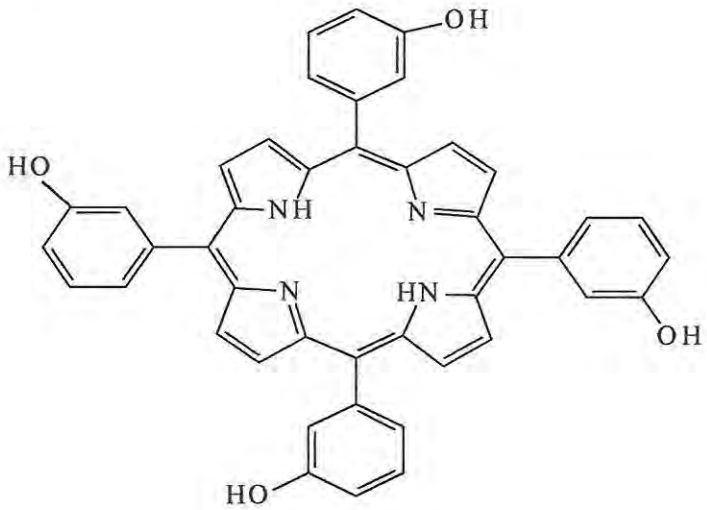

Figure 1.12 The structure of *m*- tetrahydroxyphenylchlorin.

Synthesis of Foscan is easy, it has a longer absorption wavelength (650 nm) than photofrin and is good on early stage tumours.[58] The drug however causes photosensitivity which lasts for extended periods and yet it takes about a week to accumulate enough in the desired zones after introduction before light treatment. Foscan has been used to treat patients with squamous cell carcinoma of the throat, superficial esophageal tumors and bronchial tumors. Foscan is in phase II /III clinical trials for the neck and head cancers in Europe and the United States of America.[58]

Many other sensitizers are in clinical trials and some are summarised in Table 1.[55,56,60,61,62]

Table 1 Sensitizers in clinical trials.

Compound	Disease treated	Company or country
benzochlorins	age related mascular degeneration	USA
lutetium texaphyrin	metastatic brain tumours, breast cancer artherosclerotic plaques	USA
ALA	skin, stomach, mouth, bladder, colon cancers	USA
hexyl ether derivative of pyrophephorbide-a	esophageal cancer	USA
purpurin-18-alkyl amides		USA
monoaspartyl chlorin e_6	skin cancers	Meiji Seika

Mpc complexes which have been tried on biological media as sensitizers include AlTspc[52], Znpc,[60, 63] Gepc,[59,64] Sipc,[65] Rupc[56] and some naphthalocyanines.[66] The presence of a metal in the macrocycle has been observed to cause an increase in the production of singlet oxygen in pcs. The nature of the metal helps to determine the efficiency of the sensitizer. The metal chosen must increase the chances of intersystem crossing for the sensitizer, and must increase the life time of the excited triplet state. Paramagnetic metals do not have this desired effect,[67] thus it is not surprising to note that so far, all the metals favoured are diamagnetic[68] i.e Aluminium(III), zinc(II), germanium(IV), and silicon(IV) pc complexes[69] have shown some sensitizing activity.

Since the Mpcs are insoluble, the complexes have to be substituted to improve their solubility. The solubility of Mpcs is improved by attaching sulphonate or carboxylate moieties on the ring peripheral position to produce negatively charged sensitizers or alkyl ammonium groups to make positively charged adducts. Metals like Al, Ge, Ru and Si which have higher coordination abilities can carry axial ligands that are used to reduce aggregation which can sometimes result from adding the sulphonate groups peripherally. Water soluble analogs of Mpc achieved through sulphonation are the most studied complexes for possible use in PDT so far. Mono or disulphonated Mpcs were found to be the most effective.[70] The higher the number of sulphonate substituents, the more hydrophilic the complex.[53]

The di-sulphonates which are the most efficient sensitizers present a problem of existing as a complex mixture of isomers. When preparing disulphonated aluminium phthalocyanine ($AlPcS_2$), the

sulphonate groups can be accommodated in sixteen different ways giving sixteen regioisomers.[52] The ratio of regioisomers that result cannot be synthetically controlled from batch to batch. This becomes a problem for the synthesis of a pure sample, since different combinations give different efficacies. Reverse phase high performance liquid chromatography (HPLC) separation of the isomers is possible[71] and yet they are not separated in practice because the efficiency of the mixtures has been observed to be higher than that of individual isomers.[72] $ClAlPcS_2$ with sulphonate groups located on two adjacent pyrrole rings have been reported to be particularly efficient photosensitizers,[69] probably because it does not aggregate at all even at high concentrations as reported by Dhami and Phillips.[71] However, in Russia the sodium salt of $AlPcS_4$ is at the end of second stage of clinical trials as a PDT sensitizer under the name Photosens.[70] Photosens is used for treatment of skin, intracutaneous metastases of breast cancer, pharynx, mouth, oesophagus and stomach.

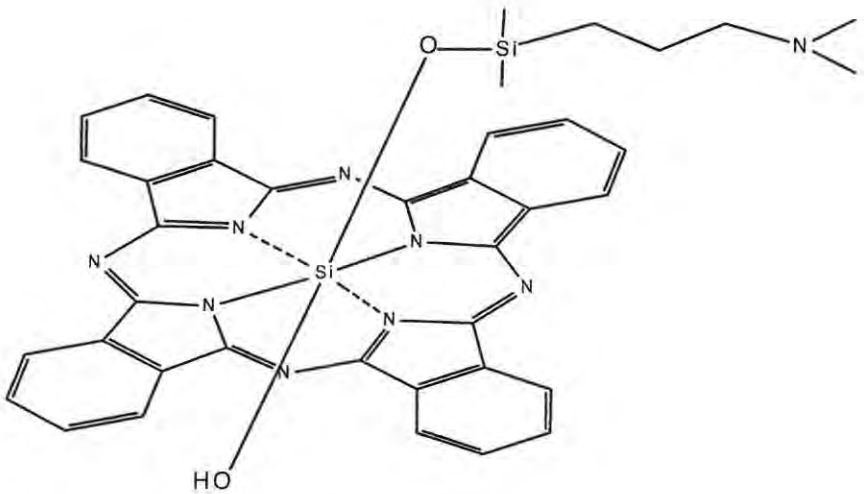

Figure 1. 13 Structure of Pc4.[65]

Amine bearing Sipc derivatives have been investigated for their PDT sensitizer potential.[65] Pc4, with a monoaminosiloxy group, Figure 1.13, and other Sipc derivatives were found to be as efficacious as Photofrin in *in vivo* PDT studies and thus, Pc4 is in advanced clinical trial stages. Amine bearing silicon pc complexes are taken up well by tumour cells and are cytotoxic when irradiated with light at 675 nm, a higher wavelength and better tissue absorption than when using Photofrin. These Sipc complexes can be prepared in high purity and they were found to cause much less photosensitivity than Photofrin at therapeutic doses. The effectiveness of the sensitizer depends on the drug delivery mechanism, its coordinating abilities to both the hydrophobic and the hydrophilic structures it passes through in the body.[54,73]

Ge(IV)pc derivatives with cholesterol, cholestan and long fatty acids residues as axial ligands have been synthesized and their phototherapeutic properties were tried on tumour bearing mice. Good phototheraupetic efficiency was reported at very low drug doses.[64] The Gepc derivatives were selectively retained by the tumour although to a lesser extent when compared with liposoma Znpc sensitizers, and the Gepc complexes were released relatively fast from the body promising not to lead to phototoxicity.

As already stated the energy of singlet oxygen is about 94 KJ/mol above $O_2(^3\Sigma_g)$ so the energy of the triplet state of the sensitizer has to be higher than this value to allow generation of a singlet oxygen.[52] When the Q band wavelength of the sensitizer is too high the possibility of the energy being too low for the generation of singlet oxygen exists. Naturally occurring chlorophyll derivatives

and naphthalocyanines whose absorption lies way into the near infrared light region have a problem of generating low quantities of singlet oxygen because their triplet state energy lie below that of singlet oxygen. However, molecules that possess such status may still be good sensitizers through the Type I mechanism.

Treatment of tumours deficient in oxygen is still a problem. Mechanisms for using pcs as sensitizers in such environments have been suggested whereby the cytotoxic hydroxy radical is generated through direct photooxidation of water by the sensitizer, Equation 5. This can be achieved by making a pc with enhanced oxidation powers.[44]

$$Mpc + H_2O \xrightarrow{h\nu} OH^{\cdot} + H^{+} + Mpc^{\cdot -} \qquad ...5$$

Photoproperties that need to be considered when designing a sensitizer include improving the efficiency of producing singlet oxygen, quantitatively described as the quantum yield of singlet oxygen (ϕ_Δ). ϕ_Δ is a measure of how much singlet oxygen is produced per quanta of light absorbed, for usable sensitizers this value ranges from 0.2 - 0.8. Quantum yield of any photo-process is to a photochemist what overall yield is to an organic chemist. The values of the quantum yields for singlet oxygen production give an approximation of what to expect in *in vivo* applications. Some molecules like the bacterichlorophyll that have ϕ_Δ as high as unity, have proved not to be such good sensitizers in *in-vivo* studies.

The fate of an excited triplet state is not just the production of singlet oxygen, thus the quantum yield of the competing processes such as phosphorescence or non radiative processes must also be determined. Also, the quantum yield of fluorescence must be determined since fluorescence can be used to probe the position of the dye in the body,[74] but high efficiency of the fluorescence process is not desired as it would lead to lower quantum yields of the triplet state of the sensitizer. Table 2 gives photophysical properties that have been determined for some Mpc complexes. These values are solvent dependent.

Table 2 Photophysical data on Mpc sensitizers in methanol. Where ϕ_F and ϕ_τ represent quantum yields of fluorescence and triplet state of the photosensitizer, respectively and ϕ_Δ is the singlet oxygen quantum yield obtained. *R= phenyl ring R`= O-$(CH_2)_{17}CH_3$.[76]

sensitizer	λ_{max}	ϕ_Δ	ϕ_τ	ϕ_F	References
$AlPcS_2$	675	0.2	0.3	0.4	[75]
$ZnPcS_2$	665	0.52	0.46	0.3	[53]
Photofrin	628	0.3	0.6	0.1	[75]
*Gepc[OSi(R_2)R`]$_2$	667	0.39	0.38		[76]

It has been suggested that some molecules that are produced from the tumour cells through either Type I or II methods can revert back to the sensitizer and oxidise it. This leads to the "self destruction" of the sensitizer in a process called photobleaching. Quantum yields of photobleaching allow for the prediction of the photostability of the sensitizer, knowing exactly whether to expect

enough sensitizer to remain to produce the cytotoxic species after exposing the molecules to light. Photostability depends on many factors including the structure, concentration, nature of solvent and intensity of the light. High photobleaching quantum yields are not desired, however some degree of photobleaching helps to clear dye molecule from the body resulting in reduced phototoxicity.[54]

Only a few reports of the use of Ge[64] and Snpc complexes for the generation of $O_2(^1\Sigma_g)$ have been published, yet non-transition metals are expected to be good sensitizers. Also porphyrazines have not been fully explored for use in generation of $O_2(^1\Sigma_g)$. Positively charged pcs are better than negatively charged pcs in the generation of $O_2(^1\Sigma_g)$,[73] hence the aim of my study is to determine the $O_2(^1\Sigma_g)$ quantum yields of the non-transition metals Ge, Si, Sn and Zn tmtppa complexes which are water soluble and positively charged.

1.7.4 Other PDT applications.

PDT can be applied for other purposes other than cancer cure. PDT has been used to treat artherosclerotic plaques.[60] When plaque builds up inside the walls of the arteries, it can slow down the flow of blood considerably resulting in the hardening of the arteries. As in tumours, sensitizers were found to accumulate in plaque. Exposure to light disintegrates the plaque without causing any damage to the neighbouring healthy tissue. Lutetium texaphyrin (Lu-Tex) sensitizer has been used for such purposes.[60] Using Toluidine blue, total disinfection on extracted teeth has been achieved.[77] This suggest that mouth sterilization can be done with the teeth still in place which would produce healthy teeth that can still regenerate the bone, and tooth fillings will be a thing of the past.

5-Aminolaevulinic acid (ALA) is itself not a senstizer but a precursor in the natural biosynthesis of haemoglobin, an iron based porphyrin.[62,75] Through homeostasis the body regulates the amount of ALA to be produced by a feedback mechanism. The high levels of haemoglobin can reduce the production of an enzyme ALA synthetase which is responsible for the production of ALA. Iron chelators fed into the system together with excess ALA inhibits this feedback mechanism. Thus leading to a continuous process that produces the porphyrin structure in heam, protoporphyrin (PPIX), which is devoid of the metal. PPIX is a sensitizer with distinct fluorescence characteristics, it can therefore be probed easily within the body. PPIX fluoresces more in malignant tissue than in normal cells which means it is selectively produced or retained by the former. Exposing the tumour with PPIX to light has resulted in positive PDT therapy.

PPIX levels were also found to be higher in non-malignant inflammatory and proliferative lesions, which makes ALA a suitable candidate for treating rheumatoid arthritis and eye diseases using PDT. ALA has also been included in topical creams for treating pimples and other dermatological problems successfully. An advantage of using ALA comes from the fact that the resultant sensitizer clears within hours of production so it has very limited phototoxicity potential and it does not take long to generate desirable levels of PPIX after the introduction of ALA.

PDT has been used to treat age-related macular degeneration, the most common cause of blindness in older people. Vertoporfin[58] has had extensive use in such applications. PDT inactivation of viral infection has been investigated with Photofrin. PDT can be used to treat microbial infections

of the blood and psoriasis. The potential of treating contaminated blood using PDT is under investigation.[51, 58, 62]

1.8 Theoretical background on electrochemistry

Electrochemistry as an analytical tool has many techniques, in this section cyclic voltammetry and bulk electrolysis will be discussed as techniques used in characterisation of the compounds.

1.8.1 Cyclic voltammetry

Cyclic stationary electrode voltammetry often referred to as just cyclic voltammetry (CV) is the most commonly used electrochemical technique. It offers a rapid scanning of the electroactive substance to locate the redox potentials.[78] CV involves linearly scanning the potential on a stationary, solid working electrode made of either platinum, gold or carbon in an unstirred deaerated solution. Dry nitrogen gas or argon are the inert gases normally bubbled through to achieve quiescent, oxygen free atmosphere before the scanning.

The method is termed cyclic because the potential is increased from an initial value E_i to a final value E_f then back to E_i again. When the potential is scanned positively, anodic current response increases rapidly as the potential characteristic of the redox system approaches, until a peak current is obtained when the species gets oxidised. On reversing the scan direction the oxidation product that would have accumulated around the electrode gets reduced and a similar response of a cathodic peak is observed at the potential at which the product gets reduced, hence the term cyclic voltammetry. Figure1.14 shows typical response current-potential plot, a voltammogram, produced for a reversible system.

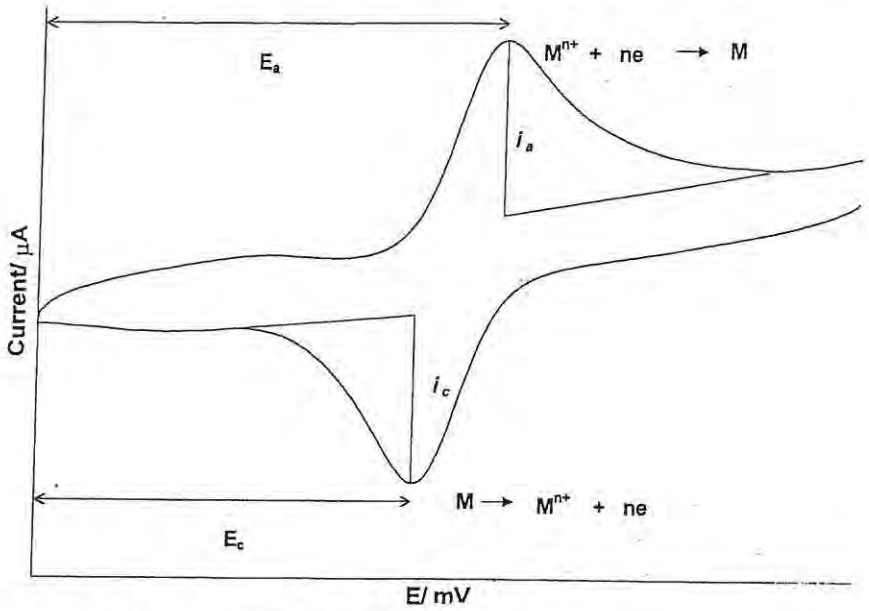

Figure 1.14 A typical cyclic voltammogram

Important parameters from a voltammogram are the anodic peak current, i_a, the cathodic peak current, i_c the anodic potential E_a and the cathodic potential E_c. These can be used to obtain information on the reversibility of the reaction and the stability of the products hence CV's ability to rapidly provide information on the thermodynamics of the redox processes. A redox couple in which both the reduced and the oxidised species are stable and allow a rapid exchange of electrons with the working electrode is called an electrochemically reversible couple.[79] Measurement of the potential difference between cathodic and anodic potential (ΔE_p) in volts and applying them to Equation 6 can be used to characterise a reversible redox system.

$$\Delta E_p = E_a - E_c = \frac{RT}{nF} = \frac{0.058}{n} \text{ at } 25\,^{\circ}\text{C.} \qquad \ldots 6$$

where n is the number of electrons transferred, F the Faraday constant, R the gas constant and T is the temperature in Kelvin. This separation is independent of the scan rate for a reversible couple. For reversible systems the ratio of the peak currents is unity, and i_c and i_a are propotional to the square root of the scan rate according to the Randle-Sercik equation, which applies at 25°C,[80] Equation 7.

$$i_p = 2.69 \times 10^5 \times n^{3/2} AD^{1/2} Cv^{1/2} \quad \ldots 7$$

where n = moles of electrons, D = diffusion coefficient, C = bulk concentration, A = area of the electrode and v = the scan rate. A common approximation for a reversible system is given in Equation 8.

$$E^\circ \sim E_{1/2} = \frac{E_a + E_c}{2} \quad \ldots 8$$

Where E° is the standard potential for a redox reaction. $E_{1/2}$ is characteristic potential of a species. It is possible to observe multi-electron-transfer processes which will have several distinct peaks if there is no overlap between the potentials of the individual redox steps.

Irreversible systems are a common occurrence in organic complexes. These are redox reaction that have slow electron exchange with the working electrode. Totally irreversible systems are

characterised by voltammograms with a single oxidation or reduction peak without the reverse peak current. In some cases the peaks are normally widely separated and reduced in size. Totally irreversible systems also show a shift of the peak potential with the scan rate and the separation of the peak potentials is greater than 0.058/n volts and is independent on the scan rate.

Cyclic voltammetry can be carried out using micro fibre electrodes as well. Micro electrodes are of the micrometer dimensions or smaller. They have a high application as probes in biological analysis. During an electrochemical process, ions move by diffusion, stirring and migration. Without stirring and adding an electrolyte to minimize migration, a diffusion controlled system results. The diffusion of molecules to the microelectrode can be described by Fick`s second law, Equation 9;

$$\frac{\partial c}{\partial t} = D\nabla^2 C \qquad \ldots 9$$

Where C is the concentration, D the diffusion coefficient and ∇^2 is the Laplacian diffusion operator. Diffusion operator changes with the form of geometry of the electrode surface.[81] For a microfibre electrode the surface is not planar and its diffusion expression can be used to describe current as Equation 10;

$$i_t = nFADC\left(\frac{1}{\sqrt{\pi Dt}} + \frac{1}{r_o}\right) \qquad \ldots 10$$

where r_o is the radius of the electrode and t is the experimental time. n, F, D, A and C as defined for

Equations 8 and 9. At long experimental times, current behaviour approaches a non zero steady state value represented by Equation 11;

$$i_{t=\infty} = 2\pi nFr_0DC \qquad ...11$$

In steady state situation, the current obtained is time independent and this can be observed during low scan rates using microelectrodes. Voltammograms can be obtained even with low concentrations of the supporting electrolyte if the diffusion layer is larger than the electrode size. Generally the casing for the microelectrode is more bulky compared with the size of the active tip, thus the reference electrode is far from the working electrode and high resistance is generated resulting in distortions in the shape of the voltammogram. Very low scan rates can be applied when using microelectrodes and this helps to separate the potentials that overlap in multi-electron transfer systems.[15]

1.8.2 Bulk Electrolysis

Electrochemistry can be carried out to generate the product for further probing with a different technique. To carry out bulk electrolysis particular care is taken to ensure that the ratio of the area of the working electrode to the volume of the solution is very large, big electrodes are therefore used. The oxidation and the reduction occur in different compartments in order to generate products. To ensure maximum movement of particles, the solution is stirred.

1.8.3 Electrochemical properties of metallophthalocyanines.

In this work, electrochemical data is used to explain some of the observed photochemical behaviour of the Tmtppas, hence an overview of the electrochemistry of Mpc follows. Metallophthalocyanines are highly electroactive due to their ability to accept or donate electrons without the destruction of their structure, or a compromise to their stable stature. In solution, their electrochemistry show multiple often reversible processes. Mpcs have two localities on which redox reaction can occur, the metal centre and/or the phthalocyanine ring.

The pc ring is a dianion which can undergo further oxidation into a singly charged ion or an uncharged ion in the order; $Pc^{2-} \rightarrow Pc^{-} \rightarrow Pc^{0}$. The ring can also be reduced by four successive electron reductions from Pc^{2-} to Pc^{6-},[82] as discussed earlier in section 1.4. For some transition metal pc complexes, the metal centre can be redox reactive depending on the solvent, the substituents, the electrolyte and the metal itself. Mpc complexes with metal centres prone to redox processes have their occupied d-orbitals lying between the HOMO and the LUMO gap of the ring. Examples of redox active Mpcs are Copc, Fepc, Mnpc and Crpc.

Non transition metals pcs are redox inactive at the central metal, ie all their electrochemical processes occur on the ring and not on the metal. Non-transition metals do not have any occupied d-orbitals accessible between the HOMO - LUMO gap of the ring. The first ring reduction is separated from the first ring oxidation by ≈1.5V in main group Mpcs.[18] This value corresponds to the separation of the energy levels involved in such redox processes. The value still varies from metal

to metal depending on the polarization power of the metal ion, metals with higher polarization being easier to reduce. Deviations are also observed if the metal is too large to fit in the pc centre.

Ge^{IV} , Sn, Zn, and Si are non-transition metals hence their oxidation or reduction occurs at the phthalocyanine ring.

1.8.4 Electrochemical properties of the tetraazatetrapyridinoporphyrazines.

The tppas have more or less the same structures as the pcs, thus it is expected that their electrochemical behaviour will be the same. However, N atoms in pyridine groups in tppas have a higher electron withdrawing power than the C atoms in the benzene groups of the pc, this causes a destabilization of the π-π conjugate system making tppa more easily reduced species than pc. The Mtmtppas would be expected to be even more easily reduced since they are positively charged. Literature reports are available for the electrochemistry of Cotmtppa[41] and Pdtmtppa and Pttmtppa.[15] Two reduction processes were observed on Pt electrodes for the Pt and Pd tmtppas which were assigned as the reduction of the ring followed by the reduction of the methyl groups on the pyridine substituents whereas for the CoTmtppa complexes, the couples were assigned to the reduction of the central metal (Co^{II}/Co^{I}) followed by the reduction of the ring.[42] Reduction in Copc complexes is known to occur at the metal. The potential of the reduction couple for Cotmtppa occur at more positive values than the (Co^{II}/Co^{I}) couples in Copc complexes due to the electron withdrawing power enhancement by the presence of the positive charge. Spectroscopic confirmation of the observed redox results is normally essential in order to determine whether the reduction is on the ring or on the

metal.

Studies on $[Zntmtppa]^{4+}$, $[Cotmtppa]^{4+}$, $[Cutmtppa]^{4+}$, and $[Nitmtppa]^{4+}$ using polarography have also been reported.[83] Photoreduction of $[Zntmtppa(-2)]^{4+}$ solution in dimethylformamide (DMF)-water in the presence of electron donors such as ethylenediaminetetraacetic acid (EDTA) and cysteine results in the reduction of $[Zntmtppa(-2)]^{4+}$, forming a product with an absorption maxima at 570 nm. The product forms very easily and quickly,[83] and was identified as the ring reduced species $[Zntmtppa(-3)]^{3+}$. The product could be reoxidized by dioxygen back into the original species, $[Zntmtppa(-2)]^{4+}$. $[Zntmtppa(-3)]^{3+}$ can be further reduced to a second reduction product with an absorption maxima at 500 nm. The second reduction product occurs as a purple precipitate and was identified as the doubly reduced $[Zntmtppa(-4)]^{2+}$species. Both these reduction products have short wavelength absorption bands comparable to the corresponding pcs. The nature of the photoreduction products was found to depend on the strength of the donor molecules such that with some molecules e.g. EDTA only the first reduction product was obtained or sometimes only the second product formed without going through the first product. $[Cotmtppa]^{4+}$ was also readily reduced in the presence of ascorbic acid without photolysis.[83]

Polarographic measuremants show that $[Nitmtppa]^{4+}$ has a $E_{½}$ value of -0.3 V vs normal hydrogen electrode (n.h.e.) For the first reduction process. CV studies reflected the non reversibility of these redox processes.

1.9 Photochemical methods

1.9.1 Singlet oxygen determination.

Photochemical processes are said to take place when an excited molecule takes part in the initial steps, `primary`, of a chemical reaction. This can lead to either a final product or to some unstable species which can then react in secondary processes through dark reaction to give the photoproducts. As has been indicated earlier, for PDT the triplet excited state of the sensitizer is the reactive species, therefore the efficiency of the other processes that deactivate this state including its non-radiative decay and phosphorescence must be minimal or controlled, for best PDT results. Knowing the overall efficiency of the different photochemical steps thus becomes important. The efficiency is expressed as quantum yield, which has been defined as the number of molecules of the process of interest formed for each photon of light absorbed. Several methods have been used to determine quantum yields.[52,67,68,84]

In this work the determination of the O_2 ($^1\Delta_g$) quantum yield (ϕ_Δ) was carried out for the Ge, Si, Sn, and Zn phthalocyanine and porphyrazine complexes, using a quencher to react with O_2 ($^1\Delta_g$) as soon as it was produced. 1,3-Diphenylisobenzofuran (DPBF) is a pure, efficient chemical quencher for O_2 ($^1\Delta_g$) which reacts stoichiometrically with the O_2. DPBF permits the use of spectroscopic methods to follow its disappearance by monitoring its absorption maximum, $\lambda = 416$ nm. The decay can be directly correlated to ϕ_Δ through the following reactions, Equations 12-16.

$$O_2(^1\Delta_g) \xrightarrow{k_d} O_2(^3\Sigma_g) \text{ (Natural decay)} \quad ...12$$

$$O_2(^1\Delta_g) + \text{DPBF} \xrightarrow{k_q} \text{Oxidation products (Chemical quenching)} \quad ...13$$

$$O_2(^1\Delta_g) + \text{DPBF} \xrightarrow{k_p} O_2(^3\Sigma_g) + \text{DPBF (Physical quenching)} \quad ...14$$

$$\text{Mpc} + O_2(^1\Delta_g) \rightarrow O_2(^3\Sigma_g) + \text{Mpc (Physical quenching)} \quad ...15$$

$$\text{Mpc} + O_2(^1\Delta_g) \rightarrow \text{Chemical reaction (Chemical quenching)} \quad ...16$$

DPBF acts exclusively as a chemical quencher in DMSO[85] and in other organic solvents,[67] hence equation 14 is not important for DPBF and is ignored. ϕ_Δ does not depend on concentration of the Mpc at the concentrations used, thus even physical quenching by Mpc can be ignored. The pathway for the decay involving chemical reaction with Mpc according to Equation 16 is negligible compared to the rate of the reaction with DPBF. Only Equations 12 and 13 are important in the decay of O_2 ($^1\Delta_g$). The rate of disappearance of DPBF in the presence of O_2 ($^1\Delta_g$) is given by Equation 17.

$$\frac{-[\text{DPBF}]}{dt} = k_q [\text{DPBF}] [O_2(^1\Delta_g)] \quad ...17$$

Applying steady state approximation for O_2 ($^1\Delta_g$) and rearranging gives Equation 18:

$$O_2(^1\Delta_g) = \frac{\Phi_\Delta I_{abs}}{k_q[DPBF] + k_d} \quad ...18$$

Substitution of Equation 18 into 17 gives 19.

$$\frac{-[DPBF]}{dt} = \frac{k_q \Phi_\Delta I_{abs}[DPBF]}{k_d + k_q[DPBF]} \quad ...19$$

where I_{abs} is the amount of light absorbed from a photon by the sensitizer. Since:

$$\Phi_{DPBF} = \frac{\frac{d[DPBF]}{dt}}{I_{abs}} \quad ...20$$

substituting 20 into 19 gives Equation 21:

$$\Phi_{[DPBF]} = \frac{k_q \Phi_\Delta [DPBF]}{k_d + k_q[DPBF]} \quad ...21$$

At low [DPBF] concentrations, $k_d >> k_q$ [DPBF], and 21 becomes:

$$\Phi_{[DPBF]} = \frac{k_q \Phi_\Delta [DPBF]}{k_d} \quad ...22$$

The reaction kinetics are first order at these low DPBF concentrations, whereas at high [DPBF] a zero-order law is obeyed, i.e. the rate of the reaction becomes independent of the concentration of

the DPBF, a situation that is not wanted in this case. Thus at low DPBF concentration, Equation 23 applies for porphyrazine and phthalocyanine complexes.

$$\Phi_{DPBF}^{Mpc} = \Phi_{\Delta}^{Mpc} \frac{k_q}{k_d} [DPBF]^{Mpc} \quad ...23$$

where Φ_{DPBF}^{Mpc} is the quantum yield for DPBF in the presence of Mpc sensitizer, Φ_{Δ}^{Mpc} is the quantum yield of singlet oxygen in the presence of Mpc and $[DPBF]^{Mpc}$ is the concentration of DPBF in the presence of Mpc.

$$\Phi_{DPBF}^{Znpc} = \Phi_{\Delta}^{Znpc} \frac{k_q}{k_d} [DPBF]^{Znpc} \quad ...24$$

Where Φ_{DPBF}^{Znpc} is the quantum yield of DPBF in the presence of Znpc and Φ_{Δ}^{Znpc} is the quantum yield of singlet oxygen of Znpc and $[DPBF]^{Znpc}$ is the concentration of DPBF in the presence of Znpc. Using the ratio of Equation 23 over 24, the Φ_{Δ} of the unknown Mpc can be determined through Equation 25.

$$\Phi_{\Delta}^{Mpc} = \Phi_{\Delta}^{Znpc} \times \frac{\Phi_{DPBF}^{Mpc}}{\Phi_{DPBF}^{Znpc}} \times \frac{[DPBF]^{Znpc}}{[DPBF]^{Mpc}} \quad ...25$$

From the relationship shown by Equation 26:[52]

$$\Phi_{DPBF} = \frac{(C_o - C_t)v}{I_{abs} \times t} \quad ...26$$

where v is the volume of the sample in the cell, t is the photolysis time and C_0 and C_t are the initial concentration of DPBF and after time t of photolysis, respectively. I_{abs}, the light absorbed is determined by Equation 27:[52]

$$I_{abs} = \frac{\alpha\ SI}{N_a} \quad ...27$$

where S is the cell area irradiated, I is the intensity of light from the lamp, and N_a is Avogadro`s number, α is the fraction of the light absorbed and I_{abs} is the light absorbed. Then Equation 28 can be obtained by substituting Equation 27 into 26, then 26 into 25.

$$\Phi_{\Delta}^{Mpc} = \Phi_{\Delta}^{Znpc} \frac{(C_o - C_t)^{Mpc}}{(C_o - C_t)^{Znpc}} \times \frac{(\alpha\ t)^{Znpc}}{(\alpha\ t)^{Mpc}} \times \frac{[DPBF]^{Znpc}}{[DPBF]^{Mpc}} \quad ...28$$

Where $(C_0 - C_t)^{Mpc}$, $(C_0 - C_t)^{Znpc}$, are the changes in DPBF concentration in the presence of Mpc and Znpc, respectively. The photolysis time in the presence of Znpc and Mpc are represented by t^{Znpc} and t^{Mpc}, respectively. S, v, and N_a are the same for both the Mpc and the standard Znpc, hence

cancel in Equation 28. I is constant when the same interference filter is used for both Mpc and the Znpc reference. The determination of α will be discussed in the experimental section. Equation 28 was used for calculating the Φ_Δ of the Mpc, Mtppa and Mtmtppa complexes (where M was Si, Ge, Sn and Zn).

DPBF is a useful quencher in non-aqueous media, for determination of Φ_Δ in aqueous media, two water soluble $O_2(^1\Delta_g)$ quenchers used are α,α`-(anthracene-9,10-diyl)bimethylmalonate (ADMA) and a combination of n-nitrosodimethylanaline (NA) with imidazole .[86] ADMA has several absorption peaks in the UV region of the spectra but usually the peak at 380 nm is the one monitored. The use of ADMA has however been limited by its chemical reaction with the sensitizers and/or the products of the photochemical processes, hence it was not employed in this study. The reactions may lead to formation of a precipitate which interferes with the passage of light during the running of the experiments.

In the NA method a mixture of differently sulfonated AlPc ($AlPcS_{mix}$) was employed as a reference. $AlPcS_{mix}$ has a known $\Phi_\Delta = 0.38$ which is used in the this method.[87] Equation 28 was used with DPBF being replaced by NA. Remembering that the derivation of Equation 28 does not include the physical quenching by DPBF, the use of this Equation for NA also assumes negligible physical quenching by this species.

1.9.2 Quantum yield of photobleaching

The quantum yields of photobleaching for the compounds can be determined using Equation 26 with Φ_{DPBF} replaced by $\Phi_{photobleaching}$. V is the volume of the solution used in the reaction, S the cell area irradiated, t is the time of irradiation, N_A the Avogadro's number and I_{abs} light intensity after correction with the α coefficient. I_{abs} can be determined according to Equation 27. The determination of the intensity of light (I) and α will be discussed in the experimental section.

In Equation 27, C_t and C_o in mole $^{-1}$ are the concentrations of the sensitizers after and prior to irradiation respectively. The overall change in concentration between these should not be greater than 15% where only first order kinetics apply. The concentrations of the sensitizers are obtained using the Q band extinction coefficients from the Beer's law relationship: $A = \epsilon cl$. Where A is the absorbance, ϵ the extinction coefficient, c the conentration and l is the path length of the cell.

1.10 Aims of the thesis

PDT has several mechanisms that bring about sensitization, however Type I and Type II methods are still very commonly suspected to be the dominating mechanisms. As a step towards determining the efficiency of any sensitizer, its singlet oxygen quantum yield is determined. The qualities for a good sensitizer were listed earlier in section 1.7.1 and in addition, it has been observed that the uptake and the killing of cells is higher for positively charged sensitizers than for neutral or negatively charged ones.[73] With this in mind, soluble positively charged molecules were the target

in this work. The aim was thus to synthesize positively charged pyridinoporphyrazine with non-transition metal centres and to determine their efficiency as singlet oxygen producers in photoactivated reactions.

The singlet oxygen quantum yields were determined in organic solvents and in some cases in water. Comparisons with the respective Mpc complexes was undertaken and the change in the trend of the quantum yields when Mpc complexes were derivatised by attaching different halogens as axial ligands was also studied. The photostability of the Mpc and the pyridinoporphyrazine derivatives was also studied. The central metals used are Ge, Si, Sn and Zn.

2. Experimental

The solvents quinoline, dimethylsulfoxide (DMSO), dimethylformamide (DMF) and dimethylsulfate were distilled before use. The reagents $GeCl_4$ (Fluka), $SiCl_4$ (Aldrich), $ZnCl_2$ and $SnCl_2.2H_2O$ (Saarchem), 2,3-pyridinedicarboxylic acid (Aldrich) were used without further purification. Na_2SO_4 (Holpro) was recrystallized from water and tetraethylammonium perchlorate (TEAP, Aldrich) was recrystallized from ethanol before use as electrolytes for electrochemical studies. 1, 3-Diphenylbenzofuran (DPBF, Aldrich) and a mixture of imidazole (Saarchem) with n-nitrosodimethylanaline (NA, Aldrich) were used as $O_2(^1\Sigma_g)$ quenchers without further purification. The tppa complexes of Sn, Si and Ge have not been reported before, thus part of their characterisation is reported at the end of their synthetic procedures. The detailed characterisation including a table for the IR data, the UV-vis spectrophotometric data and NMR data will be presented in the chapter 3.

Instrumentation

UV-visible spectra were recorded on a Varian 500 UV/visible/NIR spectrophotometer. IR spectra (KBr pellets) were recorded on a Perkin-Elmer spectrum 2000 FTIR spectrometer. The light intensity was measured using a power meter (Lasermate). The NMR spectra were collected on a 400 MHz Bruker 400AMX spectrometer. Electrochemical data were collected with the BioAnalytical Systems (BAS) model 100B/W electrochemical workstation connected to a low current Module (MF-9047) for microelectrode studies. A BAS CV 27 voltammograph was employed for bulk electrolysis.

2.1 Synthesis of compounds

Synthesis of the $(Cl)_2$Gepc, $(OH)_2$Gepc,$(Cl)_2$Sipc and $(OH)_2$Sipc, complexes was carried out as outlined in literature.[88, 89] $(OH)_2$Snpc, $(Cl)_2$Snpc, $(Br)_2$Snpc and $(I)_2$Snpc complexes were synthesized according to the method of Dirk et al[89] and Znpc was purchased from Aldrich.

2.1.1 Preparation of the siliconphthalocyanine derivatives.(Scheme 8)

The method adopted from Bello and Bello,[88] involving the conversion of the dicyano template into 1,3 diiminoisoindoline before the addition of the metal salt was found to be the most reliable for the synthesis of dichlorosilicon pc, and hence was used in this work.

Synthesis of 1,3-diiminoisoindoline **(2)**

Dry ammonia was bubbled into a mixture containing o-phthalonitrile **(1)**(5 g, 0.0325 mmoles) and sodium metal (0.031 g, 1.35mmoles) in methanol (20 ml) for 40 minutes. The mixture was then brought to reflux for 3½ hours with continuous stirring and additions of small amounts of ammonia at about 30 minutes intervals. The resultant mixture was then allowed to cool at room temperature before filtering. A yellowish green residue obtained was then washed with diethyl ether and dried in air, according to the literature.[88] The work up was repeated on the filtrate which had stayed overnight yielding 1,3-diiminoisoindoline **(2)**; overall yield 2.45 g (0.017 mmol, 47%).

*Synthesis of dichlorosiliconphthalocyanine (**3**, Cl_2Sipc)*

Following literature methods[88], a mixture of 1,3-diiminiisoindoline **(2)** (2.2 g, 0.015 mol), silicon tetrachloride(2.5 cm^3, 0.022mol) and 15 ml quinoline under nitrogen was refluxed (while stirring) for 30 minutes. The product was filtered while still hot ~ 180 °C. Washing of the product with quinoline, benzene, methanol and acetone then followed. The product was then dried into a powdery green solid of $(Cl)_2Sipc$ (**3**); yield 0.932 g (40%).

*Preparation of dihydroxylphthalocyaninosilicon (**4**, $(OH)_2Sipc$)*

A mixture of the Cl_2Sipc (0.8g) and 0.5 g of sodium metal in 5 cm^3 methanol were added to a 20:1 ratio of ethanol to water as reported in literature.[88] The resulting suspension was refluxed for an hour, cooled and filtered to give $(OH)_2SiPc$ (**4**); yield 0.54g (70 %).

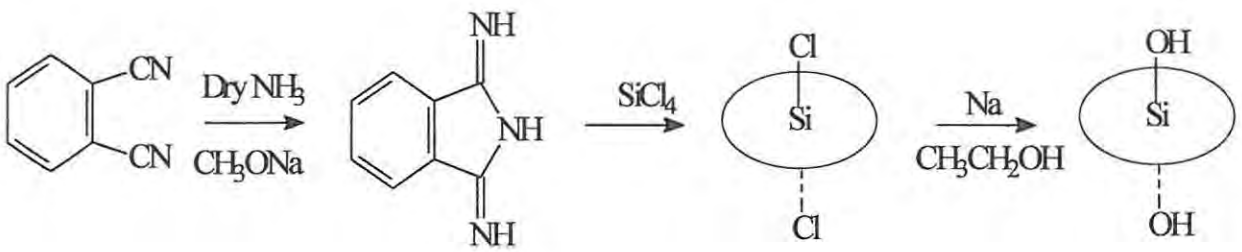

1 **2** **3** **4**

Scheme 8 Synthesis of Sipc derivatives. The circles represent the pc ring.

The complexes **3** and **4** gave similar characterization to those reported in the literature.[88]

*2.1.2 Preparation of dichlorogermanium phthalocyanine (**5**, $(Cl)_2$Gepc)-Scheme 9*

Dichlorogermanium phthalocyanine was synthesized and purified according to the method adopted from Joyner and Kenny,[90] and modified by Dirk et al.[89] Germanium tetrachloride (2.5 ml, 0.022 mol) was added under nitrogen to freshly distilled quinoline (20 ml) and was brought to reflux quickly. When the temperature of the mixture was 200 °C, phthalonitrile **(1)** (6 g, 0.039 mol) was added and the mixture was left to reflux at 210 °C for a further 4 hours. The mixture was then cooled slowly to room temperature and filtered. The residue was then washed with DMF, xylene and ether to give purple microcrystalline dichlorogermanium phthalocyanine **(5)**; yield 2 g (31 %).

Preparation of dihydroxylgermaniumphthalocyanine **(6)**

Dihydroxygermanium phthalocyanine was obtained by hydrolysis of the dichloride. A mixture of the dichloride (0.7 g) with NaOH(aq) in pyridine (40 ml) were refluxed for 6 hours. Filtration of the mixture gave blue microcrystals of $(OH)_2$Gepc **(6)**.

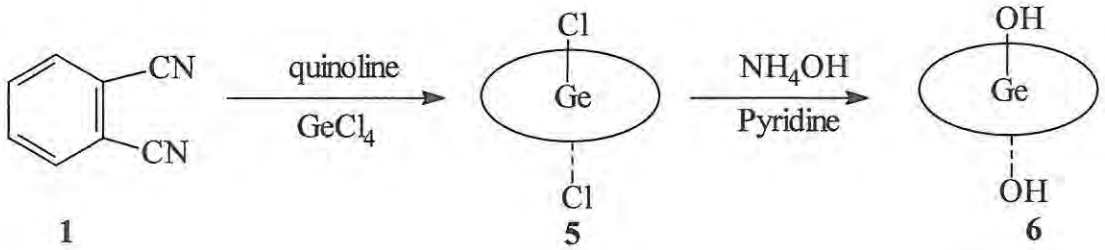

1 **5** **6**

Scheme 9 Synthesis of $(Cl)_2$Gepc and $(OH)_2$Gepc. The circles represent the pc ring.

Spectral characterisation was similar to literature reports.[89] IR (KBr) shows the Ge-O asymmetric stretch at 644 cm^{-1} and the O-H stretch at 3496 cm^{-1}.[89,91] Anal. Calcd. for $C_{32}H_{18}GeN_8O_2.2H_2O$: C,61.95; H,2.94 and N,18.06%. Found. C, 61.09; H,2.91 and N, 17.49%.

2.1.3 Preparation of Mtppa complexes: $(OH)_2$Getppa, $(OH)_2$Sitppa, $(OH)_2$Sntppa and Zntppa

Dichlorogermanium, dichlorosilicon, dichlorotin and zinc tetra-2-3-pyridinoporphyrazine (tppa) complexes, Cl_2Getppa, Cl_2Sitppa Cl_2Sntppa and Zntppa, respectively, were synthesized and purified according to the method similar to that reported by Smith et al,[11] (see Scheme 7 in section 1.3) for the synthesis of the cobalt (II) pyridinoporphyrazine complex. The general procedure was as follows: urea (0.8g, 13 mmol), ammonium molybdate (0.0315g, 0.07mol) and 2,3-pyridinedicarboxylic acid (0.35g, 2 mmol) were ground together to form a homogenous mixture. The mixture was refluxed in 1,2,3-trichlorobenzene (40ml) at 160°C for an hour. For the Si and the Ge complexes another 0.625g urea was added slowly to the mixture after 4.5 ml (42 mmol) of germanium tetrachloride (Fluka) or 3 ml silicon tetrachloride (Aldrich), respectively, had been added to the mixture in one portion, under nitrogen. The conditions were then maintained for a further 3.5 hrs during which further refluxing was carried out at 210°C. For the respective tin and zinc complexes, 0.25g of the zinc chloride (Saarchem) and 0.3g tin chloride (Saarchem) were each ground together with the additional 0.625g urea and slowly added to the reflux mixture. The temperature was then allowed to rise to 210°C and maintained for a further 3.5 hrs. The mixture was allowed to cool and attempts to remove the solvent by vacuum distillation were not successful, so filtration was employed. The

crude product was then washed with benzene (70 ml), crushed, washed successively with ethanol, aqueous 5% NaOH, and 2.5% hydrochloric acid using warm water washing in between each step according to literature methods.[11] Attempts to purify the products further using concentrated hydrochloric acid caused decomposition of the products. The synthesis and characterization of Zntppa has been reported.[83] The purification method incorporates washing with 5% NaOH (Saarchem), which seems to bring about the hydrolysis of the Sn, Si, and Ge complexes into $(OH)_2$Sntppa, $(OH)_2$Sitppa and $(OH)_2$Getppa, respectively. The UV/vis and detailed IR data for the complexes is discussed in chapter 3.

$(OH)_2$Getppa. Yield 42%. IR (KBr): ν_{Ge-O} = 646cm^{-1} and a strong O-H stretch at 3489 cm^{-1}, confirm hydrolysis. Anal. Calcd. for $C_{28}H_{14}GeN_{12}O_2$. $6H_2O$: C, 45.99; N, 22.30; H, 3.56 %. Found. C, 45.47; N, 23.83; H 2.75 %.

$(OH)_2$Sitppa. Yield 37%. IR(KBr): ν_{Si-O} = 830 cm^{-1}. Anal. Calcd. for $C_{28}H_{14}SiN_{12}O_2.5H_2O$: C, 50.29; N, 25.15; H, 3.59%. Found. C, 51.14; N, 25.78; H, 2.49%.

$(OH)_2$Sntppa. Yield 28%. IR(KBr): ν_{Sn-O} = 556 cm^{-1}.

2.1.4 Preparation of the Mtmtppa complexes: $(OH)_2$Getmtppa, $(OH)_2$Sitmtppa $(OH)_2$Sntmtppa and Zntmtppa

N, N′, N″, N‴ -tetramethyl-2,3-tetrapyridinoporphyrazine (Tmtppa) complexes of tin

($[(OH)_2Sntmtppa]^{4+}$), germanium ($[(OH)_2Getmtppa]^{4+}$), zinc ($[Zntmtppa]^{4+}$) and silicon ($[(OH)_2Sitmtppa]^{4+}$) were obtained by methylation of the corresponding Mtppa complexes using freshly distilled dimethyl sulphate (Aldrich) following a procedure reported before,[11] Scheme 10. The conversion yields from the corresponding Mtppa to the Mtmtppa were as follows: $[(OH)_2Sntmtppa]^{4+}$ (~ 10 %, highly hygroscopic complex); $[(OH)_2Getmtppa]^{4+}$ (60%); $[Zntmtppa]^{4+}$ (71%); and $[(OH)_2Sitmtppa]^{4+}$ (70%). All the Mtmtppa complexes were readily soluble in aqueous solutions.

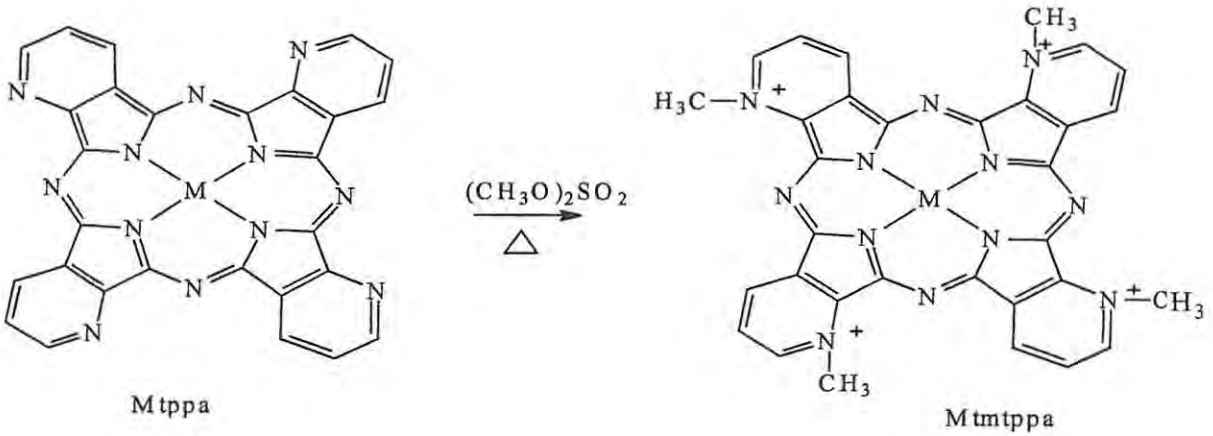

Scheme 10 Synthetic route for the preparation of the Mtmtppa complexes. M is Ge, Si, Sn and Zn. The counter anion is $[SO_3(OCH_3)]_4^-$.

2.2 Photochemical studies

Photochemical studies undertaken include the determination of the quantum yields and the photodegradation studies. It is necessary to determine the response of the molecules to light before trying to quantify any of the behaviour so that changes can be rightfully attributed to the causative

factor.

2.2.1 Studies of degradation in the dark.

The photostability of the Mtppa and the Mtmtppa derivatives was studied using a spectrophotometric cell of 1-cm pathlength using either DMF or DMSO as solvents. The solubility of the Mtppa complexes in the solvents was low and slow, and thus they were prepared about 4 hours before use. The absorption spectra of the Mtppa complexes during this period showed a gradual increase in the intensity of absorption of the dye until a constant value was reached. The solution was then used for studying photochemical properties.

The first step was the determination of the stability in the dark. The solutions of the sensitizers were prepared in the dark with the absorbance of about 1. The absorbance was recorded for the solutions over a period of 12 hours. This step is necessary so as to ascertain that there are no changes or any dark reactions taking place before or during the study of the other photochemical experiments.

2.2.2 Beer-Lambert law

Solutions were prepared in water for the Mtmtppa complexes and for the Mpc, Mtppa and in DMF and in DMSO with different concentrations with the highest absorbance at ~1.4 . Beer's law dependence was then studied.

2.2.3 Determining the light intensity.

For all the photochemical studies, 2 ml solution of the complex (about 1 x 10^{-5}mol l^{-1}) was introduced to a spectrophotometric cell and photolysed in the Q band region of the dye with a General electric Quartz lamp (300W). A 600 nm cut off filter (Schott) and a water filter were used to exclude ultraviolet and far infrared radiation. Interference filters (Intor, 650 nm, 670 nm or 700 nm with a 20 nm bandwidths) were placed in front of the sample in the line of the light during the determination of the quantum yields, using the setup shown in Figure 2.1.

The transmittance of the interference filter was such that it overlapped with the Q band absorption of either the Mpc, Mtppa or Mtmtppa complex under study. A differential computation

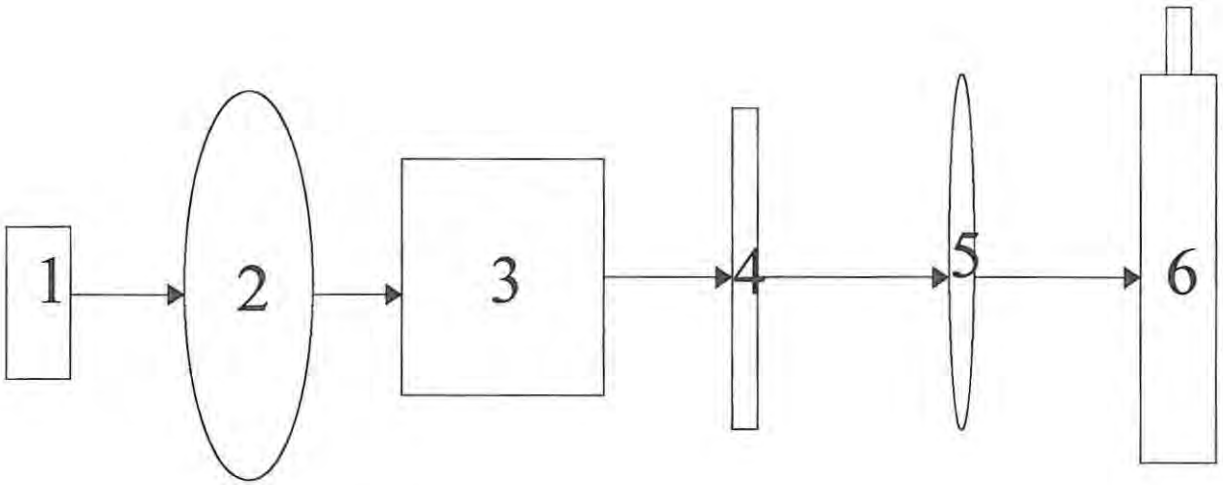

Figure 2.1 A diagrammatic representation of the photolysis setup. 1 = light source, 2 = focusing lens, 3 = water filter for IR and for cooling, 4 = 600 nm cut off filter, 5 = interference filter and 6 = sample holder.

was performed to determine the fraction of light that goes through the filter and gets to the sensitizer. An illustration of the computation is shown as Table 3 where 0.419 and 0.369 are the transmittance (T) of the dye at 650 nm and 660 nm, respectively, while 0.176 and 0.732 are the transmittance of the interference filter at 650 and 660 nm, respectively.

Table 3 An illustration of the computation to determine the α coefficient. T_{dye} is the transmittance of the dye , T_{filter} is the transmittance of the filter.

λ(nm)	T_{dye}	$1 - T_{dye}$	T_{filter}	$T_{filter}(1-T_{dye})$
650	0.419	0.581	0.176	0.102256
660	0.369	0.631	0.732	0.461892
			$\sum T_{filter}$	$\sum T_{filter}(1-T_{dye})$

From the information α can be calculated using Equation 29.

$$\alpha = \frac{\Sigma_{T_{filter}}(1-T_{dye})}{\Sigma_{T_{filter}}} \qquad ...29$$

Where α fraction of the overlap integral of light for use in Equation 27 and 28 on page 53. For a good overlap, α ranges from 0.3-0.85. For every new solution the α coefficient was determined and used for Equation 28.

Light intensity measured with a power meter (Lasermate) was found to be 5×10^{16} photons s^{-1}

cm^{-2}. This was obtained using the standard relationship, Equation 30.

$$\Delta E = \frac{hc}{\lambda} \qquad ...30$$

where h is planck`s constant and *c* is the speed of light. The energy of light at any wavelength could be calculated using Equation 30. Inserting the values of h and *c* reduces the expression to :

$$\text{Energy at } \lambda = \frac{\text{kJ}}{\text{mole}} = \frac{1.194 \times 10^5}{\lambda \text{ (nm)}} \qquad ...31$$

where the λ is the wavelength of the interference filter. Using the power of the lamp which was typically found to be 40 mW, considering the area of the power meter and the sample cell exposed and remembering that 1 W = J/s, the intensity was calculated to be 5×10^{16} quanta s^{-1} cm^{-2}.

Determining the quantum yields of photobleaching requires the knowledge of the extinction coefficients *(ϵ)* of the sensitizers so that concentration can be calculated as discussed in section 1.9.2. Because of the low solubility of the sensitizers, the ϵ values could not be obtained for all the sensitizers except for the Getppa. The ϵ values for Zntppa, Znpc, Zntmtppa have been reported before.[83]

Relative photobleaching kinetics were studied for the compounds whose ϵ coefficients were not known, hence for these compounds, solutions of the Mtppas and the Mtmtppa in DMSO with an absorbance of ≤ 1 were prepared and photolysed. The plot of A/A_o against the photolysis time (t) gave

the kinetics of the photobleaching reaction where A and A_o are the absorbance at time (t) and before photolysis, respectively. For comparative reasons, the studies were done under the same conditions, using the cut off filter (600 nm) but leaving out the interference filter for all samples. Experiments were also performed whereby the solutions were deaerated with N_2 gas or saturated with O_2 in order to study the role of oxygen in the mechanism for photobleaching.

2.2.4 Singlet oxygen quantum yields determination

For singlet oxygen determination the typical procedure was as follows: DMSO solutions containing the porphyrazine or pc derivative under study (absorbance below 1 at the irradiation wavelength) and 1,3 diphenylbenzofuran (DPBF) (3×10^{-5} mol l^{-1}) were prepared in the dark. Experiments were carried out in air without bubbling oxygen using a 2.0 ml sample of solution and this was irradiated in the Q band region using the setup described in Section 2.3. DPBF absorption decay at 416 nm was then monitored. The values of ϕ_Δ were calculated using Equation 28 on page 53 with Φ_Δ^{Znpc} (the singlet oxygen quantum yield for ZnPc in DMSO), = 0.67[92] and ϕ_Δ = 0.56 in DMF.[52] In some experiments diazabicyclo-(2,2,2)-octane (DABCO) was used in addition to DPBF as a quencher.

For experiments in aqueous solutions, a combination of imidazole and n-nitrosodimethylanaline (referred to as NA method in this thesis) was employed instead of DPBF as a singlet oxygen quencher. A stock solution (NA) of imidazole (1×10^{-2} mole l^{-1}) and n-nitrosodimethylanaline (4×10^{-5} mole l^{-1})

was prepared. A solution of the Mpc, Mtppa or Mtmtppa was prepared in the stock solution and illuminated as described above for DPBF. All the experiments were carried out at room temperature (23 – 25 °C).

2.3 Electrochemical studies

2.3.1 Cyclic voltammetry studies

For cyclic voltammetry in water, triply distilled deionised water was used. An undivided cell was employed. The working electrode was either a platinum disc (1.6 mm diameter) or a Bioanalytical systems (MF 2007) platinum disc microelectrode (11 μm diameter). Platinum wire and Ag | AgCl (3 mol dm^{-3} NaCl) were employed as auxiliary and reference electrodes, respectively. pH 7 buffer was employed as an electrolyte for some electrochemical experiments, for some studies water containing Na_2SO_4 was employed as an electrolyte. Microelectrode studies were done in DMSO without an added electrolyte.

2.3.2 Spectroelectrochemical methods (Bulk electrolysis)

For bulk electrolysis a two compartment cell was employed. The working and auxiliary electrode compartments being separated by a fine glass frit. The working electrode was the platinum plate of area 2 cm^2, the auxiliary was also a platinum electrode (area = 2.2 cm^3) and a silver wire pseudo reference electrode was employed. The working compartment contained the Mtmtppa complexes of Sn and Zn together with the electrolyte solution (DMSO/TEAP). The auxiliary

electrode compartment contained only the electrolyte. The concentration of the tetra methyltetrapyridinoporphyrazine complexes were of the order of $\approx 10^{-4}$ mol dm^{-3} for the cyclic voltammetry studies and $\approx 10^{-5}$ mol dm^{-3} for bulk electrolysis. Nitrogen was bubbled through the solution for the entire duration of the experiment. The solution in the working electrode compartment was sampled every 3-10 minutes for recording the electronic absorption spectra. The cell for bulk electrolysis was connected to a BAS CV 27 Voltammograph analyser.

3. Characterisation of phthalocyanine and porphyrazine complexes

3 .1 Electronic absorption spectra

The absorption spectral data is presented in Table 4, here the absorption peaks in different solvents are given as well as the extinction coefficients for those compounds where these could be determined. Figure 3.1 shows the absorption spectra of Mpc complexes in DMSO.

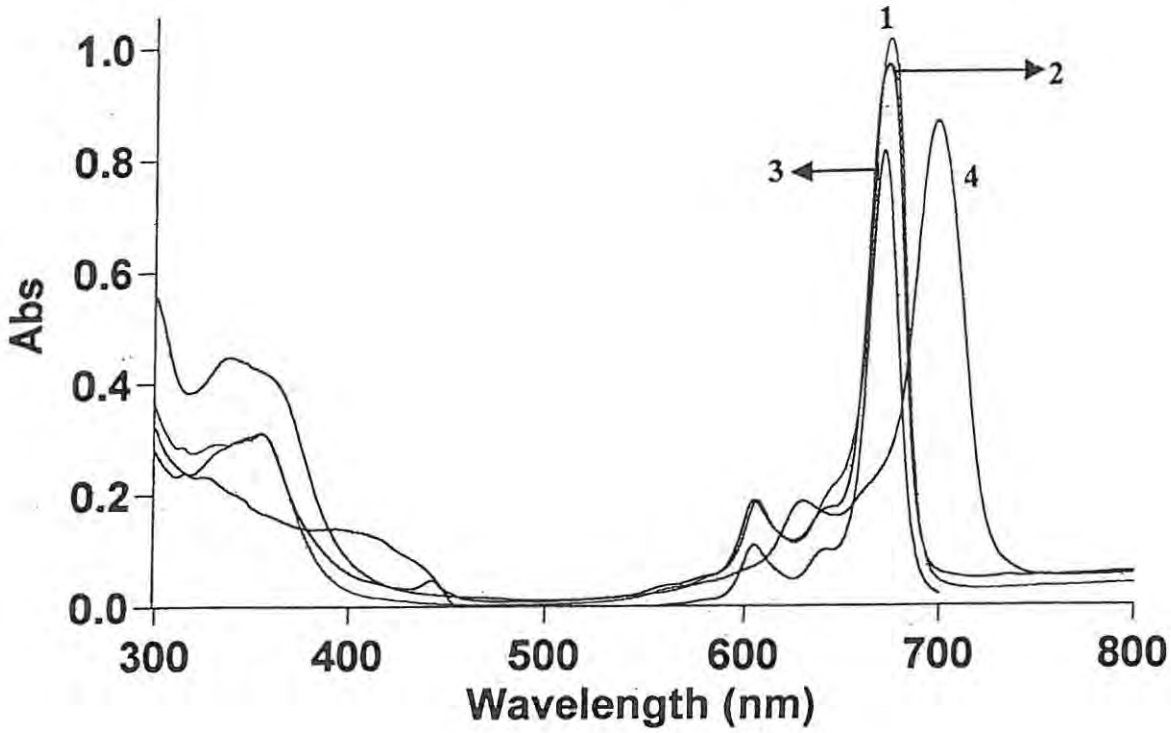

Figure 3.1 Absorption spectra of 1 = $(OH)_2$Gepc, 2 = Znpc, 3 = $(OH)_2$Sipc and 4 = $(OH)_2$Snpc.

Table 4 Absorption spectral data for tetra-2,3-pyridinoporphyrazine, *N, N′, N″, N‴*-tetramethyltetra-2,3-pyridinoporphyrazine and phthalocyanine complexes of Ge, Si, Sn and Zn. * shows that the product was reduced.

Complex	Solvent	λ_{max} / nm (log ϵ)
$(Cl)_2GePc$	DMF	695 625 365
$(OH)_2GePc$	pyridine	675 647 608 356
	DMSO/DMF	676 647 609 357
$(OH)_2Getppa$	pyridine	641 585 515 336
	DMSO	642(4.71) 583(4.00) 515(4.05)
$[(OH)_2Getmtppa]^{4+}$	DMSO	687 631 312
	Water	632 574 360
ZnPc	DMSO	672 607 345
Zntppa,	DMSO	647 584 331
	DMF	646 588 326
$[Zntmtppa]^{4+}$	Water	648 637 365
	DMSO	655 641 583 390
$(OH)_2SiPc$	DMSO	672 641 602 446 341
$(OH)_2Sitppa$	DMSO	645 587 330
$[(OH)_2Sitmtppa]^{4+}$	*DMSO	653 590 400
	*Water	630 519

Table 4 continued...				
$(Cl)_2SnPc$	DMSO	699	630	335
$(OH)_2SnPc$	DMSO	697	630	337
$(OH)_2Sntppa$	DMSO	648	604	337
$[(OH)_2Sntmtppa]^{4+}$	DMSO	642	574	
	Water	633	570	353

3.1.1 Phthalocyanine complexes

The absorption spectral data of $(OH_2)Sipc$, $(OH_2)Gepc$ and $(OH_2)Snpc$ had λ_{max} of the Q band at 672, 675, and 697 nm respectively, are in agreement with literature reports.[87] All Q band spectra had a weak shoulder to the blue due to the vibrational modes within the electronic transition. The shoulder observed in the spectrum of $(OH)_2Sipc$ is located at 640 nm while those of $(OH)_2Gepc$ and $(OH)_2Snpc$ are located at 647 and 665 nm respectively. The Soret bands are found near 340 nm. For the elements in the same group a progressive red shift of the Q band is observed as the electronegativity of the central metal decreases, i.e Sn > Ge > Si as one moves down the group. A change in the electron density of the metal causes a change in the interaction of the metal's bonding electrons with the HOMO of the ring. The higher the electron density, the stronger the interaction, which pushes the HOMO to a higher energy level. This results in a smaller HOMO-LUMO gap and a lowering of the

energy of transitions. This only holds true if the LUMO energy level does not change with the change in the central atom.

3.1.2 Tetra-2,3pyridinoporphyrazines complexes: (OH_2)Getppa, (OH_2)Sitppa, (OH_2)Sntppa, Zntppa

As the solubility of the unsubstituted Mtppa complexes is extremely low, extinction coefficients could not be obtained for most of them. Extinction coefficients were obtained for (OH_2)Getppa, and literature values (determined in DMF) $\epsilon = 5.91 \times 10^4$ was used for Zntppa.[83] Slight solubility in DMF and DMSO was achieved which permitted suitable concentrations of solutions for spectroscopic and photochemical studies. $(OH)_2$Sitppa and $(OH)_2$Sntppa complexes were less soluble than the corresponding $(OH)_2$Getppa and Zntppa which explains why the ϵ coefficients of the former could not be obtained. The pyridinoporphyrazines under study were monomeric in solution as shown by their absorption spectra. These possessed a single, unsplit, sharp Q band at 642, 647, 645 and 648 nm for Ge, Zn , Si and Sn tppa complexes, respectively, and vibrational satellites in the 580-590 nm region for all the complexes. Figure 3.2 shows the UV/Vis spectrum of Getppa, which is representative of the spectra of the other Mtppa complexes.

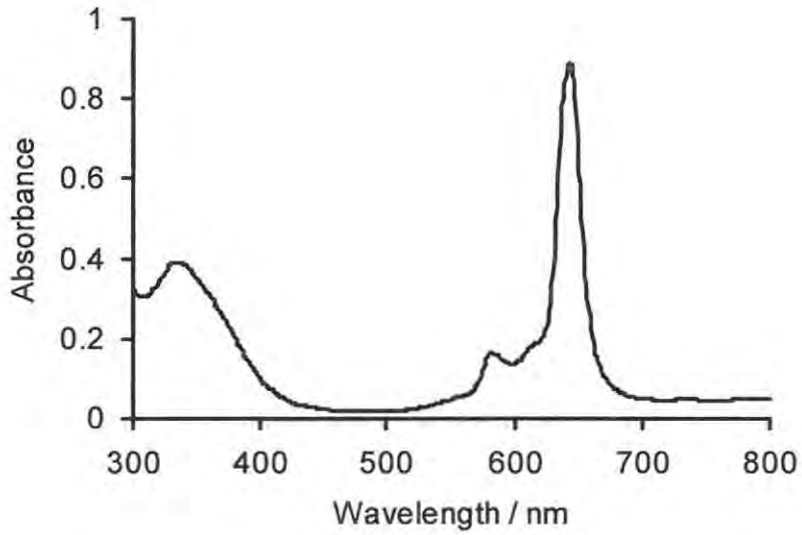

Figure 3.2 The absorption spectrum of $(OH)_2$Getppa in DMSO.

The blue shift of about 30 nm of the pyridinoporphyrazine Q band relative to the phthalocyanine is expected [91] and was observed as recorded in Table 4. The blue shift is due to the electron withdrawing power of the pyridine group which have replaced the benzene moiety in the ring. The Mtppa solutions obeyed Beer-Lambert`s law in both DMF and DMSO solutions at low concentrations, of the order ~10^{-5}, as shown in Figure 3.3 for $(OH)_2$Getppa. The variation of the concentration of the $(OH)_2$Getppa complex with the absorbance had a linear relationship with an intercept close to 0. Thus at the concentrations of Figure 3.3, the Mtppa complexes are not aggregated.

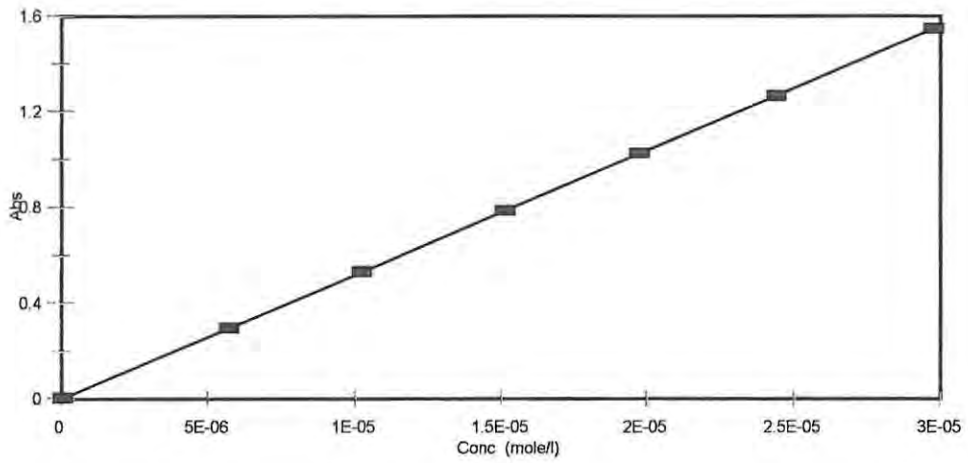

Figure 3.3 A graph of concentration of $[(OH)_2Getppa]^{4+}$ in DMF versus absorbance shows a linear relationship

3.1.3 Tetramethyltetrapyridinoporphyrazine complexes of Si, Ge, Sn and Zn.

As discussed in the introduction, the phthalocyanine and the porphyrazine rings carry a charge of 2^-, hence may be represented as pc(-2) and pa(-2), respectively. Hence for the following discussion, Mtmtppa are represented as $[Mtmtppa(-2)]^{4+}$ before reduction or oxidation. Singly or doubly reduced species are represented as $[Mtmtppa(-3)]^{3+}$ and $[Mtmtppa(-4)]^{2+}$, respectively. The Mtmtppa complexes are water soluble and display a different spectroscopic behaviour to that of the Mtppa complexes. Electronic absorption spectral studies in water showed that the synthesized (OH_2)Sitmtppa complex was reduced since it gave a purple solution in water with a broad absorption

band obtained around 500-600 nm. This is typical behaviour for reduced Mtmtppa complexes.[83] $[(OH)_2Sntmtppa]^{4+}$ complex gave a blue solution of the $[(OH)_2Sntmtppa(-2)]^{4+}$ species with a sharp Q band at $\lambda max = 633$ nm and a vibration satellite at 570 nm characteristic of monomeric species, Figure 3.4(c) and did not show evidence of the presence of reduced species. The Zntmtppa and $(OH)_2Getmtppa$ complexes were partly reduced as evidenced by broad bands in the 500 nm region.

The bands due to the reduced species were observed in addition to the Q band in some of the complexes, see Figure 3.4 (b, and d), showing that the complexes were partly reduced. Sitmtppa was reduced to a much higher extent when compared to Zn and Ge tmtppa complexes. The peak near 500 nm has been associated with doubly reduced $[Zntmtppa(-4)]^{2+}$ complexes, hence is assigned to the $[(OH)_2Sitmtppa(-4)]^{2+}$ complex in Figure 3.4 (a).

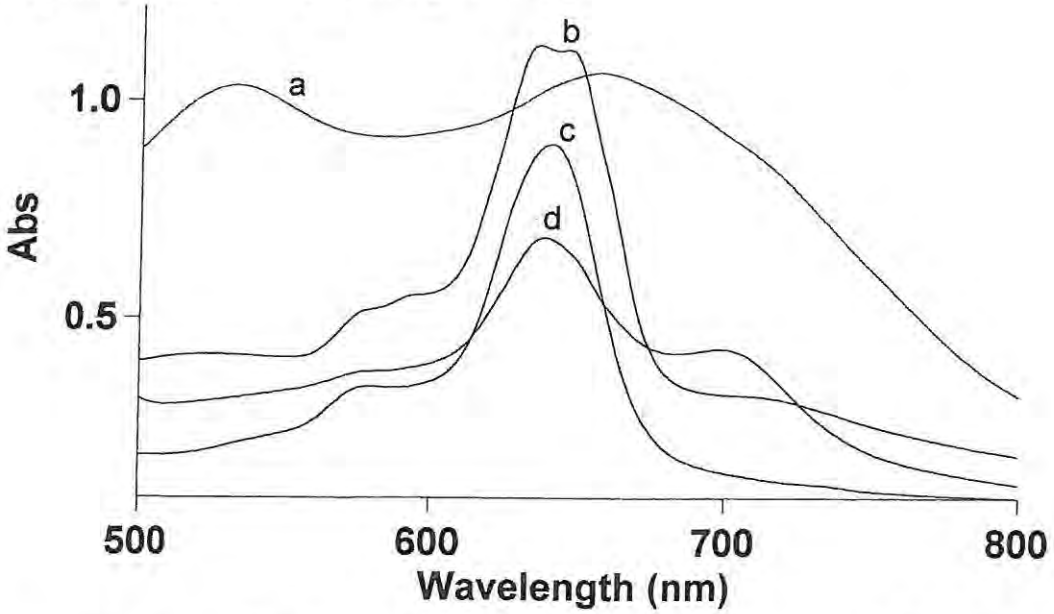

Figure 3.4 The absorption spectra of: a = $[(OH)_2Sitmtppa(-2)]^{4+}$, b = $Zntmtppa(-2)]^{4+}$, c = $[(OH)_2Sntmtppa(-2)]^{4+}$ and d = $[(OH)_2Getmtppa(-2)]^{4+}$ in aqueous media.

[Zntmtppa]$^{4+}$ spectra were measured at pH 4 in Figure 3.4 while the others are in water. The extent of reduction of the complexes in water was dependent on the pH, in that at low pH there was generally a more intense Q band and a smaller amount of the reduced species. For [Zntmtppa(-2)]$^{4+}$species in water, the absorption maxima are in agreement with those reported in literature.[83] Mtmtppa complexes are known to decompose in basic media.[83] The synthesized Mtmtppa complexes dissolved well in water although in common solvents their solubilities were poor, a behaviour that has been reported for Nitmtppa.[12] Their solubility in DMF was so poor that it did not permit photochemical studies, but in DMSO the solubility was modest enough to make solutions for use in photochemical studies. It was possible to further prove that the distortion in the absorption spectra was due to reduction, as chemical oxidation using Br_2 fumes produced a normal spectra typical of monomeric porphyrazines, Figure 3.5 and caused a change in colour from purple to the typical blue for $(OH)_2$Sitmtppa. For $(OH)_2$Getmtppa and Zntmtppa complexes, blue solutions with a spectra which did not show the reduction peaks, were obtained for some preparation batches. It is still not clear what factors influenced the extent of reduction of these species during their synthesis.

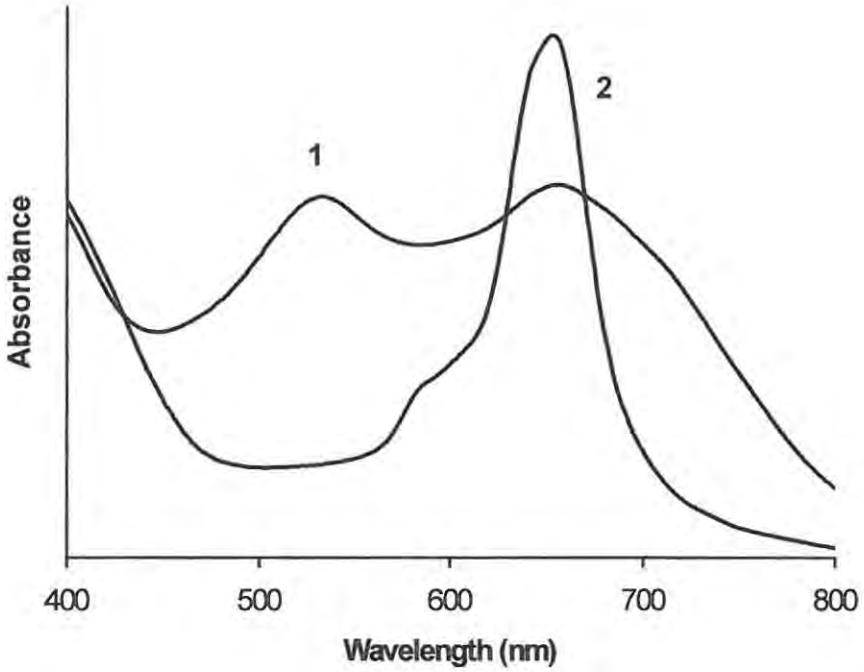

Figure 3.5 Absorption spectra of $(OH)_2$Sitmtppa in DMSO; 1 = without Br_2 and 2 = with Br_2

Fresh solutions of $(OH)_2$Sitmtppa, $(OH)_2$Getmtppa and Zntmtppa in DMSO also gave a purple colour with broad bands around 500 nm indicative of the reduced species. The extent of the ring reduction was dependent on the nature of the solvent as indicated by the different behaviour exhibited in DMSO when compared with that in water. The formation of reduced products during synthesis has not been reported in any of the earlier works on the Mtmtppa (M = Zn, Ni, Cu, and Co) complexes.[11,15,83] This implies that the formation of the reduced species may also depend on the nature of the central metal in addition to experimental conditions. The purple solutions in DMSO were found to turn blue if left in the dark for a prolonged period (overnight) resulting in $[(OH)_2$Sitmtppa(-2)$]^{4+}$, $[(OH)_2$Getmtppa(-2)$]^{4+}$, and [Zntmtppa(-2)$]^{4+}$ as the main products. Figure 3.6 shows the visible

spectra of solutions of the Mtmtppa complexes of Si, Sn, Ge, and Zn in DMSO following prolonged times in the dark after dissolving in DMSO.

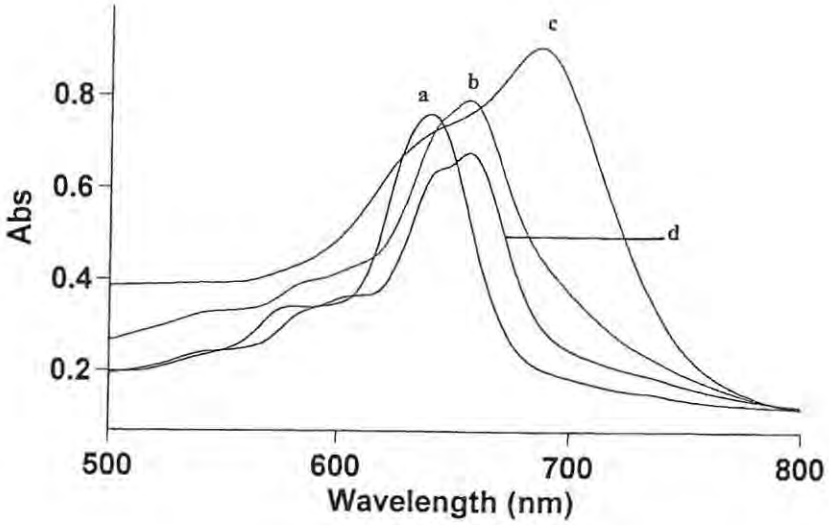

Figure 3.6 Absorption spectra of $[Mtmtppa(-2)]^{4+}$ solutions where M = Sn (a), Si (b), Ge (c) and Zn (d) in DMSO after leaving overnight.

The spectrum of $[(OH)_2Sntmtppa(-2)]^{4+}$ is typical of monomeric Mpc species. The spectra of $[(OH)_2Sitmtppa(-2)]^{4+}$ and $[Zntmtppa(-2)]^{4+}$ show a split Q band due to the presence of symmetrical and unsymmetrical constitutional isomers as has been reported before for the Zn complex.[83] Zntmtppa complex is not known to be aggregated in solution but under our conditions Beer`s law was only obeyed at low concentration ($< 1.6 \times 10^{-5}$), Figure 3.7. For $[(OH)_2Getmtppa(-2)]^{4+}$ the spectrum in Figure 3.6(c) with a broad Q band is typical of aggregation in Mpc complexes.

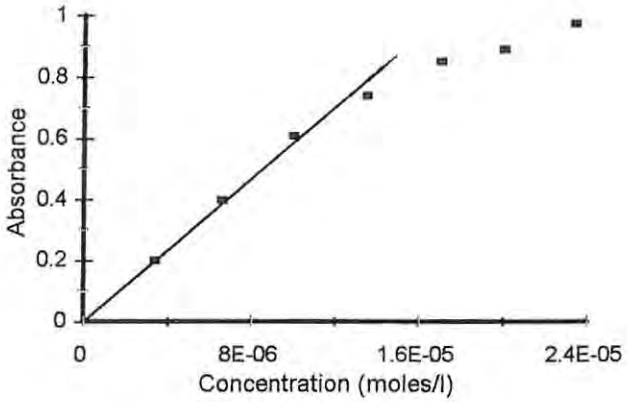

Figure 3.7 A plot of concentration *vs* absorbance for $[Zntmtppa]^{4+}$ in DMSO.

Beer's law showed considerable aggregation for Ge and Si tmtppa complexes.

^{1}HNMR studies for $[(OH)_2Sitmtppa(-2)]^{4+}$ and $[Zntmtppa(-2)]^{4+}$ did not yield conclusive results concerning the presence of the isomers in that the signals of the pyridino protons were not resolved. However, unexpectedly, the presence of isomers was proven for the seemingly monomeric Sn complex by the ^{1}HNMR spectrum obtained, Figure 3.8.

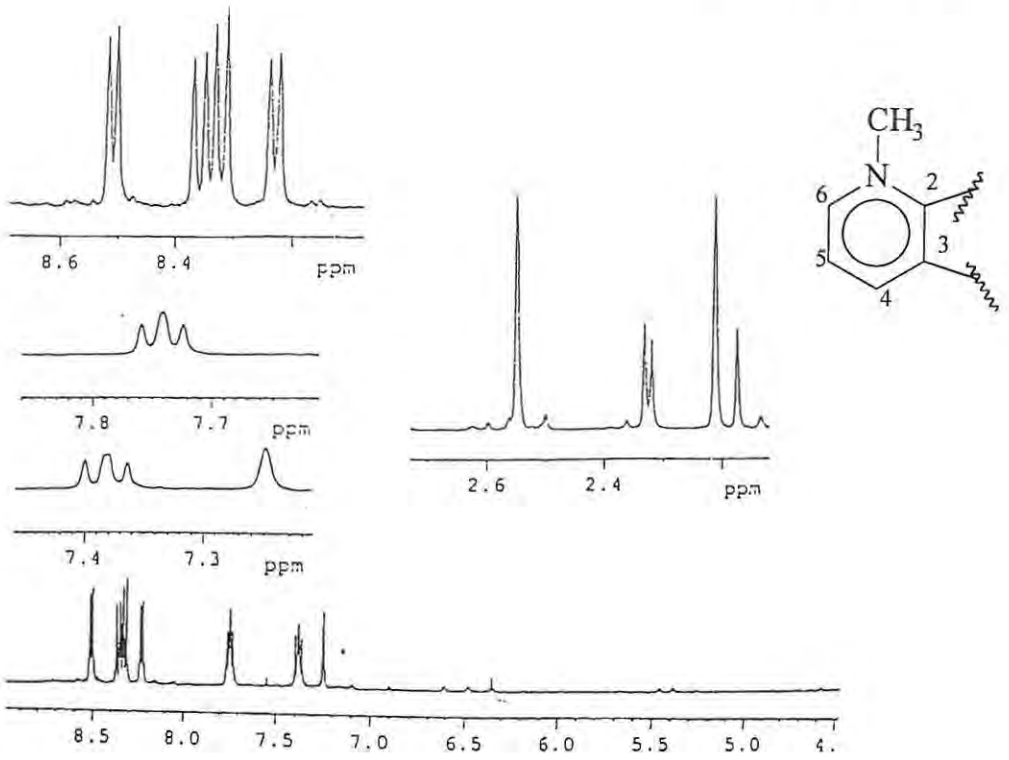

Figure 3.8 The ^{1}HNMR spectra of Sntmtppa in D_2O. The insert shows a simplified part of the molecule showing positions of the carbon groups.

The ^{1}HNMR spectra confirms the presence of the methylated pyridinoporphyrazine and existence of isomers. For Sntmtppa in D_2O, the spectra shows the methyl groups on the pyridine nitrogen as multiple singlets as reported in literature for the Zntmtppa complex.[91] The orientation of the pyridine groups with respect to the core of the ring causes the methyl groups of the pyridine to experience different magnetic environments, leading to the multiple signals observed. Using the pyridine model and the simplified numbering on Figure 3.8, two doublets are observed (for each isomer between 8.0 and 8.6 ppm) due to the protons on position 4 and 6 of the pyridine. The proton on 5 is influenced by the protons at 4 and 6 and appears as a triplet for each isomer. The triplet at 7.4

ppm and the doublets at 8.2 and 8.5 ppm belong to the same isomer and they are expected signals on the NMR spectrum. What appears as a quartet is in fact two sets of doublets overlapping at 8.35 ppm with the triplet found at 7.75 ppm due to another isomer.

In literature it has been reported that the Zntmtppa complex has a DMF soluble fraction and a DMF insoluble fraction which can be explained as a mixture of constitutional isomers.[83] This was observed with the Mtmtppa complexes of Sn, Si and Ge where a small fraction was soluble in DMF while the bulk of the compound was not. The solubility in DMF was however so low that solutions for UV/visible and ^{1}HNMR studies could not be obtained for the separated fractions. From the structure of the Mtmppa complexes, four constitutional isomers can be expected which have the symmetries C_{4h}, D_{2h}, C_{2v} and C_s. However, ^{1}HNMR data only shows signals that would be observed for protons in the C_{4h} and D_{2h} because the other symmetries are a combination of these two. The proton signal in the C_{4h} isomer has an 80% excess over the signals observed for a D_{2h} arrangement. This is because there exists spatial interaction of the methyl groups and thus the steric hindrance does not afford the formation of the other isomers in large amounts. The assumption that electrostatic repulsion and steric hindrance would totally block the formation of isomers does not hold. From this observation, one concludes that the Mtppa complexes must also exist as mixtures of constitutional isomers.

3.2 Infrared spectra

The infrared spectral data for $(OH)_2$Gepc, $(OH)_2$Snpc and $(OH)_2$Sipc complexes matched band for band with the literature reports by Dirk et al.[89] For $(OH)_2$Gepc the Ge-O asymmetric stretch is assigned at 646 cm^{-1}. The Sn-O stretch in the $(OH)_2$Snpc was found at 560 cm^{-1} and the Si-O at 830 cm^{-1} for $(OH)_2$Sipc. The IR spectra of these Mpc complexes is not shown on the tables below since they have been reported before.[89]

The following bands characteristic of the phthalocyanines have been identified for tppa complexes, Table 5, bands around 730 cm^{-1} due to the C-H out of plane bending modes; the 1030 cm^{-1} band due to C-H in plane bending while C-H stretching vibrations lead to the 3030 cm^{-1} band; C-C stretching vibrations of the benzene rings at 1600 - 1680 cm^{-1} and the C-N stretching vibrations at around 1650 cm^{-1}.

The assignment of bands for the Mtppa complexes is more or less the same as that of Mpcs which can be expected considering the similarities in structure between the two groups. Table 5 shows the infrared absorption frequencies for the tppa complexes of Sn, Ge, Si, and Zn. Figure 3.9 compares the frequency bands of Getppa and $(OH)_2$Gepc as an illustration for the other metal complexes under study.

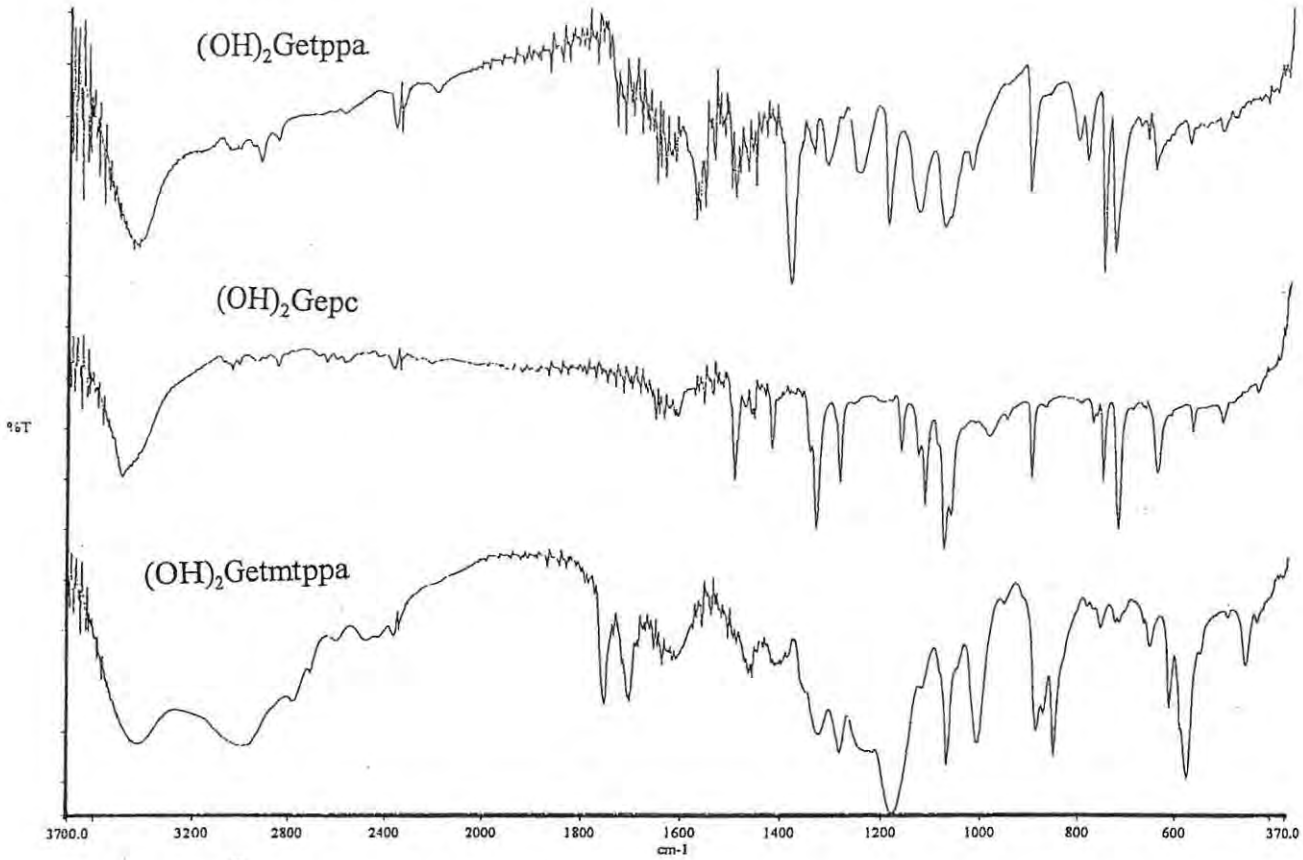

Figure 3.9 IR spectra of $(OH)_2$Getppa, $(OH)_2$Gepc and $[(OH)_2Getmtppa]^{4-}$ on KBr pellets.

Table 5 Infrared absorption bands of Mtppa complexes of Sn, Ge, Si and Zn using KBr pellets in wavenumbers (cm^{-1}). The relative intensities are given as b = broad, w = weak, s = strong, sh = shoulder and m = medium

Sntppa	Getppa	Sitppa	Zntppa	Assignment
376w	377w	_	_	
385w	387w	_	385m	
399	401	_	_	
413	_	_	(415)	
419	420	426w	(426)	C-C ring deformation
443b	_	449	_	
_	487	_	_	
535sh	515	535sh,(549)	_	C-C
556vs	_	_	_	Sn-O
_	583w	_	582w	C-C
_	647s	_	_	Ge-O
_	669w	_	_	Ge-Cl stetch
691	685	691vw	_	
737	736vs	737	734vs	π(C-H)
758	759	753	756	C-H out of plane
781vs	792m	781sh(794)	792	
813w	811w	810m	810s	C-H
_		830w		Si-O
_	870	_	_	(C-H)
902s	909s	900m	900s	
-	-	940w		O - Si -O

Table 5 continued.

_	_	960w	933 sh 960w	
1027vw	1030w	1029	1028s	C-H in plane bend
1064w	1072sh	1066sh	1066sh	C-H
1089	1084s	1075s	1088s	C-N stretch
	1137s	1129m	1129s	C-H in plane
			1188vs	
1252w	1251m	1251s	1251s	C-C vibrations
1363	1311m	_	1311	
1388sh	1388vs	1388s	1385s	C-C
1401	1476	1461	1479	
1569w	1572vs	1569m	1578vs	C-C stretch
	1627	1605	1655	C-C stretch
1737s	1737	1730w	1729	
2779w	2927w	_	_	
	3040m	3036w	3058w	C-H stretch

Table 6 gives the infrared bands of the Mtmtppa complexes. The major observed difference between the frequencies of Mtmtppa with Mtppa is the presence of a strong S - O stretch at around 1060 and 1180 and the C - O vibrational stretch at around 1015 cm^{-1} which are due to the counter anion for Mtmtppa complexes.

Table 6 Infrared absorption bands of Mtmtppa complexes of Sn, Ge, Si and Zn using KBr pellets in wavenumbers (cm^{-1}).

Sntmtppa	Getmtppa	Sitmtppa	Zntmtppa
376vw	377vw		370w
_	388vw		-
402w	395w		-
433w	434w	447s	-
456s	457s		-
_	_	532m	-
_	_	543w	547w
577vs	577vs	581s	578s
613s	616s	_	612sh
_	647m	648m	_
662m	667sh	_	_
670m	_	690s	_
_	728m	740m	732s
_	759m	751s	755vs
780m	786w	_	_
850vs	851s	836s	_
_	863w	_	_
_	873m	_	_
885vs	882vs	_	898s
_	951w	_	901w

Table 6 continued.

1016s	1009s	1025s	1002s
1070vs	1070vs	1067w	1048s
_	_	_	1117w
1179vs	1178vs	1183s	1183s
_	1753s	1725m	1468s
2781w	2780w	_	1591s
2985w	2995m, b	_	1742w
_	2980	_	3073s
3405s	3436s,b	3450s	3444s

4. Electrochemistry of tmtppa complexes of Si, Ge, Sn and Zn

Cyclic voltammetry (CV) was performed both on macroelectrodes (Pt diameter 1.6mm) and microelectrodes (platinum microelectrode, diameter11 μm) working electrodes; with macroelectrode data collected in water and microelectrode in DMSO. As the Mtppa complexes were not soluble enough for CV, these were not studied. The CV data for Gepc, Sipc, Snpc and Znpc complexes is known.[93] Only CV data for tmtppa complexes of Ge, Si, Sn and Zn is discussed below. Electrochemical data has been reported before for Zntmtppa[83] hence only its microelectrode data is presented.

It is important to note that $(OH)_2$Getmtppa and Zntmtppa complexes used for cyclic voltammetry were partly reduced in water as noted before in section 3.1. In addition to the weak spectral bands indicative of the reduced species these complexes still had intense Q band. $(OH)_2$Sitmtppa complex was reduced to a much larger extent than the Ge and Zn complexes, see Figure 3.4. Only the $(OH)_2$Sntmtppa complex showed no evidence of reduction before use in CV. Figure 4.1 shows the cyclic voltammogram of $[(OH)_2Sntmtppa(-2)]^{4+}$ in water containing Na_2SO_4 on platinum disc electrode.

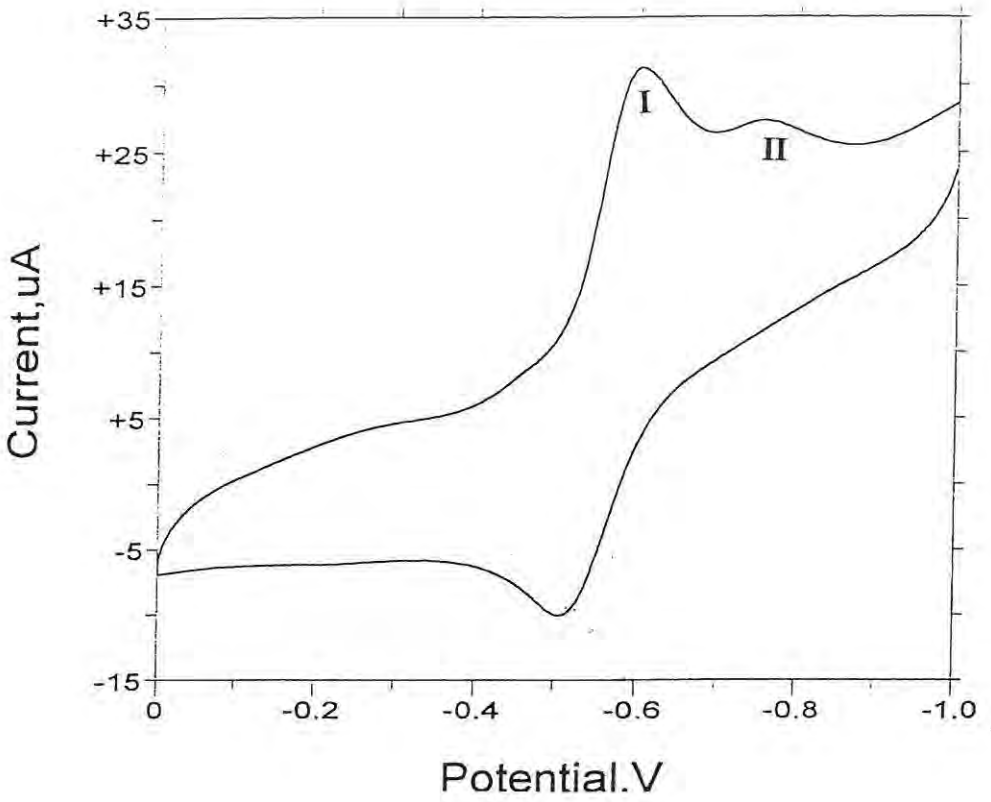

Figure 4.1 Cyclic voltammogram of $[(OH)_2Sntmtppa]^{4+}$ in water, vs Ag|AgCl. Scan rate100 mV/s.

Two reduction processes were observed, the first at a half-wave potential of $E_{1/2}$ = -0.57 V (process I) and the second as a peak at -0.76 V (process II) vs Ag|AgCl for $[(OH)_2Sntmtppa]^{4+}$. The second reduction did not show a reverse peak on the reverse scan showing that it is irreversible. The shape of the peaks due to process I and process II did not change with change in scan rate showing that no intermediate products were produced. The positions of the reduction processes also did not change with scan rate, Figure 4.2.

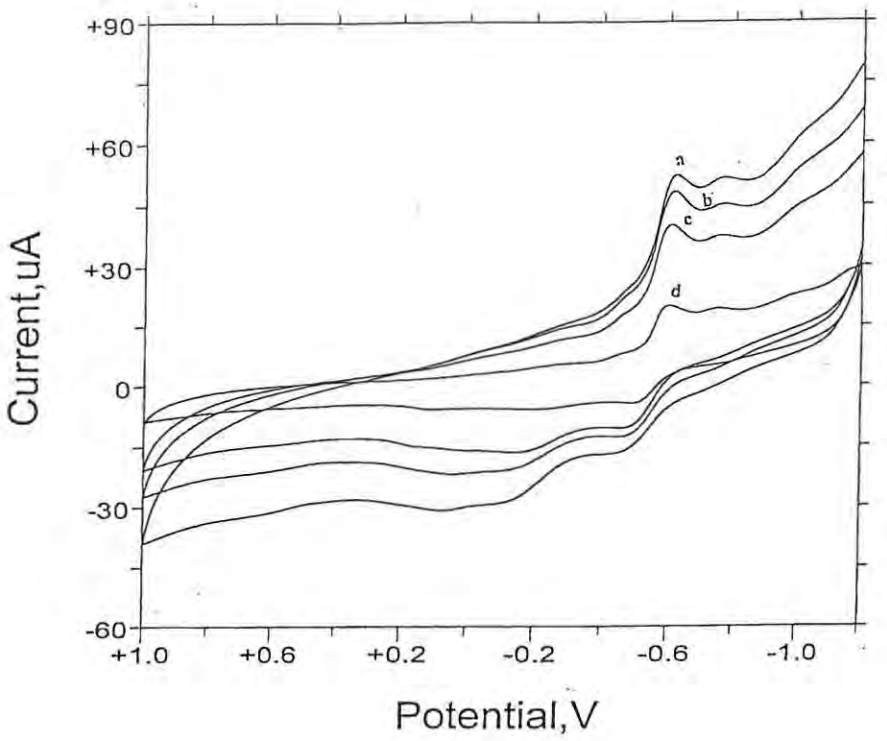

Figure 4.2 Cyclic voltammograms (*vs* Ag|AgCl) of $[Sntmtppa]^{4+}$ as the scan rate is varied on a platinum electrode. Scan rates starting from the outside are (a) 400, (b) 300, (c) 200 and (d) 50 mV/s. Water containing Na_2SO_4 as an electrolyte.

The plot of the i_c of the first reduction couple (process I) *vs* square root of the scan rate gave a linear relationship which indicates that the process was diffusion controlled, Figure 4.3.

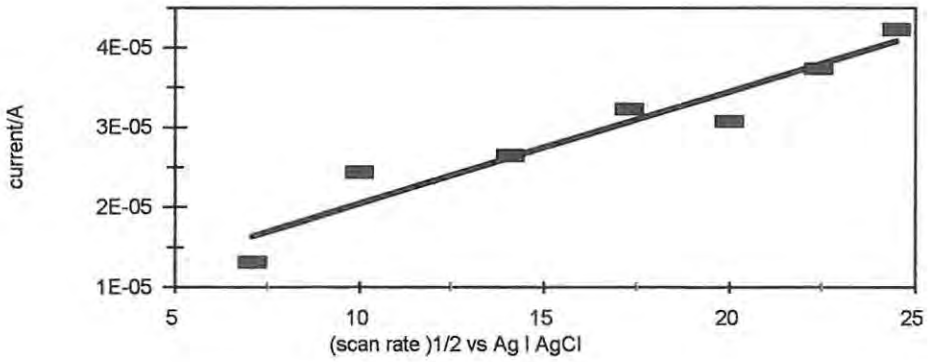

Figure 4.3 Plot of i_c *vs* square root of the scan rate for process I (first reduction couple) for $(OH)_2$Sntmtppa.

A summary of the half wave potentials for the $[Mtmtppa]^{4+}$ under study in this work is given in Table 7 below.

Table 7 Electrochemical data ($E_{1/2}$) for Mtmtppa complexes of Ge, Si, Sn and Zn. Where ME = Microelectrode and * indicates no reverse peak.. ME studies done in DMSO without an electrolyte.

Complex	$E_{1/2}$ /V or E_p /V (vs Ag/AgCl)	ΔE/mV	i_c / i_a	# of ME peaks.
$[(OH)_2Getmtppa(-2)]^{4+}$	-0.54 -0.63	230	1.9	4
$[(OH)_2Sntmtppa(-2)]^{4+}$	- 0.57 - 0.76*	78	1.8	6
$[(OH)_2Sitmtppa(-2)]^{4+}$	- 0.50	243	0.21	4

Process I was observed at $E_{1/2}$ -0.50 and -0.54 V for $[(OH)_2Sitmtppa(-2)]^{4+}$ and $[(OH)_2Getmtppa(-2)]^{4+}$, respectively. Even though these complexes are partly reduced, the peaks for process I were

similar in shape to the peak observed in Figure 4.1 for the unreduced $[(OH)_2Sntmtppa(-2)]^{4+}$ species. The first reduction process agrees with the order of the electron donating abilities of the central metals in question. Tin, being the least electronegative of the three metals in group IV, imparts the least electron withdrawing tendency of the three on the ring. This is confirmed by the reduction potential being the most negative at -0.57 V for$[(OH)_2Sntmtppa(-2)]^{4+}$, followed by $[(OH)_2Getmtppa(-2)]^{4+}$ (-0.54 V) and lastly $[(OH)_2Sitmtppa(-2)]^{4+}$ at -0.50 V.

As explained in the introduction on page 43 a system is said to be reversible if the separation between the cathodic and the anodic currents (ΔE) is 58 mV for one electron systems. ΔE values slightly higher (70- 100 mV) than this are still considered reversible, depending on the reversibility of an internal standard such as ferrocene. Total irreversibility can be concluded when the reverse peak does not exist at all, thus process I was found to be reversible for $[(OH)_2Sntmtppa(-2)]^{4+}$ where $\Delta E =$ 78 mV was obtained, while process II is irreversible because no return peak was observed for it. For $[(OH)_2Getmtppa(-2)]^{4+}$ process II showed some reversibility in that there was a return peak. The ratio of anodic to cathodic currents were however not unity for process I which implied that true reversibility was not obtained for $[(OH)_2Sntmtppa(-2)]^{4+}$. For $[(OH)_2Getmtppa(-2)]^{4+}$ and $[(OH)_2Sitmtppa(-2)]^{4+}$ the ΔE values were greater than 200 mV implying irreversibility of the couples. This could be due to the fact that these species are partly reduced hence complicating the CV.

The magnitudes of the reduction currents were not the same for processes I and II suggesting that the number of electrons transferred during these processes were not the same, with process I showing larger currents than process II. From the work reported earlier[15] only two processes were

observed for the $[Pttmtppa]^{4+}$ and $[Pdtmtppa]^{4+}$ complexes, with one process a multi-electron reduction step.[15] Comparing this observation with the results above, it is assumed that the process I with the large currents could also be a multielectron reduction process. In comparison with literature[15], process I is therefore, tentatively assigned to the multielectron reduction of the methyl pyridyl groups. A closer look at Figure 4.1 shows a broad peak just before process I (~ E = 0.45 V). This peak has been observed before[15] and was assigned to ring reduction in $[Pttmtppa]^{4+}$ and $[Pdtmtppa]^{4+}$ complexes prior to the reduction of pyridyl methyl groups at process I.

Cyclic voltammery on a Pt microelectrode was carried out to determine the nature of the reduction process for the Mtmtppa complexes under study. The number of peaks obtained are listed in Table 6 and Figure 4.4 shows the cyclic voltammogram obtained for $[(OH)_2Sitmtppa(-2)]^{4+}$ on a platinum micro fibre electrode and in DMSO. In Figure 4.4 four reduction processes of similar peak heights (I to IV) were observed; four peaks were also observed for $[(OH)_2Getmtppa(-2)]^{4+}$. For $[(OH)_2Sntmtppa(-2)]^{4+}$, six reduction processes were observed. The four peaks suggest that for $[(OH)_2Sitmtppa(-2)]^{4+}$ and $[(OH)_2Getmtppa(-2)]^{4+}$ the methyl groups of the pyridine complexes are being reduced and that $E_{½}$ values of their redox processes were so close that they overlapped on macroelectrode for process I. The same assumption still holds for $[(OH)_2Sntmtppa(-2)]^{4+}$, the additional two peaks being probably due to redox processes on the ring. A close look at Figure 4.4 shows that prior to process I there is a weak peak, labeled I*, which could be due to ring reduction also observed in Figure 4.1 before process I. Ring reduction is known to occur before the reduction of methyl pyridyl groups in Pt, Pd, Zn, Cu, and Ni tmtppa complexes.[15,83]

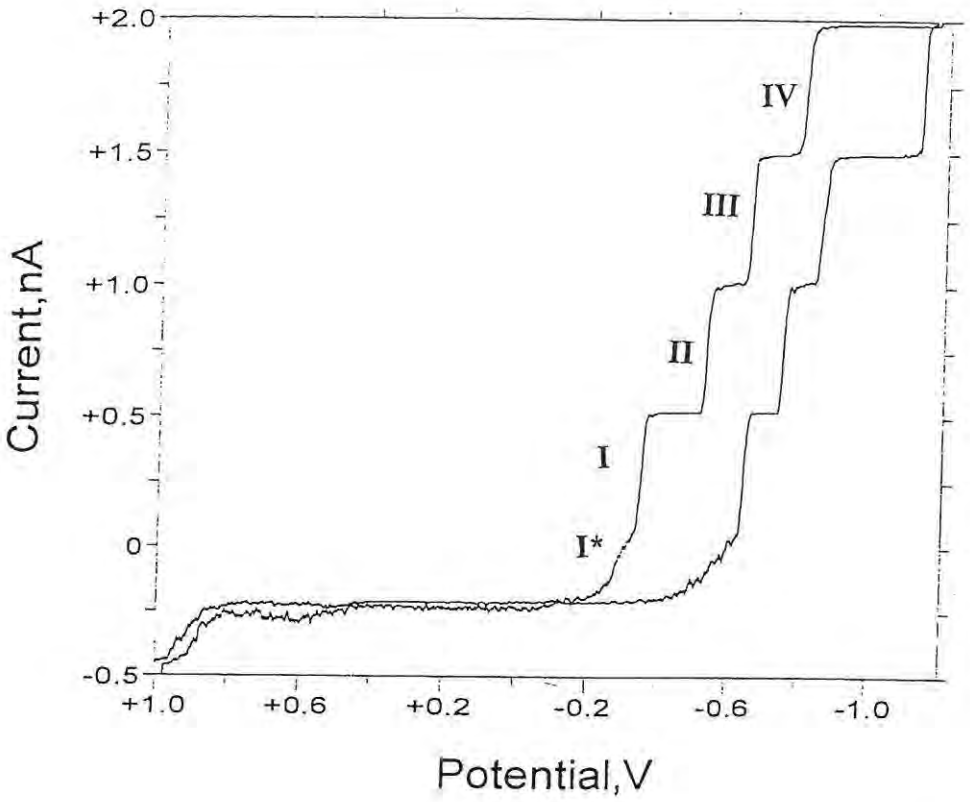

Figure 4.4 Cyclic voltammogram obtained for $[(OH)_2Sitmtppa(-2)]^{4+}$ in DMSO on a microfibre electrode with a silver wire psuedoreference electrode. Scan rate 1 mV/s.

Bulk electrolysis of $[Mtmtppa]^{4+}$ in DMSO at a potential of -0.7 V resulted in spectral changes shown in Figure 4.5 for $[Zntmtppa(-2)]^{4+}$. Similar results were observed for $[(OH)_2Sntmtppa(-2)]^{4+}$. Attempts to reduce $[(OH)_2Getmtppa(-2)]^{4+}$ and $[(OH)_2Sitmtppa(-2)]^{4+}$ by bulk electrolysis were unsuccessful. This was probably due to the larger extent of reduction in these complexes, as evidenced by a larger background in the 500 - 600 nm region, Figure 3.6, where reduction peaks are located. Where reduction occurred, solutions changed from blue to purple for $[Zntmtppa(-2)]^{4+}$ and $[(OH)_2Sntmtppa(-2)]^{4+}$complexes. The products obtained could not be reoxidized electrochemically, however, dioxygen could regenerate > 50% of the original $[Mtmtppa(-2)]^{4+}$ species. The reduction

products were only obtained when DMSO was used but not in water solution, showing that the donor abilities of the solvent play an important role in the electrochemical reduction process.

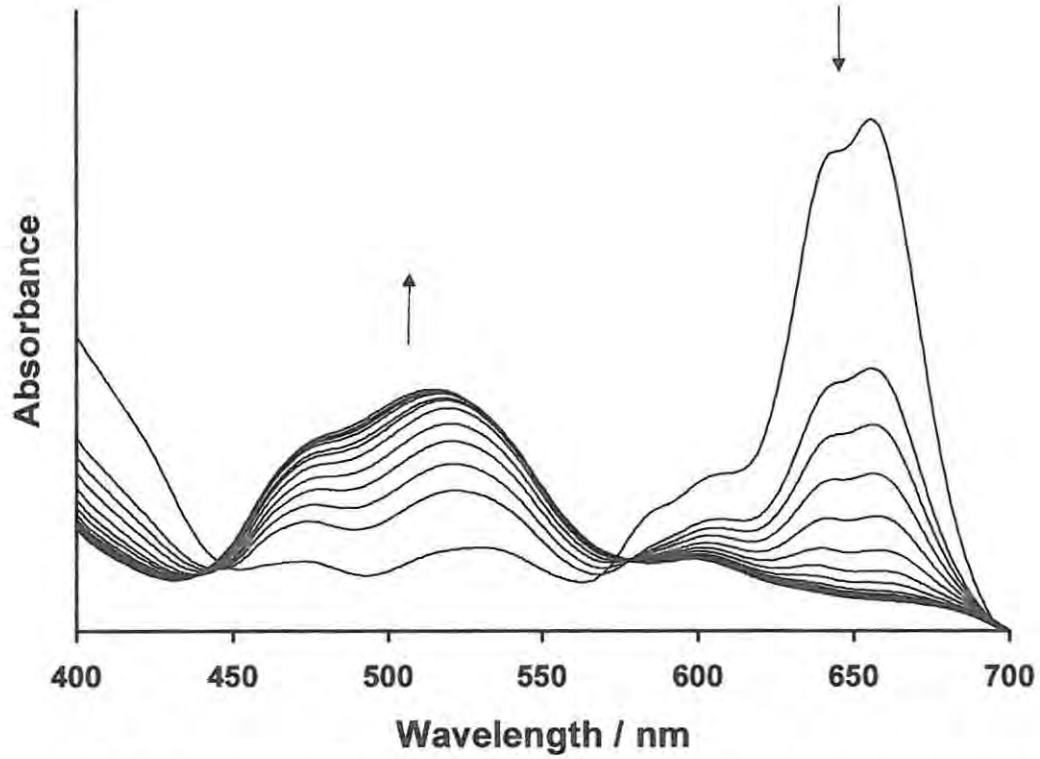

Figure 4.5 Absorption spectral changes observed during the electrochemical reduction of [Zntmtppa] in DMSO containing TEAP.

Figure 4.5 shows that the reduction occurs with isosbestic points at 573 and 445 nm. Isosbestic points are not formed with the original starting spectra, suggesting that more than two processes occur during the bulk electrolysis. The peaks observed for the reduced species are similar to those reported for the doubly reduced $[Zntmtppa(-4)]^{2+}$ species. The peak due to the formation of $[Zntmtppa(-3)]^{3+}$ at ~570 nm was not observed, hence suggesting that $[Zntmtppa(-3)]^{3+}$ is formed and is rapidly converted to $[Zntmtppa(-4)]^{3+}$, resulting in the lack of isosbestic points with the starting spectra, since

more than two species are present in solution. The final solution following bulk electrolysis showed a precipitate, a typical behaviour for the formation of $[Mtmtppa(-4)]^{2+}$ species. The lack of total reversibility is consistent with the CV data for process I. Reduction of $[Zntmtppa(-2)]^{4+}$ complex is known[83] to occur at the ring first, with the reduction at methyl pyridyl groups occurring later. It is possible that the reduction of the methyl groups also starts to proceed at the potentials used for bulk electrolysis.

5. Photochemical studies of tppa, tmtppa and pc complexes of Si, Ge, Sn and Zn

5.1 Photobleaching of Mtppa complexes

Figure 5.1 shows the absorption spectra changes observed on photolysis of Zntppa in DMSO in the Q band region. Photolysis was performed with the set-up shown in Figure 2.1, without the interference filter in place. Gradual decrease in the Q band absorption intensity without formation of new peaks in the UV and the visible regions takes place. This kind of photoprocess is termed photobleaching and reflects the breaking down of the conjugated chromophore structure of the dye.

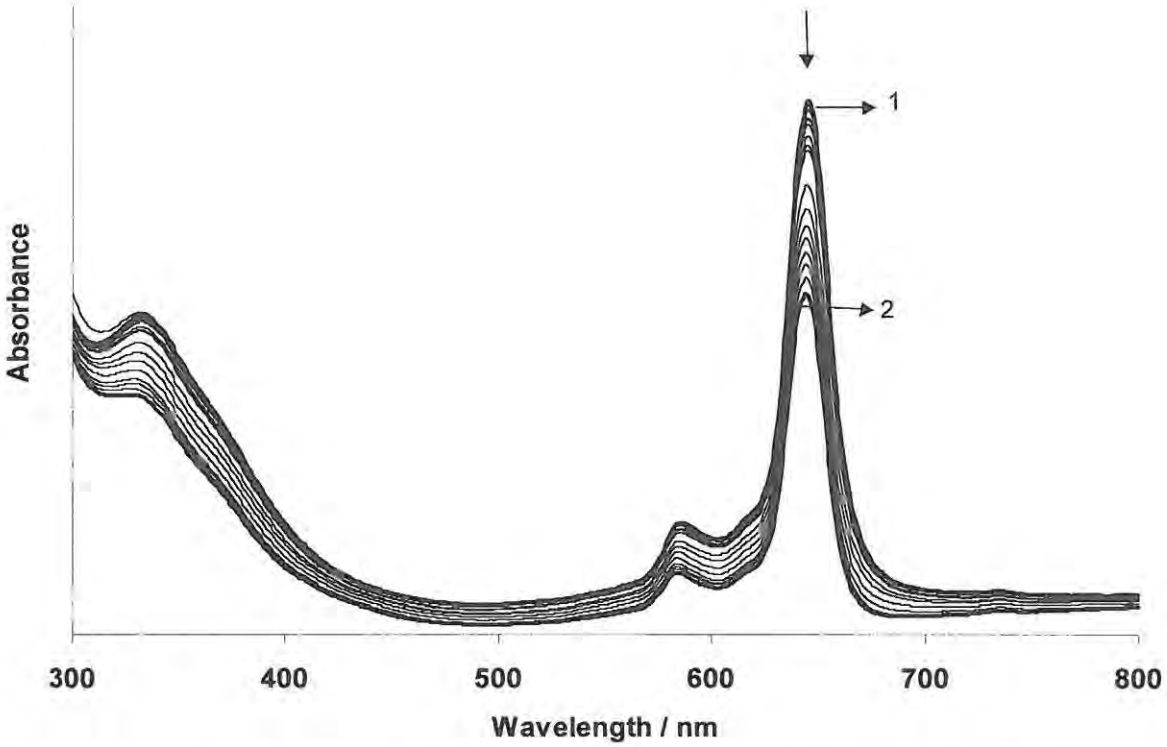

Figure 5.1 Absorption spectral changes during photolysis of Zntppa in DMSO. Photolysis time 1 = 0 and 2 = 20 min

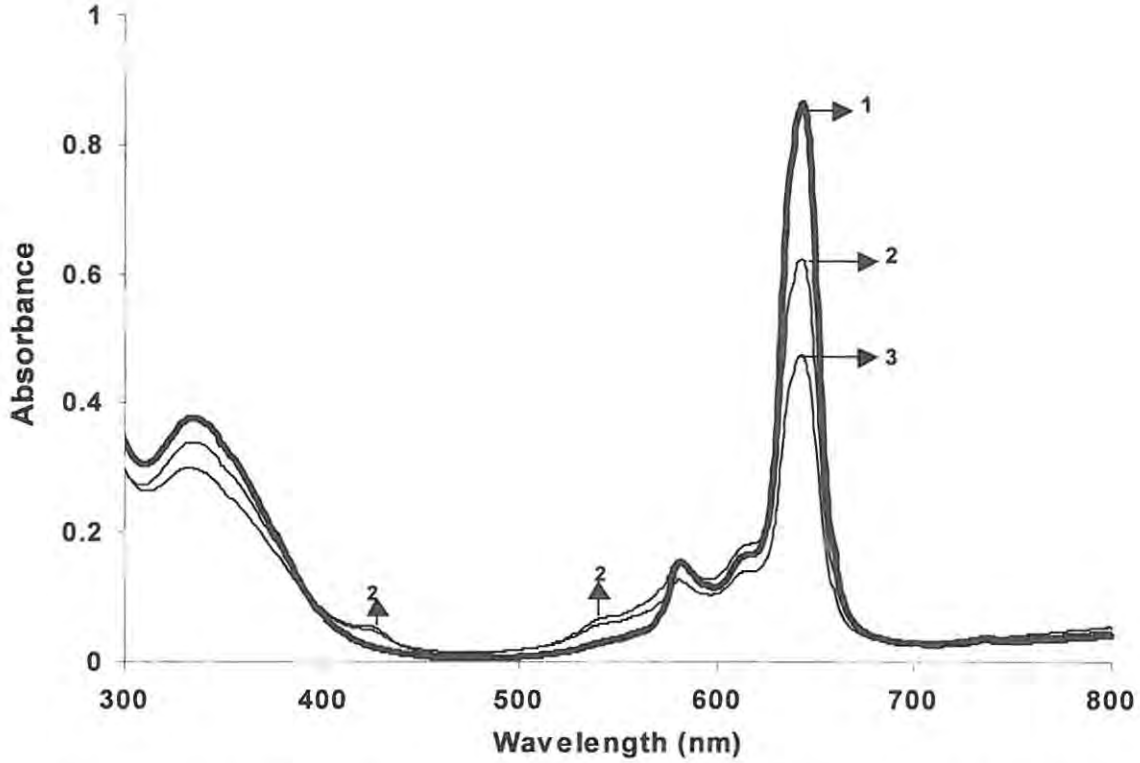

Figure 5.2 Spectral changes observed during photolysis of $(OH)_2$Getppa in DMSO at photolysis times (1) 0 min, (2) 30 sec and (3) 12 min.

The complexes, $(OH)_2$Getppa, $(OH)_2$Sntppa and $(OH)_2$Sitppa display slightly different behavior from that observed for Zntppa (Figure 5.1) under the same conditions. As demonstrated using $(OH)_2$Getppa, Figure 5.2, as an example, photobleaching and photoinduced change in the Q band absorption may be divided into two parts. The first part consists of up to 25% fast decrease in the Q band intensity with simultaneous increase of absorption in the short wavelength region around 420, 540 and 620 nm (spectra 2 in Figure 5.2). The peak at 540 nm is at the same wavelength as the peak due to the ring reduced species in porphyrazine complexes as discussed in section 3.1 hence

confirming photoreduction of the species. The peak at 420 nm is associated with ring reduction in Mpc complexes.[94] Chemical reduction (using sodium borohydride) of $(OH)_2$Getppa resulted in the formation of the same bands, hence confirming that the photobleaching is accompanied by reduction of the complexes. The reduction peaks at 420, 540 and 620 nm reached their peak absorbance within 30 seconds of photolysis. They then decreased in intensity as photolysis progressed, -clear photobleaching process was observed after this time. The relative kinetic curves for the decrease in the Q band absorption obtained under identical conditions, ($\lambda > 600$ nm excitation and without the use of an interference filter) for all the Mtppa complexes in DMSO, are presented in Figure 5.3.

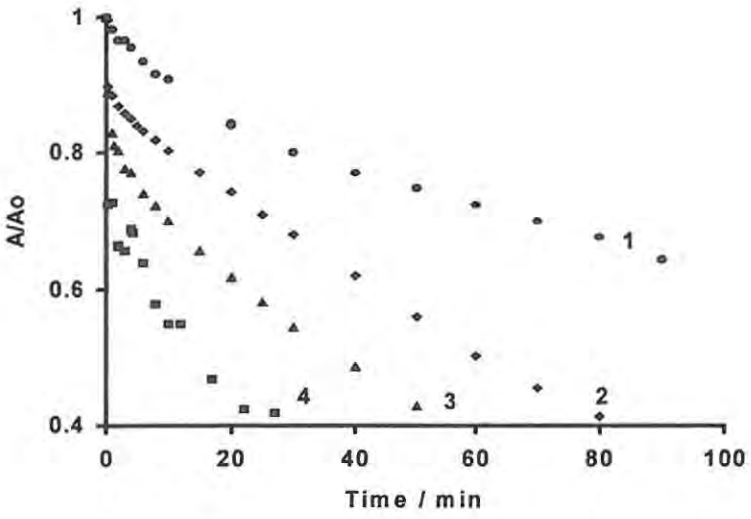

Figure 5.3 Kinetic curves for the photobleaching in DMSO in air for (1) Zntppa, (2) $(OH)_2$Sitppa, (3) $(OH)_2$Sntppa and (4) $(OH)_2$Getppa.

The plots in Fig. 5.3 show an initial fast decrease in Q band during the first 30 seconds of photolysis due to the reduction process described above, followed by a gradual decrease in the Q band

intensity as photobleaching progresses. Photobleaching rates of compounds under investigation differ slightly, with the lowest rate being for Zntppa and the highest rate for the $(OH)_2$Getppa complex.

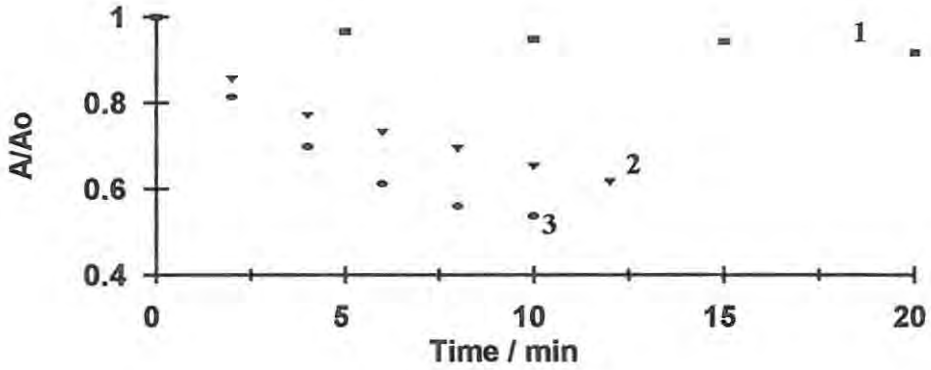

Figure 5.4 Kinetic curves for the photobleaching of $(OH)_2$Getppa in (1) oxygen, (2) air and (3) nitrogen saturated solutions.

Kinetic curves for the photobleaching of $(OH)_2$Getppa in DMF saturated with O_2, air or N_2 are presented in Figure 5.4. The curves shown represent only the photobleaching component, excluding the first step that leads to the initial formation of the reduced species. The quantum yields of photobleacing were calculated to be $(7.5 \pm 0.5) \times 10^{-5}$, $(5.0 \pm 0.5) \times 10^{-4}$ and $(1.2 \pm 0.2) \times 10^{-3}$, respectively, for O_2, air and N_2 saturated solutions of $(OH)_2$Getppa. The results obtained demonstrate that photobleaching rates and quantum yields of $(OH)_2$Getppa in DMF decrease with increase in oxygen concentration. The increase of photobleaching rate under nitrogen when compared to oxygen and air saturated solutions was observed for $(OH)_2$Getppa in DMSO as well. This observation is

inconsistent with macrocycle photooxidation by oxygen as the first photochemical step, but in agreement with photobleaching initiated by the photoreduction of the dye molecule. Photoreduction is thus responsible for the degradation of $(OH)_2$Getppa in DMF and DMSO solutions. A similar photobleaching pattern was observed for $(OH)_2$Gepc in DMF. In their study on the phototransformation of Zntppa in the presence of electron donors, Wohrle and coworkers [83] found that the electron-withdrawing effect of the annelated pyridine rings resulted in reductive quenching of the excited states of the Zntppa species. Thus, electron or hydrogen atom transfer from the solvent (S-H in the scheme below) to the excited porphyrazine molecule (Pz*) may be assumed as the first step in the photobleaching process.

$$Pz^* + S\text{-}H \rightarrow Pz^{\bullet -}(PzH^{\bullet}) + S\text{-}H^{\bullet +}(S^{\bullet}) \quad (1)$$

$$Pz^{\bullet -}(PzH^{\bullet}) + O_2 \rightarrow Pz + O_2^{\bullet -}(HO_2^{\bullet}) \quad (2)$$

$$S\text{-}H^{\bullet +}(S^{\bullet}) \xrightarrow{O_2} \text{peroxides} \quad (3)$$

$$O_2^{\bullet -}(HO_2^{\bullet}) \xrightarrow{S\text{-}H} H_2O_2 \quad (4)$$

$$Pz^{\bullet -}(PzH^{\bullet}) \xrightarrow{O_2} \text{oxidized products} \quad (5)$$

$$Pz \xrightarrow{H_2O_2,\ \text{peroxides}} \text{oxidized products} \quad (6)$$

Scheme 11 Proposed mechanism for photobleaching of the Mtppa and Mpc macrocycles.

H abstraction produces highly chemically reactive free radicals during step 1 of the photoreduction process. The free radicals react preferentially with residual oxygen. Interaction of semi-reduced dye radicals with oxygen results in the recovery of the dye according to step 2 of the Scheme. Examination of the recovery of $(OH)_2$Getppa after photolysis under N_2 conditions showed that bubbling dioxygen through a solution with 30-40% of photobleaching leads to about 50% recovery of the original Q band absorption of the dye, which may be considered as confirmation of step (2) of the Scheme. Further reactions of primary radicals may give oxidation products shown in reactions (3-6). The relative efficiency of the processes depends on the dye structure. Thus, primary photoreduction of dye in the presence of residual oxygen leads ultimately to degradation of the dye through oxidative process given by steps 3 to 6 of the Scheme. This type of substrate photooxidation initiated by photoreduction is known in organic photochemistry as photooxidation with chemical sensitization.

The relationship between photobleaching rates and electronic structure of dye molecules is consistent with a key role for dye photoreduction in photobleaching. Pyridinoporphyrazine macrocycle possesses higher electron accepting abilities than phthalocyanine. Thus, the kinetic curves presented on Figure 5.5 show that $(OH)_2$Getppa with electron-withdrawing pyridine rings in macrocycle structure have a significantly higher photobleaching rate than $(OH)_2$GePc.

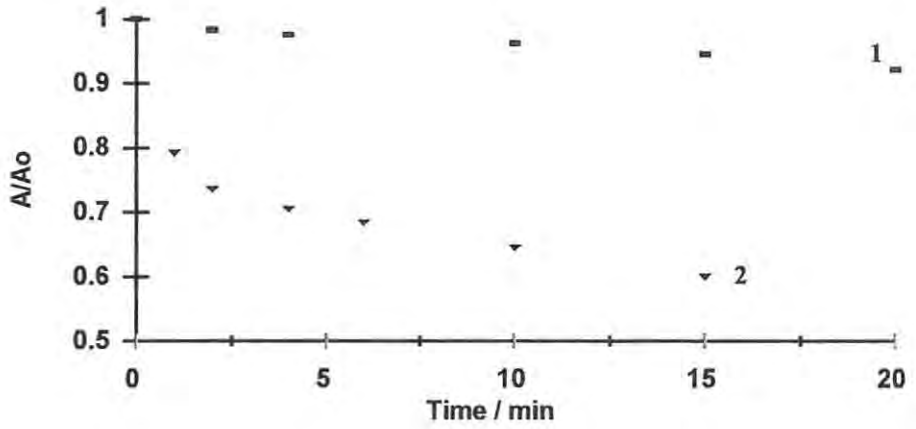

Figure 5.5 Kinetic curves for photobleaching in air for solutions of: (1) $(OH)_2$Gepc and (2) $(OH)_2$Getppa in DMF.

5.2 Singlet oxygen quantum yields of Mtppa complexes.

Singlet oxygen quantum yields (Φ_Δ) for $(OH)_2$Getppa, $(OH)_2$Sitppa, $(OH)_2$Sntppa and Zntppa are summarized in Table 8.

Table 8 Singlet oxygen quantum yields of porphyrazine metallocomplexes. The spectra in DMSO was recorded after allowing the solution turn blue. (a) corresponds to values in DMF (b) in water, no buffer.

Compound	ϕ_Δ
	DMSO
$(OH)_2$GePc	0.25 (0.38)[a]
$(OH)_2$Getppa	0.17 (0.22)[a]
$[(OH)_2$Getmtppa(-2)$]^{4+}$	<0.01 (0.48)[b]
$(OH)_2$SiPc	0.28
$(OH)_2$Sitppa	0.21
$[(OH)_2$Sitmtppa(-2)$]^{4+}$	0.01
$(OH)_2$SnPc	0.26
$(OH)_2$Sntppa	0.15
$[(OH)_2$Sntmtppa(-2)$]^{4+}$	0.02
Znpc	0.67 [92]
Zntppa	0.16
$[$Zntmtppa(-2)$]^{4+}$	0.06

Table 8 shows values of Φ_Δ ranging 0.15 to 0.21 for Mtppa complexes. Φ_Δ is thus only slightly affected by the nature of the central metal atom in the series of complexes studied. For comparison,

literature or experimental data of Φ_Δ values for the corresponding MPc complexes are also presented. Quantum efficiency of singlet oxygen production was generally measured in DMSO solutions -for $(OH)_2$GePc and $(OH)_2$Getppa the experiments were performed in DMF as well, with Φ_Δ value of 0.38 and 0.17, respectively. Values of Φ_Δ are higher in DMF when compared to DMSO, and for $(OH)_2$GePc in DMF, the Φ_Δ value is close to that reported in the literature (Φ_Δ = 0.42 for GePc complexes containing bulky axial substituents).[76] The information shown in Table 8 gives evidence for lower singlet oxygen quantum yields for the porphyrazine complexes when compared with the corresponding phthalocyanines. The low efficiency of singlet oxygen photogeneration by porphyrazines may be explained in terms of their short triplet state lifetimes. Triplet state lifetimes (τ_T) for some Mtppa (M = Mg, Zn, Cd, H) were found to be only ca. 10^{-7}s,[83] shorter than phthalocyanines containing a similar central metal, values as high as τ_T = 0.3 ms have been recorded for Znpc complex.[95] Since singlet oxygen is generated by energy transfer from the excited triplet state of the photosensitizer to ground state triplet oxygen, the high triplet state lifetime is an important prerequisite for efficient singlet oxygen photogeneration.

5.3 N, N′, N″, N‴-tetramethyl-2,3- tetrapyridinoporphyrazines phototransformation

The spectral changes, induced by Q band excitation (without an interference filter) of $(OH)_2$Sntmtppa in DMSO in the presence of air, are shown on Figure 5.6. A decrease of Q absorption band intensity and relative increase of short-wavelength absorption provide evidence for the formation

of a one-electron reduction product (absorption about 580 nm). There is also the formation of a weak broad band at 550 nm.

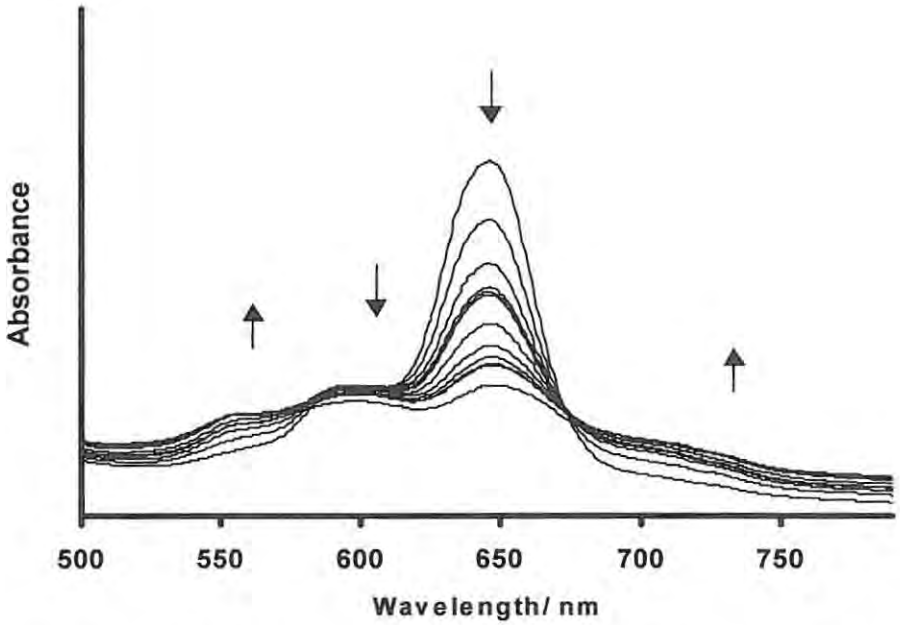

Figure 5.6 Electronic spectral changes during the photolysis of $[(OH)_2Sntmtppa]^{4+}$ in DMSO.

The lack of sharp isosbestic points in Figure 5.6 implies the presence of more than two species. This supports the suggestion that a stepwise transition from $[(OH)_2Sntmtppa(-2)]^{4+}$ to $[(OH)_2Sntmtppa(-3)]^{3+}$ and finally the $[(OH)_2Sntmtppa(-4)]^{2+}$ takes place. This is further evidenced by the observation that the band at 580 nm decreases in intensity after some time, while the one at 550 nm is progressively increasing in intensity. The product of the photoreduction reacts in a slow dark process with dioxygen resulting in recovery of the original $[(OH)_2Sntmtppa(-2)]^{4+}$ species with a Q band maxima at 642 nm. Addition of bromine increases the rate of regeneration of the $[(OH)_2Sntmtppa(-2)]^{4+}$ species thus confirming that the product is a reduced species. The spectral

changes are similar to those observed during the electrochemical reduction of $[(OH)_2Sntmtppa(-2)]^{4+}$ in DMSO as discussed in chapter 4. Photolysis of the $[Zntmtppa(-2)]^{4+}$ species in DMSO displays a similar photoredox behaviour to that shown in Figure 5.6 for $[(OH)_2Sntmtppa(-2)]^{4+}$. The results obtained confirm the conclusion of other researchers,[91] that alkylated tetramethyl-2,3-tetrapyridinoporphyrazines show a strong tendency towards photochemically induced reductive quenching of excited states by electron donors. DMSO may be acting as an electron donor in this case. Figure 5.7 presents the kinetics for the photoreduction of $[(OH)_2Sntmtppa(-2)]^{4+}$, the decrease in the Q band intensity obeys pseudo first-order rate law. Ge and Si complexes did not exhibit the photoreduction process observed for Sn and Zn complexes as shown in Figure 5.6. $[(OH)_2Getmtppa(-2)]^{4+}$ and $[(OH)_2Sitmtppa(-2)]^{4+}$ showed photobleaching as explained above for Mtppa complexes.

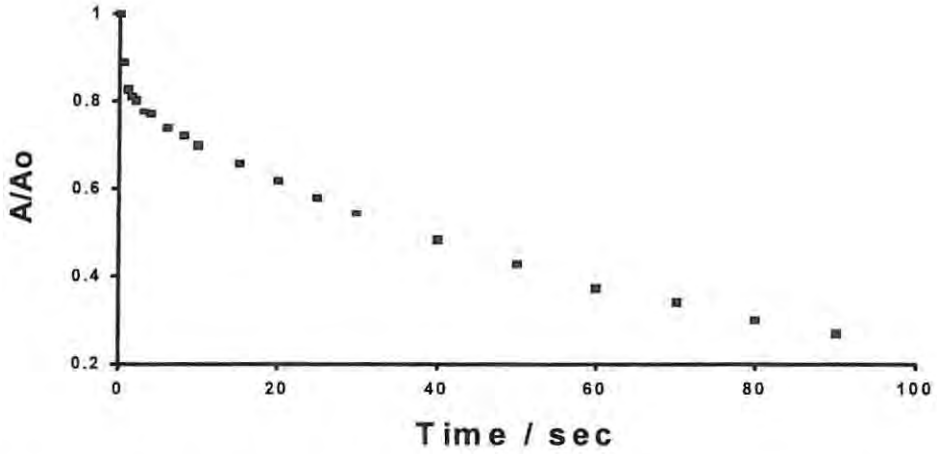

Figure 5.7 The plot of absorbance vs time during the spectroscopic changes observed for Sntmtppa in Figure 5.6.

Unlike in the behaviour reported above for DMSO and DMF, no light induced photoreduction of the $[Mtmtppa(-2)]^{4+}$ complexes was observed in water solutions, in the absence of added electron

donors. As discussed earlier in section 3.1, the spectra of the Zntmtppa and Getmtppa were partially reduced with broad bands in the 480 to 600 nm region in addition to the Q band. During photolysis, the initial flash of light brings about oxidation of the reduced component as evidenced by the decrease of short-wavelength absorption in the 480 to 600 nm, and a slight increase in the intensity of the Q band of the $[Zntmtppa(-2)]^{4+}$ species. Gradual photobleaching then follows as evidenced by the decrease in the spectra without formation of new peaks. Figure 5.8 shows spectral changes observed during the photolysis of $[Zntmtppa(-2)]^{4+}$ in acidic aqueous conditions where we obtained a more pronounced Q band and less of the reduced species when compared to pH 7.4 conditions.

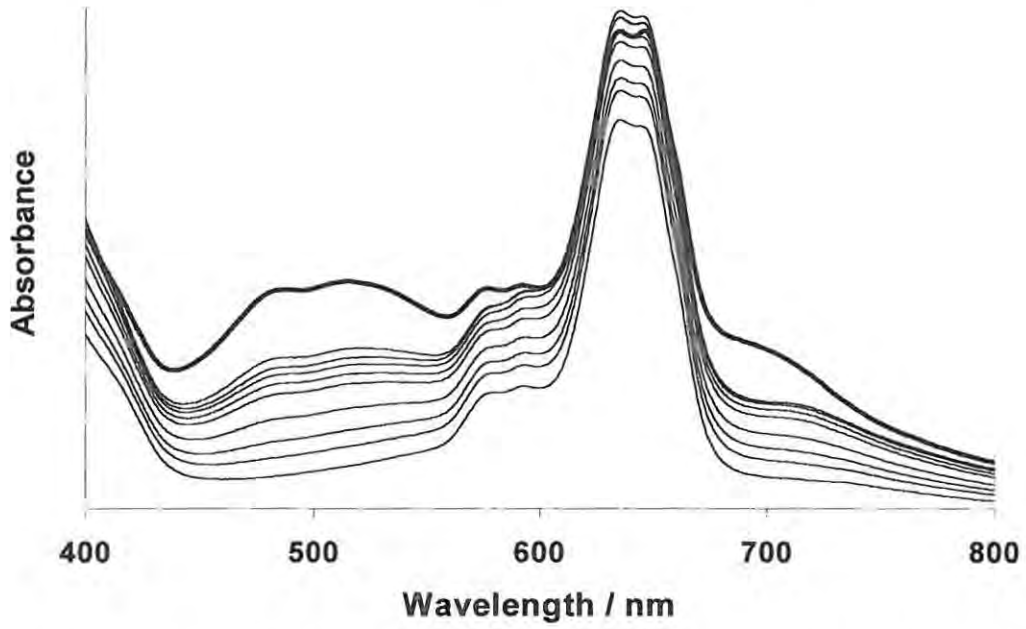

Figure 5.8 Spectral changes observed during the photolysis of $[Zntmtppa(-2)]^{4+}$ in pH4 buffer. The heavy line shows the original spectra.

Similar decrease of Q band with photolysis was observed for $[(OH)_2Sntmtppa(2-]^{4+}$,

$[(OH)_2Getmtppa(2-)]$, and $[(OH)_2Sitmtppa(-2)]^{4+}$ in water. The quantum yields of photobleaching are 6.60×10^{-5}, 1.8×10^{-5} and 5.4×10^{-6} for $[Zntmtppa(2-)]^{4+}$, Zntppa, and Znpc , respectively. In agreement with the proposed photobleaching mechanism involving initial reduction of the ring, is the fact that it is easier for porphyrazine macrocycles to photobleach than for pthalocyanine molecules bearing the same metal centre. Comparing the $[Zntmtppa(2-)]^{4+}$ with the Zntppa, the former is more easily reduced due to the extra methyl groups on the ring. This results in the $[Zntmtppa(-2)]^{4+}$ complex being more easily photobleached than the Zntppa species.

5.4 Singlet oxygen quantum yields of Mtmtppa complexes

Singlet oxygen quantum yields of $[Mtmtppa(-2)]^{4+}$ complexes in DMSO solution are summarized in Table 8, page 106. The Φ_Δ values, reflecting the state of aggregation of the compounds under investigation, are negligible ($\Phi_\Delta \leq 0.01$) for $[(OH)_2Getmtppa(-2)]^{4+}$ and $[(OH)_2Sitmtppa(-2)]^{4+}$ complexes. As discussed in Chapter 3 the $[(OH)_2Getmtppa(-2)]^{4+}$ and $[(OH)_2Sitmtppa(-2)]^{4+}$ are aggregated in DMSO solution as judged by the spectra and Beer`s law dependence at the concentrations used for this study. The monomeric complexes, $[Zntmtppa(-2)]^{4+}$ and $[(OH)_2Sntmtppa(-2)]^{4+}$ show slightly higher Φ_Δ values when compared to the aggregated Ge and Si complexes, but show low efficiencies of singlet oxygen photosensitization when compared to the corresponding Mpc and Mtppa complexes, Table 8. The generally low singlet oxygen formation for Mtmtppa complex when compared with Mtppa and Mpc complexes may be caused by low excited state lifetimes of the Mtmtppa complexes due to their enhanced degradation caused by competitive

reductive quenching.

Confirmation that the decay of DPBF was due to its reaction with singlet oxygen was done by adding a competitor singlet oxygen quencher 1,4-diazabicyclo [2.2.2]-octane (DABCO) to the experimental mixture, containing the dye and DPBF, in an air-tight sample cell. Photolysis of this control mixture reflected no change in the DPBF concentration. This indicated that the reaction between DPBF and $O_2(^1\Delta_g)$ was not taking place. In order to further confirm that DPBF is a quencher for singlet oxygen, the solution containing the dye and DPBF was deaerated with nitrogen and then photolysed in a tightly closed cell. Here again there was no change in DPBF concentration

As already discussed, the Mtmtppa complexes are generally reduced in water following synthesis except for Sn complex. The extent of reduction of $[(OH)_2Getmtppa]^{4+}$ depended on the synthesis conditions. Φ_Δ values were obtained only for the batch of $[(OH)_2Getmtppa]^{4+}$ species which showed minimum reduction in water. Interestingly, the Φ_Δ value for this batch of $[Getmtppa]^{4+}$ in water is much higher than even its corresponding Mtppa complex, Table 8. The value is close to the literature values for the highly alkalyted Gepc complexes in CH_3Cl. This observation confirms the reasoning above that aggregation is the reason behind the low Φ_Δ values in DMSO, because, as can be seen from Figure 5.9, this batch of Getmtppa was monomeric in water.

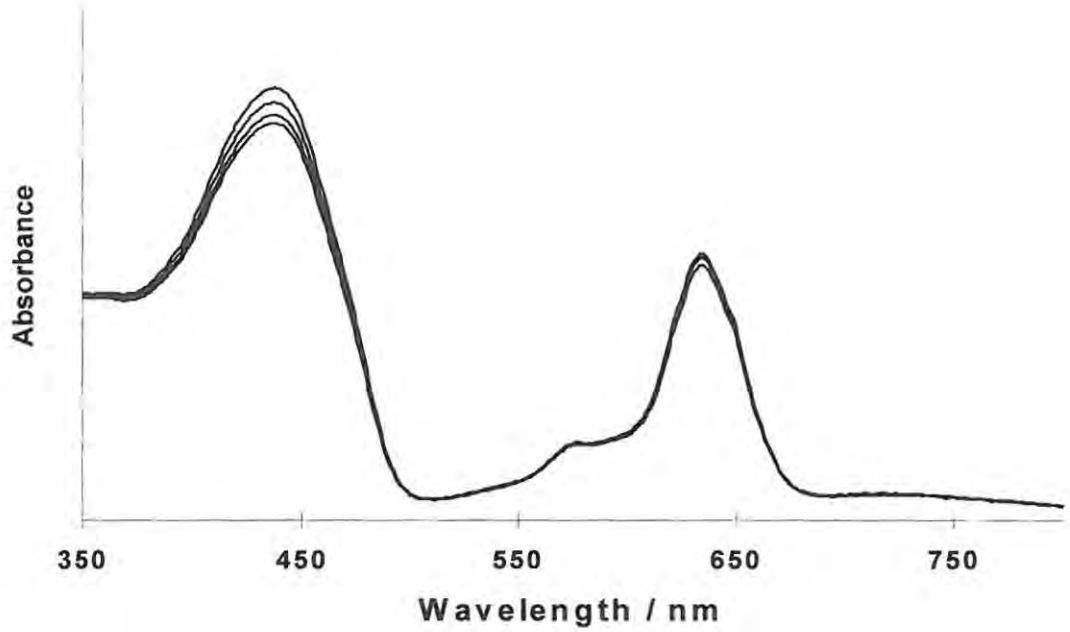

Figure 5.9 Spectral changes observed during the photolysis of $[(OH)_2Getmtppa(2-)]^{4+}$ in the NA Φ_Δ determination in aqueous medium.

5.5 Singlet oxygen quantum yield for Mpc complexes

Table 9 Singlet oxygen quantum yields for axially ligated Snpc complexes.

Compound	ϕ_Δ in DMSO
Br_2Snpc	0.25
I_2Snpc	0.35
Cl_2Snpc	0.37
$(OH)_2Snpc$	0.25

Values of ϕ_Δ obtained for $(X)_2$Snpc complexes where x is OH^- or halogens are summarised in Table 9. Values of ϕ_Δ vary from 0.25-0.37 for the Snpc complexes with varying ligands showing that the nature of the ligand can considerably affect the value ϕ_Δ. It is expected that the Snpc complexes containing heavier axial ligands such as I_2 should have higher intersystem crossing and hence higher triplet excited state yields. This would then result in higher Φ_Δ values. But as Table 9 shows, this is not the case, suggesting that other factors such as triplet state life-times are important.

6 Future studies and conclusion

It is well known that complexes of phthalocyanines with non-transition metals have long-lived excited states, high triplet state quantum yields and therefore sensitize singlet oxygen efficiently. Phthalocyanines and their derivatives are thus promising sensitizers for different applications including PDT. In the present study the efficiency of phthalocyanine pyridine analogs, tetra-2,3-pyridinoporphyrazine complexes with diamagnetic metals, such as Zn, Si, Sn and Ge in sensitization of singlet oxygen were examined for the first time. It was found that the increase in the electron-withdrawing character of the phthalocyanine macrocycle periphery leads to a decrease in singlet oxygen quantum yields, probably due to enhanced excited states reductive quenching in DMSO. Conversely in water, the quantum yield of Getmtppa was found to be even higher than for Gepc. The most outstanding property of tetra-2,3-pyridinoporphyrazines is their enhanced ability to act as oxidizing agents. Under visible light excitation and in organic media, the pyridinoporphyrazines sensitize the formation of radicals in electron transfer process, through a Type I mechanism. Since Type I mechanism is also important for PDT, tetra-2,3-pyridinoporphyrazines and their water-soluble quaternized forms cannot be ruled out as promising sensitizers for this application and need further investigations. Due to enhanced oxidizing ability pyridinoporphyrazines may be interesting also as photoredox sensitizers for functional materials.

In order to confirm reasons behind the low singlet oxygen quantum yields, further studies on the other photophysical aspects of these compounds need to be done. As earlier said, the knowledge of the rest of the photophysical data on these compounds would provide a better insight into whether

they can be expected to be good sensitizers even through Type I mechanism..

Future work could also include studying pyrazines i.e porphyrazines with two nitrogen atoms on the outer rings and investigating the effect of the electron withdrawing groups on the photophysical data of porphyrazines. A study of the effect of different electron donor and acceptor solvents would clarify the complex behaviour of the Mtmtppa studied in this work. Finally, cell studies still need to be done with the tmtppa and the tppa complexes of Ge, Si, Sn and Zn. It has been said that not only does the charge of the molecule affect the photophysical status, but also the rate of incorporation and absorption into cells during PDT. Cell studies would thus prove whether this applies with these porphyrazine type molecules.

References

1. R. L. Milgrom in *Colours of Life: An introdution to chemistry of porphyrins and related compounds.* Oxford University Press (1977).
2. A. P. B. Lever, *Adv. Inorg. Radiochem.*, 1965, 7, 27.
3. R. P. Linstead, E. G. Noble, J. M. Wright, *J. Chem. Soc.*, 1937, 911.
4. J. M. Robertson,*J. Chem. Soc.*, 1935, 615.
5. T. Nyokong, *S. Afr. J. Chem.*, 1995, **48**, 23.
6. J. M. Robertson, *J. Chem. Soc.*, 1936, 1195.
7. T. Torres, *J. Porphyrins Phthalocyanines.* 2000, **4**, 325.
8. M. K. Lowey, A. J. Starshak, J. N. Esposito, P. C. Krueger, M. E. Kenney, *Inorg. Chem.*1965, **4**, 128.
9. P. C. Krueger, M. E. Kenney, *Inorg. Chem*, 1963, 3379.
10. E. Ağar, S. Şaşmaz, İ. E. Gümrükçüoğlu, M. Özdemir, *Dyes and Pigments*, 1998, **36,** 407.
11. T. D. Smith, J. Livorness, H. Taylor, *J. Chem. Soc. Dalton Trans.*, 1983, 1391.
12. K. Kasuga, M. Morisada, M. Handa, *Inorg. Chim. Acta,* 1990, **174**, 161.
13. M. J. Danzig, C. Y. Liang, E. Passaglia, *J. Am. Chem. Soc.*, 1963, **85**, 668.
14. R. Gerdes, D. Wohrle, W. Spiller. G. Scheider, G. Schnurpfeil, G. Schulz-Ekloff, *J. Photochem. Photobiol. A: Chem.*, 1997, **65**, 95.
15. M. Sekota, T. Nyokong, *J. Porphyrins Phthalocyanines,* 1999, **3**, 477.
16. M. Thamae, T. Nyokong, *J. Electroanal. Chem.* 1999, **470**, 126.
17. M. Gouterman in D. Dolphin (ed) *The porphyrins: Physical Chemistry*, Vol 3, part A, Academic Press New York, 1978, 1.

18. A.B.P. Lever, S. Licoccia, K. Magneli, P. C. Minor, B. S. Ramaswamy, *J. Am. Chem. Soc.* 1982, **11**, 237.

19. M. J. Stillman, T. Nyokong in C. C. Leznoff and A. B. P. Lever (ed) Phthalocyanines: Properties and Applications, VCH, Vol 1, Chapt. 3, 1989.

20. B. W. Dale, *Trans. Faraday Soc.*, 1969, **65**, 311.

21. A. B. P. Lever, M. R. Hempstead, C. C. Leznoff, W. Liu, M. Melnik, W. A. Nevin, P. Seymour, *Pure and Appl. Chem.* 1986, **58**, 1467.

22. D. W. Clark, J.R. Yandle, *Inorg. Chem.* 1972, **11**, 1738.

23. T. Nyokong, Z. Gasyna, M. J. Stillman, *J.Am. Chem. Soc.*, 1986, 309.

24. T. Nyokong, *Polyhedron*, 1993, **12**, 375.

25. G. Knor, *Inorg. Chem.*, 1996, **35**, 7916.

26. N. Sasa, K. Okada, K. Nkamura, S. Okada, *J. Molecular Structure,*1998, **448**, 163.

27. M. M. Nicholson in C.C.Leznoff and A. B. P. Lever (eds) Phthalocyanines: Properties and applications, VCH, Vol 1, Chapt. 2, 1989.

28. P. Vasudevan, N. Phougat, A. K. Shukla, *Applied Organometallic Chemistry,* 1996, **10**, 591.

29. N. R. Armstrong, *J. Porphyrins Phthalocyanines,* 2000, **4**, 414.

30. J. H. Zagal, *Coord. Chem. Rev.*, 1992, **119**, 89.

31. K. Hanabusa, R. P. Shirai, in: C. C. Leznoff, A. B. P. Lever (eds.) Phthalocyanines: Properties and Applications,VCH, Vol. 2, New York, 1993.

32. N. Kobayashi, W. A. Nevin, *Appl. Organomet. Chem.*. 1996, **10**, 591.

33. R. M. Ion, *Prog. Catal.* 1998, **2**, 113.

34. J. Limson, T. Nyokong, *Electroanalysis,*1998, **10**, 988.

35. S. L. Vilakazi, T. Nyokong, *Polyhedron,* 1998, **17**, 4415.

36. S. Vilakazi, T. Nyokong, *Polyhedron,* 1999, **19**, 229.

37. J. Oni, T. Nyokong, *Polyhedron,* 2000, **19**, 1355.

38. J-Z. Li, X-Y. Pang, D. Gao, R-Q. Yu, *Talanta*, 1995, **42**,1775.

39. N. B. Mckeown, *Chemistry and Industry*, Feb 1999, **1**, 92.

40. P. Gregory, *J. of Porphyrins and Phthalocyanines*, 2000, **4**, 432.

41. P. Gregory, *J. of Porphyrins Phthalocyanines*, 1999, **3**, 468.

42. Y. Tse, P. Janda, A. P. B. Lever, *Anal. Chem.*, 1994, **66**, 384.

43. P. Janda, J. Weber, L. Dunsch, A. P. B. Lever, *Anal. Chem.*, 1996, **68**, 960.

44. O. L. Kaliya, E. A. Lukyanets, G. N. Vorozhtsov, *J. Porphyrins Phthalocyanines, 1999,* **3**, 592.

45. S. B. Brown, T. G. Truscott, *Chem in Britain*, 1993, 955.

46. D. D. Ebbing, *General Chemistry*, 5th ed. Houghton Mifflin Company, Boston USA, 1996.

47. J. D. Lee, *Concise Inorganic Chemistry*, 4th ed., Chapman and Hall, London, 1991.

48. P. Suppan, *Chemistry and Light*, 1st ed., The Royal Society of Chemistry, Cambridge. 1994.

49. A. J. MacRobert, D. Phillips, *Chemistry and Industry*, 1992, **1**, 1.

50. P. A. Wingo, L. A. G. Ries, H. M. Rosenberg, D. S. Miller, B. K. Edwards, *Cancer*, 1998, **82**, 6, 1198.

51. J. Miller, *J. Chem. Ed.*, 1999, **76**, 592.

52. W. Spiller, H. Kliesch, D. Wörhle, S. Hackbarth, B. Röder, G. Schnurpfeil, *J. Porphyrins Phthalocyanines,* 1998, **2**, 145.

53. D. Phillips, *Pure and Appl. Chem.* 1995, **67**, 117.

54. T. J. Dougherty, *Photochemistry and Photobiology*, 1987, **45**, 879.

55. D. Phillips, *Science Progress*, 1993/94, **77**, 295.

56. M. J. Abrams, *Platinum Metals Rev.*1995, **39**, 14.

57. E. D. Sternberg, D. Dolphin, *Tetrahedron*, 1998, **54**, 4152.

58. R. K. Pandey, *J. Porphyrins Phthalocyanines*, 2000, **4**, 368.

59. T. D. Mody, *J. Porphyrins Phthalocyanines*, 2000, **4**, 362.

60. J. L. Sessler, N. A. Tvermoes, J. Davis, P. Anzenbacher Jr, K. Jursikova, W. Sato, D. Seidel, V. Lynch, C. B. Black, A. Try, B. Andioletti, G. Hemmi, T. D. Mody, D. J. Magda, V. Kral, *Pure Appl. Chem.*, 1999, **71**, 2009.

61. G. Kosterich, T. Babushkina, A. Lavi, Y. Langzam, Z. Malik, A.Orestein, B. Ehrenberg, *J. Porphyrins Phthalocyanines*, 1998, **2**, 383.

62. S. B. Brown, T. G. Truscott, *Chemistry in Britain*, Nov. 1993.

63. M. Peeva, M. Shopova, N. Stoichkova, N. Michailov, D. Wöhrle, S. Müller, *J. Porphyrins Phthalocyanines*, 1999, **3**, 380.

64. K. Scheiweck, H-G. Capraro, U. Isele, E. Batt, M. Ochsner, P. van Hoogevest, W. A. Love, *SPIE*, 1994, **2078**, 165.

65. C. Y. Anderson, K. Freye, K. A. Tubesing, Y-S Li, M. Kenney, H. Mukhtar, C. A. Elmets, *Photochem. Photobiol.*, 1998, **67**, 332.

66. M. Shopova, D. Wohrle, V. Mantareva, S. Mueller, *Journal of Biomedical Optics*, 1999, **4**, 276.

67. M. Gabriela Lagorio, Lelia E. Dicelio, Enrique A. San Roman, *J. Photochem. Photobiol. B. Biol.*, 1989, **3**, 615.

68. X. Zhang, H. Xu, *J. Chem. Soc. Faraday Trans.*, 1993, **89**, 3347.

69. R. Decrèau, A. Viola, J. Richard, A. Jeunet, M. Julliard, *J. Porphyrins Phthalocyanines*, 1998, **2**, 405.

70. E. A. Lukyanets, *J. Porphyrins Phthalocyanines*, 1999, **3**, 424.

71. S. Dhami, D. Phillips, *J. Photochem. Photobiol., A: Chem.*, 1996, **100**, 77.

72. R. Edrei, V. Goddfried, J. E. van Lier, S. Kimel, *J. Porphyrins Phthalocyanines*, 1998, **2**, 191.

73. S. R. Wood, J.A. Holroyd, S. B. Brown, *Photochem. Photobiol.*, 1997, **65**, 397.

74. A. D. Sully, R. B. Ostler, D. Phillips, P. O`neill, K. M. S. townsend, A. W. Parker, A. J. MacRobert, *Bioimaging*, 1999, **5**, 9.

75. L. Milgrom, S. MacRobert, *Chemistry in Britain*, May 1998.

76. H. G. Capraro, K. Schieweck, R. Hilfiker, M. Ochsner, U. Isele, P. van Hoogevest, R. Naef, M. Buamann, *SPIE*, 1994, **2078**, 158.

77. E. Samuel, *New Scientist*, Sept. 2000, 21.

78. W. R. Heineman and P. T. Kissinger in *Laboratory Techniques in Electrochemistry*, Marcel Dekker (1996) New York.

79. A. J. Bard and L. R. Faulkner in *Electrochemical methods; Fundamentals and Application,* John Wiley & Sons, New York (1980) 1st ed.

80. J. Wang in *Analytical Electrochemistry* VCH publishers Inc. (1994) New York.

81. D. Shoup, A. Szabo, *J. Electroanal. Chem.*, 1982, **140**, 237.

82. A. B. P. Lever, *J. Porphyrin Phthalocyanine*, 1999, **3**, 488.

83. D. Wohrle, J. Gitzel, I. Okura, S. Aono, *J. Chem. Soc. Perkin Trans.*, 1985,**11**, 1171.

84. E. E. Wegner, A. W. Adamson, *J. Am. Chem. Soc.*, 1966, **88**, 394.

85. H. J. Guiraud, C. S. Foote, *J. Am. Chem. Soc.*, 1976, **98**, 1984.

86. I. Kraljic, S. Monsni, *Photochem. Photobiol.* 1978, **28**, 577.

87. J. Farnandes, M. Bilgin, L. Grossweiner, *J. Photochem. Photobiol. B,* 1997, **37**, 131.

88. C. W. Dirk , T. Inabe, K. F. Schoch, Jr., T. J. Marks, *J. Am. Chem. Soc.*, 1983, **105**, 1539.

89. K. A. Bello, I. A. Bello, *Dyes and Pigments*, 1997, **35**, 261.

90. R. D. Joyner, M. E. Kenney, *J. Chem. Soc.* , 1960, **82**, 5790.

91. J. N. Espito, L. E. Sutton, M. E. Kenny, *Inorg. Chem.* 1967, **6**, 1116.

92. N. Kuznetsova, E. Makarova, S. Dashkevich, N. Gretsova, V. Negrimovsky, O. Kaliya, E. Luk`yanets, *Zh. Obshch. Khim.* 2000, **70**, 140.

93. A. B. P. Lever, E. R. Milaeva, G. Speier, Phthalocyanines: Properties and Applications. A. B. P. Lever, C. C. Leznoff (Eds.) Vol. 3, VCH Publishers, New York, 1993.

94. M. J. Stillman,Phthalocyanines: Properties and Applications. A. B. P. Lever, C. C. Leznoff (Eds.) Vol. 3, VCH Publishers, New York, 1993.

95. J. R. Darwnt, P. Douglas, A. Harriman, G. Porter, M.-C. Richoux, *Coord. Chem. Rev.* 1982, **44**, 83.

Abstract

Metallophthalocyanine complexes containing non-transition metals are very useful as sensitizers for photodynamic therapy, a cure for cancer that is based on visible light activation of tumour localized photosensitizers. Excited sensitizers generate singlet oxygen as the main hyperactive species that destroy the tumour. Water soluble sensitizers are sort after for the convenience of delivery into the body. Thus, phthalocyanine (pc), tetrapyridinoporphyrazines (tppa) and tetramethyltetrapyridinoporphyrazines (tmtppa) with non-transition central metal atoms of Ge, Si, Sn and Zn were studied. First was the synthesis of these complexes, followed by their characterisation. The characterisation involved the use of ultraviolet and visible absorption spectroscopy, infrared spectroscopy, nuclear magnetic resonance spectroscopy, electrochemical properties and elemental analysis.

Photochemical properties of the complexes were then investigated. Photolysis of these macrocycles showed two processes; -reduction of the dye and photobleaching, which leads to the disintegration of the conjugated chromophore structure of the dye. Photobleaching is the reductive quenching of the excited state of the sensitizers. The intensity of the quenching decreased progressively from tmtppa, tppa to pc metal complexes with photobleaching quantum yields, 6.6×10^{-5}, 1.8×10^{-5} and 5.4×10^{-6} for Zntmtppa, Zntppa and Znpc, respectively.

Efficiency of singlet oxygen sensitization is solvent dependent with very different values obtained for the same compound in different solvents, for example, 0.25 and 0.38 were observed as singlet oxygen quantum yields for Gepc complex in DMSO and DMF respectively. In DMSO the efficiency of $^1O_2$ generation decrease considerably from pc to tppa and finally tmtppa. In water Getmtppa exhibits much higher singlet oxygen quantum yield, hence promising to be effective as a sensitizer for

photodynamic therapy.